UNIVERSITY OF NAIROBI

INVESTIGATING POWER GRID FREQUENCY STABILITY WITH WIND ENERGY USING PARTICLE SWARM OPTIMISATION ALGORITHM.

BY

TERRY LUMBASI CHEPKANIA

B.TECH (ELECTRICAL & COMMUNICATION ENGINEERING), MOI UNIVERSITY

F56/83018/2015

A thesis submitted in partial fulfilment of the requirements for the Degree of Master of Science in Electrical and Electronic Engineering.

University of Nairobi.

NOVEMBER 2020

DECLARATION OF ORIGINALITY

NAME OF STUDENT: Terry Lumbasi Chepkania

REGISTRATION NUMBER: F56/83018/2015

COLLEGE: Architecture and Engineering

FACULTY/ SCHOOL/ INSTITUTE: Engineering

DEPARTMENT: Electrical &Information Engineering

COURSE NAME: Master of Science in Electrical & Electronic Engineering

TITLE OF WORK: Investigating Power Grid Frequency Stability with Wind Energy using Particle Swarm Optimisation Algorithm.

1) I understand what plagiarism is and I am aware of the University of Nairobi policy in this regard.
2) I declare that this thesis is my original work and has not been submitted elsewhere for examination, award of a degree or publication. Where other people's work, or my own work has been used, this has properly been acknowledged and referenced in accordance with the University of Nairobi of Nairobi's requirements.
3) I have not sought or used the services of any professional agencies to produce this work
4) I have not allowed, and shall not allow anyone to copy my work with the intention of passing it off as his/her own work
5) I understand that any false claim in respect of this work shall result in disciplinary action, in accordance with University anti- plagiarism policy

Signature: .....

Date:.....

DECLARATION

This thesis is my original work and has not been presented to any other University for degree award.

Signature_____ Date_____

TERRY LUMBASI CHEPKANIA

F56/83018/2015

This thesis has been submitted for examination with our approval as University Supervisors.

Signature_____ Date_____

DR. PETER MOSES MUSAU

Signature_____ Date 24/11/2020

PROF. CYRUS WABUGE WEKESA

DEDICATION

This thesis is written in honour of my dear parents who with a lot of steadfastness, love, discipline and encouragement sowed a fruitful seed and laid the foundation for my life. I thank them that even in their old age have never stopped to give me advice to push a little bit further in all my endeavours.

I also wish to extend sincere and heartfelt gratitude to my lovely wife and children who have stood by me in all circumstances that I found myself in. To my lovable siblings, thank you for your relentless support and several calls you made that I could not return at times due this kind of work.

ACKNOWLEDGEMENT

I thank the almighty God for his kindness, grace and blessings in my entire life. I am highly indebted to my supervisors Dr. Peter Moses Musau and Prof. Cyrus Wekesa who relentlessly offered to guide and encourage me in carrying out this academic research while at the University of Nairobi. I wish to register my appreciation to my wife Susan and children for the family support I received from them. I also thank my parents Lumbasi Jean Chepkania and Retempta Khakasa Lumbasi for their love and care while growing up from childhood to this age. I highly appreciate the Higher Education Loans Board for the partial scholarship to fund my studies. Lastly, I acknowledge my colleagues at the University of Nairobi who kept supporting and advising me on my research work.

TABLE OF CONTENTS

DECLARATION OF ORIGINALITY ..... **II**

DECLARATION ..... **III**

DEDICATION ..... **IV**

ACKNOWLEDGEMENT ..... **V**

TABLE OF CONTENTS ..... **VI**

LIST OF TABLES, FIGURES ..... **VIII**

LIST OF ABBREVIATIONS ..... **X**

ABSTRACT ..... **XI**

CHAPTER ONE **1**

INTRODUCTION **1**

1.1 BACKGROUND OF THE STUDY 1
1.2 STATEMENT OF THE PROBLEM 3
1.3 RESEARCH OBJECTIVES 3
1.4 RESEARCH QUESTIONS 4
1.5 JUSTIFICATION OF THE STUDY 4
1.6 CONTRIBUTIONS OF THE THESIS 5
1.7 SCOPE OF WORK 5
1.8 THESIS ORGANIZATION 5

CHAPTER TWO **6**

LITERATURE REVIEW **6**

2.1 INTRODUCTION. 6
2.2 POWER SYSTEM STABILITY 6
2.2.1 Rotor Angle Stability. *8*
(a) Small-Disturbance (Small-Signal) Rotor Angle Stability *8*
(b) Large Disturbance Rotor Angle Stability *9*
2.2.2 Voltage Stability *10*
(a) Large disturbance Voltage Stability *11*
(b) Small Disturbance Voltage Stability *11*
2.2.3 Frequency Stability *12*
2.3 LITERATURE REVIEW FOR FREQUENCY STABILITY: 13
2.4 RESEARCH GAPS 20
2.5 PROBLEM FORMULATION 21
2.6 SUMMARY OF LITERATURE REVIEW. 27
2.7 CHAPTER CONCLUSION 28

CHAPTER THREE **29**

RESEARCH METHODOLOGY **29**

3.1 INTRODUCTION 29
3.2 RESEARCH DESIGN 29

3.2.1 Previous Methods, Strengths and Weaknesses. *29*
3.2.2 Frequency Control Schemes with Wind Energy Using Simulation Approach *29*
(a) Choice of IEEE 39 bus System *30*
3.2.3 The Enhanced Frequency stability control Scheme using Particle Swarm Optimization *30*
(a) Justification for use of Particle Swarm Optimization (PSO) *31*
3.3 DATA COLLECTION AND ANALYSIS 33
3.4 ACHIEVED RESULTS. 33
3.5 CHAPTER CONCLUSION 33

CHAPTER FOUR 35

RESULTS AND ANALYSIS 35

4.1 ANALYSIS AND STATISTICS OF FREQUENCY STABILITY CONTROL SCHEMES IN THE PRESENCE OF WIND ENERGY SOURCES 35
4.1.1 Scenario I: Without Wind Farm connected to the Grid. *35*
4.1.2 Scenario II: With one Wind Farm in the Grid. *36*
4.1.3 Scenario III: With Two Wind Farms Integrated in the Grid. *40*
4.1.4 Scenario IV: With Five Wind Farms connected to the Grid *42*
4.2 ENHANCED FREQUENCY STABILITY CONTROL SCHEME USING PARTICLE SWARM OPTIMIZATION ALGORITHM. 44
4.2.1 Case 1: Without Wind Farm Integrated in the Grid *44*
4.2.2 Case 2: With One Wind Farm Integrated in the Grid Using PSO *45*
4.2.3 Case 3: With Two Wind Farms Integrated in the Grid Using PSO *49*
4.2.4 Case 4: With Two Wind farms Integrated in the Grid and generator at bus 39 Tripped *50*
4.2.5 Case 5: With Two Wind farms Integrated in the Grid and generators at bus 38 and 39 Tripped. *51*
4.3 VALIDATION OF PARTICLE SWARM OPTIMIZATION WITH OTHER EXISTING METHODS 53
4.4 CHAPTER CONCLUSION 54

CHAPTER FIVE 56

CONCLUSION AND RECOMMENDATIONS 56

5.1 FURTHER RESEARCH WORK 56

REFERENCES 58

APPENDIX B 62

PUBLISHED WORKS. 62
IEEE 39 BUS USING PARTICLE SWARM OPTIMIZATION ALGORITHM RESULTS 75

APPENDIX C. 107

CODING AND ALGORITHMS 107

LIST OF TABLES, FIGURES

Figure 1.1: Block diagram of a DFIG 2
Figure 2.1: Power system stability categories based on the nature of disturbance 7
Figure 2.2: Classification of Power System Stability 9
Table 2.1: WPP and Pre-Designed Inertial Response Control. 14
Table 2.2: Wind Speed of 10 m/s with 80 MW SG Trip-Case 1 15
Table 2.3: Wind Speed of 8m/s with 110 MW SG Trip- Case 2. 16
Table 2.4: Major Characteristics of the Wind Turbines Main Inertia Control. 17
Table 3.1: Table for Particle Swarm Optimisation Justification. 31
Table 3.2: Mapping of the Problem to the Particle Swarm Algorithm 32
Figure 3.1: Flow Chart for Implementation of PSO Algorithm 34
Table 4.1: Scenario I - Output Results without a Wind Farm Connected to the Grid Using Simulation Approach 36
Table 4.2: Magnitude and Phase Angle Profile of Power Parameters without a Wind Farm connected to the Grid 37
Table 4.3: Generation, Load and Losses from Power Flow without a Wind Farm 37
Figure 4.1: The Simulink diagram for IEEE 39 bus without a wind Farm. 38
Table 4.4: Scenario II - Output Results for One Wind Farm Integrated in the Grid Using Simulation Approach 39
Table 4.5: Magnitude and Phase Angle Profile of Power Parameters with One Wind Farm connected to the Grid 39
Table 4.6: Generation, Load and Losses from Power Flow with One Wind Farm. 40
Figure 4.2: The Simulink diagram for IEEE 39 bus with one wind Farm. 40
Table 4.7: Scenario III - Output Results for Two Wind Farms Integrated in Grid Using Simulation Approach. 41
Table 4.8: Magnitude and Phase Angle Profile of Power Parameters with Two Wind Farms connected to the Grid 42
Table 4.9: Generation, Load And Losses From Power Flow With Two Wind Farms Connected To The Grid. 43
Figure 4.3: The Simulink diagram for IEEE 39 bus with two wind farms. 43
Table 4.10: Five Wind Farms with Rated Capacities and Number of Wind Turbines in Each Wind Farm. . 44
Table 4.11: Scenario IV - Output Results for Five Wind Farm Integrated in Grid Using Simulation Approach 45
Table 4.12: Magnitude and Phase Angle Profile of Power Parameters with Five Wind Farms connected to the Grid 46
Table 4.13: Generation, Load And Losses From Power Flow With Five Wind Farms Connected To The Grid 46
Figure 4.4: The Simulink diagram for IEEE 39 bus with five wind farms. 47
Figure 4.5: Voltage Magnitude Profile without Wind Farm in the Grid 47
Figure 4.6: Frequency Plot with Disturbance without a Wind Farm. 48
Figure 4.7: Voltage Profile with One Wind Farm in the Grid Using PSO 49
Figure 4.8: Frequency Response with One Wind Farm in the Grid Using PSO 49
Figure 4.9: Voltage Profile with Two Wind Farms in the Grid Using PSO 50

Figure 4.10: Frequency Response with Two Wind Farms Displacing Conventional Sources and Closely Matched Active Power Using PSO 51
Figure 4.11: Voltage Profile with Two Wind Farms and bus 39 Generator Tripped 52
Figure 4.12: Frequency Response with Two Wind Farms and bus 39 Generator Tripped. 52
Figure 4.13: Two Wind Farms in the Grid with Two Generators at bus 38 And 39 Tripped. 53
Figure 4.14: Frequency response of two wind farms with two generators at bus 38 and bus 39 Tripped. 54
Table 4.14: PSO Results. 55
Table 4.15: PSO Validation with other methods. 55

LIST OF ABBREVIATIONS

CIGRE-	International Council on Large Electric Systems
DFIG-	Doubly Fed Induction Generator
EHV-	Extra High Voltage
EMTP-RV-	Electromagnetic Transients Program
GW-	Gigawatt
HVDC-	High Voltage Direct Current
IEEE-	Institute of Electrical and Electronic Engineers
KE-	Kinetic Energy
KenGen-	Kenya Electricity Generating Company
MPPT-	Maximum Power Point Tracking
MW-	Megawatts
PLL-	Phase-Locked Loop
PV-	Photovoltaic
ROCOF-	Rate of Change of Frequency
STFS-	Short Term Frequency Support
VSWT-	Variable Speed Wind Turbines
WF-	Wind Farm
WPP-	Wind Power Plants
WTG-	Wind Turbine Generator
WT-to-WT-	Wind Turbine to Wind Turbine

ABSTRACT

Title: Investigating Power Grid Frequency Stability with Wind Energy using Particle Swarm Optimization Algorithm.

Reg. No: F56/83018/2015.

Renewable energy sources (RES) have become a key area of concern and interest world-wide, including in Kenya where recently a 310 MW Wind Power plant was commissioned. They are clean energy technologies, in some cases occur in abundance and can mitigate against rising cost of fossil-fuels. Wind energy conversion technologies, in particular, have witnessed one of the highest growth rates in the energy sector in recent years. However, their continued integration into the utility poses serious challenges with respect to the stability of the electrical power system. They do not inherently provide system inertia from rotating masses of the rotor of the turbine. In fact, it is well documented that large scale integration of wind energy sources into the grid by displacement of the conventional sources of energy leads to frequency instability. This thesis investigated power grid frequency stability with wind energy using particle swarm optimization (PSO) algorithm. The investigation employed MATLAB/Simulink environment, in conjunction with power system analysis toolbox, on an IEEE 39 Bus Test System. The optimization employed PSO algorithm and load flow was conducted using Newton Raphson algorithm. Results obtained show that the voltage profile and frequency response profile improved significantly as the percentage wind penetration increased in the grid. The active and reactive power injections remained constant because the load was assumed constant. For the test system considered, the maximum wind power penetration level was established to be 32.1%. Notably, as the percentage of wind power penetration increased, the rate of change of frequency worsened from 0 % to 33.33 %. This is due to the intermittent nature of wind energy source.

Key Terms: Power system stability, frequency stability, wind turbines, frequency control methods, conventional sources of energy, renewable energy sources, wind energy, system inertia, particle swarm optimization.

CHAPTER ONE

INTRODUCTION

1.1 Background of the study

The focus on electricity generation has shifted to renewable energy sources globally [1].They can be replenished and cannot be exhausted and include: Solar, wind, hydro, bioenergy, hydrogen, geothermal, ocean tidal & wave energy. Due to environmental impact, rising cost of fossil-fuels, price volatility and depletion of fossil-fuel reserves, renewable energy sources are not only vital but also their utilization has increased in the whole world [2].Renewable energy penetration to the grid promises cost reduction in generation and abundance in supply [2]. However, large scale integration of wind and solar photovoltaic (PV) in the power grid causes numerous power system stability problems. They suffer from intermittency and variability due to dependency on weather patterns. Most of the renewable energy generators connect with the grid through power converters that do not inherently provide rotational inertia like conventional alternators. Hence, large presence of the renewable energy resources integrated into the grid lowers the system inertia running the risk of large frequency deviations [3]- [4].

One of the resources within the renewable energy portfolio is wind [5]. In the year 2014, the world market set a new record of the amount of installed wind capacity at 51GW [6].The Kenyan government envisages that by the year 2030 it would have an installed capacity of 2 GW of wind power in Kenya [7]. According to Wind Energy Prospectus [7], Kenya has forecasted wind energy potential of values as high as 346W/m² and wind speeds of 6m/s in parts of Kajiado, Narok Laikipia, Meru, Nyandarua, Kilifi, Lamu, Isiolo, Turakana, Samburu, UasinGishu, Marsabit, and Kiambu among others. Hence, the increased interest from the government and the world at large implies that the challenges and limitations on wind energy penetration must be addressed to enjoy the benefits of abundant wind energy supply.

Power system stability refers to a situation where synchronous machines of the power system are able to offer response to disturbance from normal operating condition and restore normalcy in operation [8].According to [9], it is the ability of an interconnected power system to retain sTable or normal operation after subjection to disturbance. The power system stability is highly degraded by power imbalances between generation and demand which are inherently present in the daily operation of the power grid [10]. Frequency deviation has an operational limit and

hence minimum inertial frequency response is required. The intermittency and variable nature of wind with reduced or zero inertia [5], increases power system frequency instability. Therefore, by lowering the system inertial response, high levels of wind penetration would contribute to power system instability.

Among the major concerns of power system stability is frequency stability [2].The displacement of conventional generators such as hydropower and thermal energy by wind energy causes a reduction in system inertial response, faster and large frequency excursions that take long to return to its nominal value [2]. This implies addition of wind power to the grid causes frequency to deviate to a large degree from the nominal value. This attribute calls for power system frequency control and regulation capability and limits the range of accepTable wind power penetration levels [2].Inadequate regulation capability of the grid would cause larger frequency excursions leading to load shedding or an entire collapse of the system [5].

Variable speed wind turbines (VSWT) have gained popularity and dominant use in wind turbine energy generation because of better efficiency and control options. They are decoupled from the grid and as a result offer reduced system inertia to support power system frequency stability [10]. A typical example of the VSWT is the doubly fed induction generator (DFIG) shown in Figure 1.1.Wind energy is characterized by intermittency and low inertia and variability [5]- [11].

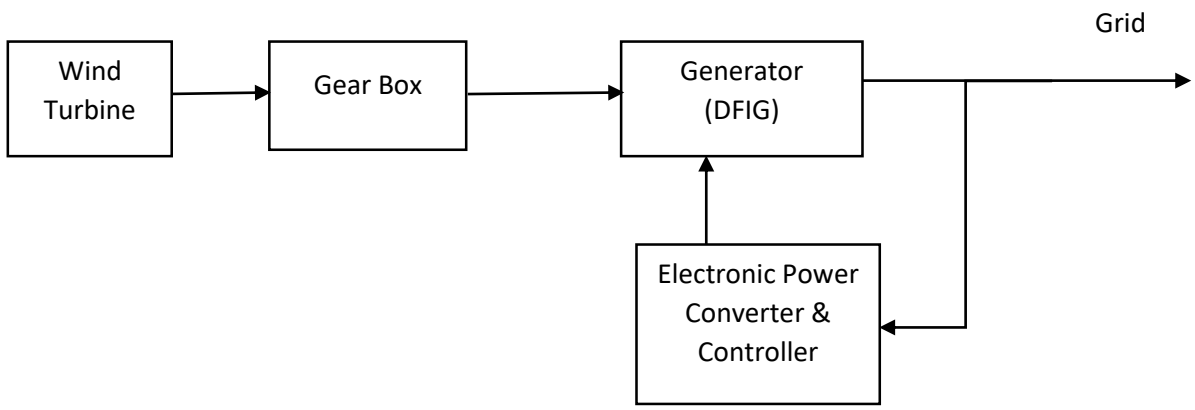

Figure 1.1: Block diagram of a DFIG

Source: Shang et al. [12]

1.2 Statement of the Problem

Wind energy conversion systems (WECs) are continuously being integrated into the power grid. Wind turbines have zero or low system inertia; hence they do not support frequency stability. This has given rise to frequency stability related challenges. They include cascaded outages and power system blackouts due to the frequent operation of under frequency load shedding relays or islanding situations (isolating part of the network due to under frequency load shedding). The amount, timing and coordination of the injection of power from the rotor masses of wind turbines with conventional power plants into the grid with a view of minimizing further frequency excursions during frequency events has been a challenge.

According to Wind Energy Prospectus Report [7], with all this wind energy potential, the existing generation and transmission systems have still experienced system disturbances where generation does not meet the load demand on some occasions or when a fault occurs on the transmission line. This has prompted either the generators or utilities to switch off an entire grid due to under frequency leading to nationwide blackouts lasting several hours. For example, in June 2016, a Monkey tripped one of the transformers at Gitaru that resulted into nationwide blackout that lasted 3 hours losing 180MW of power [12].

It is therefore expected that with the increasing generation mix and focus towards renewable energy because of reduced generation costs and emissions of greenhouse gases, better frequency stability mechanisms should be developed to cope with the ever-increasing energy demand. This motivated investigation of grid power frequency stability with wind energy using particle swarm optimization.

1.3 Research Objectives

The core objective of this research was to investigate the effect of connecting wind generators on power grid frequency using particle swarm optimization (PSO).The specific objectives were:

(i) To review frequency stability control schemes in the presence of wind energy sources.

(ii) To perform load flow studies on a test system to determine system behavior in the presence of new (wind) generation

(iii) To develop an enhanced particle swarm optimization frequency control scheme

1.4 Research Questions

(i) What and how effective are the current frequency stability control schemes in the presence of wind energy sources?

(ii) How do the voltage and frequency of the power system change in the presence of new (wind) generation?

(iii) What frequency control scheme can offer better grid frequency stability in the presence of wind energy?

1.5 Justification of the Study

The intermittent nature of wind and variability of wind energy input from wind energy conversion systems (WECS) pose power system stability challenges. The zero or low inertial response of wind turbines implies frequency excursions are common. Therefore, with the high integration and penetration of wind into the grid makes the power system suffer from frequency instability. This is further exacerbated by the dynamic nature of the load at any given time.

Renewable energy sources have found wide use and are becoming key areas of energy investment and management world-wide. They have been found to be clean, environmentally friendly and are less costly in terms of capital investments [13]. They reduce carbon dioxide emissions and subsequently global warming, decrease depletion of fossil-fuel sources and are relatively cheaper compared to thermal plants [1]. They are also readily available compared to conventional sources of energy.

The government of Kenya is focused on providing cheap and reliable power supply to its citizen. Towards this noble endeavor, it has initiated many wind energy projects in Turkana, Ngong and Isiolo and Malindi to curb the anticipated energy deficit [7].The power system is required by Kenyan law to provide ancillary services to the power system by maintaining frequency in the event of generation loss or other causes [14]. The operating frequency for the Kenyan power system is 50±0.5 Hz from practice in the field and Kenya's National Control Centre in Dandora. This narrow operating frequency range implies proper mechanisms should be put in place to ensure the frequency range is maintained. System frequencies that fall outside the narrow operating range imply under frequency load shedding or entire collapse of the power system leading to blackouts. It is therefore important that investigations are carried out to establish the effect of large scale penetration and integration of wind energy on the grid. This

will also inform the frequency control schemes suitable for smooth operation of wind energy with other sources of energy of the power system.

1.6 Contributions of the Thesis

The percentage of wind power penetration in the grid was limited to a maximum value of 32.08%. The frequency response improved from 49.9963 Hz to 49.9971 Hz. The rate of change of frequency worsened from a low value of 0.030389 Hz/s to 0.040518 Hz/sec. This showed that an increase in the percentage of wind power penetration leads to an increase in the rate of frequency change hence increasing frequency instability in the grid.

1.7 Scope of Work

The subject area reviewed the current frequency stability control methods with renewable energy existing globally. It also checked on their deficiencies and inadequacies in controlling the previous system disturbances and then developed an enhanced frequency stability control method with wind energy using particle swarm optimization. This was modelled and comparative results between the current existing method and the new proposed method were validated.

1.8 Thesis Organization

The thesis is organized as follows: Chapter one gives an introduction in renewables. Chapter two delves deeper into literature review on the types of stability and later on focused on review of frequency stability. The research methodology was covered in chapter three. Results and analysis were captured in chapter four and conclusion and recommendations in chapter five.

CHAPTER TWO

LITERATURE REVIEW

In this section, review of literature contains the following sections: Introduction, power system stability, review of frequency stability, research gaps, problem formulation and a summary of literature review.

2.1 Introduction.

According to Kundur et al., [15] since early 1920s, one of the parameters determining secure operation of a power system is power system stability. Power system instabilities have caused blackouts. In the past, transient instability was the most dominant stability problem where major focus and efforts were concentrated. Currently, due to large interconnected systems, new technologies and controls, other stability problems have arisen that includes: voltage, frequency and rotor angle stability and interarea oscillations.

2.2 Power System Stability.

Power system stability is the ability of an electric power system, given an initial operating condition, to preserve operating equilibrium, after subjection to a physical disturbance, with most system variables constrained and unchanged [15].It is highly a nonlinear system where generator outputs, loads and other system operating parameters change continuously. It is influenced by the nature of disturbance and initial operating condition.

Power system is subjected to two disturbances. Small disturbances can be load changes that occur continually. Large changes could be loss of a large generator or transmission line due to a fault. The design of stable power systems for all disturbances is not practical and economical. The design contingencies on a large extent are influenced by high likelihood of occurrence. For example, large-disturbance affecting stability has a specific scenario. A steady equilibrium set of a system has a limited area of operation; the wider the area, the better the resilience to large disturbances. Its response to a disturbance could involve several equipment, leading to weakening of the system and possibly instability.

In cases where the power system after a disturbance is stable, a new equilibrium level is reached where system reliability is maintained. Automatic controls and human system operators could be used to normalize the system. Power system instabilities might lead to cascaded outages and blackouts. Accordingly, based on the nature of disturbance, the synchronous power system

stability can be categorized into steady state stability, transient stability and dynamic stability [15]. The layout for the three categories is displayed in Figure 2.1.

Steady state stability refers to situations where the electric power system can achieve sTable condition after subjection to a small disturbance [15]. Examples could be normal load variations or operation of automatic voltage regulator. It determines the higher limit of loading of machines with gradually increasing loading before loss of synchronism [9]. Transient stability refers to ability of an electric power system to restore steady condition after subjection to a large disturbance. Typical examples are faulty line, loss due to excitation, switching operations or loss of load. The system retains synchronism after a persistent disturbance over a long period of time. Dynamic stability refers to artificial stability given to a system that is inherently unstable by automatically controlled means. Small disturbances (variations in loadings, turbine speed changes) continuously occur in the system. They are not sufficient to cause loss of synchronism nevertheless cause system excitation resulting to natural state of oscillations [9].In a dynamically stable system, the oscillations do not exceed particular amplitude and disappear quickly (well-damped). The amplitude of the oscillations is large and persists for a long time (underdamped) for a dynamically unstable system. Power system stabilizers are used to significantly improve dynamic stability. These small disturbances last between 10 to 30 seconds.

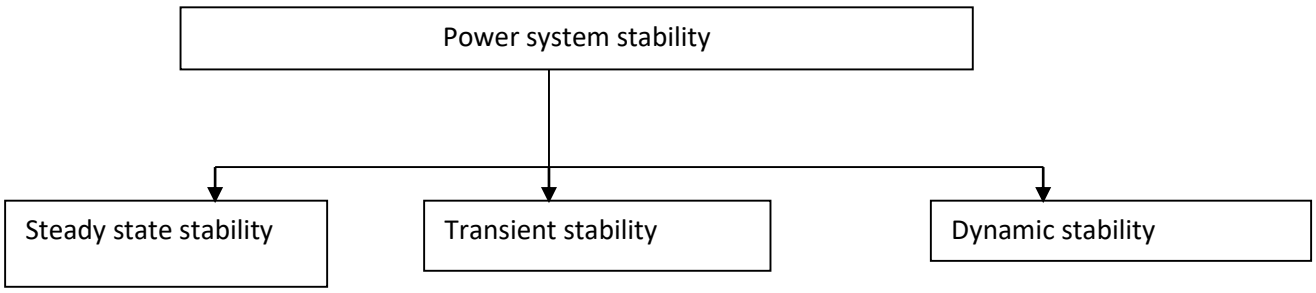

Figure 2.1: Power system stability categories based on the nature of disturbance

Source: Kundur et al. [15]

The power system is assumed to be in a true steady-state initial operating condition [15].Stability analysis, factors causing instability and methods of improving stability gave rise to categorization of power system stability as shown in Figure 2.2. Analysis and resolution of power system stability problems practically, necessitated classifications: rotor angle, voltage and frequency stabilities shown in Figure 2.2. The following aspects of the power system were

considered. The physical nature of the main power system variable where instability was detected. The size of disturbance determined stability prediction and the method of calculation. The processes, devices and time-span required to analyze stability was considered.

2.2.1 Rotor Angle Stability.

Rotor Angle stability refers to synchronous machine of an interconnected system being able to retain synchronism after subjection to a disturbance [15].It is defined by system's ability to maintain state of balance between mechanical torque and electromagnetic torque of a synchronous machine [15].This involves analysis of inherent electromechanical oscillations in power systems. The changes in electromagnetic torque in a synchronous machine could be broken down into damping torque that is in phase with speed deviation and synchronizing torque normally in phase with rotor angle deviation. The two torques determine rotor angle system stability. Synchronizing torque insufficiency leads to aperiodic or non-oscillatory stability while inadequate damping torque causes oscillatory instability. Rotor angle instability are classified into large disturbance and small-disturbance.

(a) Small-Disturbance (Small-Signal) Rotor Angle Stability

This refers a situation where the electric power system can sustain synchronism after subjection to a small disturbance [15]. Small disturbances allow system equations linearization and analysis. Insufficient synchronizing torque result into small disturbances that cause rotor angle increase by aperiodic or nonoscillatory instability mode. While inadequate damping torque leads to small disturbances to create rotor oscillations of increasing amplitude [15]. Continuously acting generator voltage regulators eliminate aperiodic mode instability. Exposure of generators operating with constant excitation to excitation limiters (field current limiters) actions lead to aperiodic mode instability.

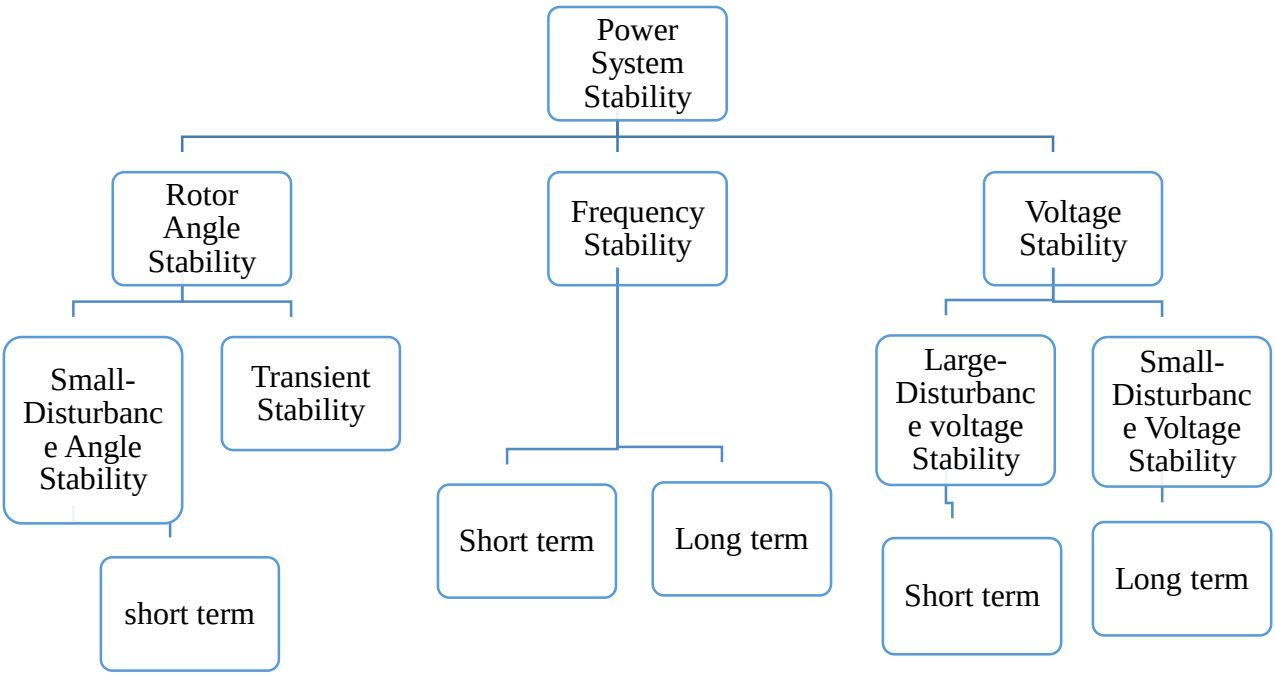

Figure 2.2: Classification of Power System Stability

Source*:* Source: Kundur et al. [15], IEEE/CIGRE Joint Task Force on Stability Terms and Definitions, May 2004.

(b) Large Disturbance Rotor Angle Stability

A situation where the electric power system can remain in synchronism after severe disturbance such as transmission line short circuit [15].Its response results into large variations in rotor angles of the generator shaped by the non-linear power-angle relationship. The rotor dynamics of a synchronous machine (generating or motoring) where friction, windage and iron losses are considered negligible is related by the swing equation [9].

$$M\frac{d^2\,\partial}{dt^2} = Pm - Pe; \tag{2.1}$$

in pu of apparent power (machine rating) as base.

$$M = \frac{H}{\pi f} \quad \text{in Pu.} \tag{2.2}$$

or

$$\frac{\mathrm{H}}{\pi \mathrm{f}} \frac{d^2\partial}{dt^2} = \mathrm{Pm} - \mathrm{Pe} \tag{2.3}$$

Where,

H-inertia constant in MJ/MVA or MW-s/MVA, f-frequency in hertz

∂ - torque angle or power angle (rotor angular displacement from synchronously rotating reference frame)

P_m -Mechanical power input per unit.

P_e -Electrical power output in per unit

M- Inertia Constant

2.2.2 Voltage Stability

Refers to situation where the electric power system is able, given initial operating condition, to sustain steady voltages at all buses after subjection to a disturbance [15].This involves power system maintaining state of balance between generation and demand. The voltage instability could be a gradual decrease or increase in voltage levels at some buses. It could result into load loss in an area, transmission line trips or other system components by their protection systems hence leading to cascading outages, partial loss of generator synchronism due to the outages or violated field current limit operating conditions.

Voltage collapse is a sequence of voltage instability events that results into blackout or abnormally low voltages in a substantial part of the electric power system [15].It is normally driven by loads in response to power system disturbance. Loads normally absorb more reactive power contributing further reduction in voltage and thus increase stress on the power system.

Voltage drop by inductive reactance of the transmission network contribute to voltage instability. The transmission network power transfer capability and voltage support are limited by voltage instability. The two parameters are also limited by some generators exceeding the field or armature current-time overload capability boundaries [15].When reactive power demand exceeds the capability of reactive power sources, it results into voltage instability.

The capacitive behaviour of the network causes overvoltage instability. For instance, Extra High Voltage (EHV) transmission lines operate under the surge impedance loading (SIL) or generators or synchronous compensators operate by under excitation limiters that prevent

excessive reactive power absorption. The generation and transmission system sometimes are not able to operate below some load level. While restoring the load power, transformer tap-changers also experience prolonged voltage instability.

The terminals of high voltage direct current (HVDC) links used for long distance transmission or end-to-end applications also experience voltage instability. This occurs where HVDC links are coupled to ac systems that are weak [15]. This happens at inverter stations or rectifiers normally linked with the undesirable reactive power "load" characteristics of the electronic power converters [15].

The active and reactive power at the ac/dc junction is controlled hence HVDC link control strategies are needed. HVDC technology developments such as voltage source converters and capacitor commutated converters have widened limits for sTable operation of HVDC links in weak ac systems as opposed to use of line commutated converters. Voltage stability categories are: Large and small disturbance voltage stability.

(a) Large disturbance Voltage Stability

This is a situation whereby the electric power system can retain steady voltages after exposure to large disturbances. Examples include faults in the system, generation loss or circuit contingencies. It is influenced by system and load characteristics and communications of both discrete and continuous controls as well as protections. It requires examination of nonlinear power system response over a study period to determine performance and interactions of devices such as motors, generator field current limiters and underload transformer tap changers [15].The period could be a few seconds to tens of minutes.

(b) Small Disturbance Voltage Stability

Refers to ability of electric power system to maintain steady voltages after being subjected to small disturbances such as system load incremental changes [15].It is influenced by system loads, discrete and continuous controls at a given instant of time. Using suiTable assumptions, system equations can be linearized for analysis to deduce sensitivity information suiTable for identifying stability factors. Both linear and nonlinear analysis are used in tap changer controls (deadbands, discrete tap steps, and time delays) since none can be used independently.

2.2.3 Frequency Stability

Refers to the ability of an electric power system to maintain steady frequency after subjection to severe system disturbance resulting in significant imbalance between generation and load [15]. It is determined by maintenance of operating balance between generation and load with minimal unintended loss of load. It is occasioned by sustained frequency swings leading to generator unit trips or load trips [15].

Generally, frequency instability is associated to equipment response inadequacies, poor coordination of control and protection equipment or generation reserve insufficiency [16]. Frequency excursions could be short or long term based on characteristic times of processes and apparatuses that will be activated [15]. For example, a fraction of seconds' device responses could be under frequency load shedding, generator controls and protections or several minutes such as prime mover energy supply systems and load voltage regulators.

When frequency excursions occur, voltage levels may change substantially in islanding conditions with under frequency load shedding [15].Voltage level changes could be greater in percentage than frequency changes and contribute to load-generation imbalance. Undesired generator trips may be caused by high voltage. In overloaded power systems, low voltage could trigger erratic impedance relays operation [15].

2.2.3.1 Background and Review of Particle Swarm Optimization (PSO) in Frequency Studies

Particle Swarm Optimization (PSO) was initiated in 1995 by Eberhart and Kennedy as a population evolution algorithm. Compared with other optimization techniques, it is easy and has fast convergence and fits well engineering and scientific applications [17].

According to AlRashidi [18], the simplicity is enshrined in the PSO two model equations and coordinates of each particle is associated with the two vectors: position (xi) and velocity (vi). A swarm consists of a group of particles or solution candidates that operate through a given feasible solution region or space where optimal solutions exist. AlRashidi and El-Hawary [19] reviewed PSO in various electric power systems applications. PSO, has been applied in distributed generation and battery storage systems to find the optimal operational settings of the system [19].

The variable frequency converters (VFC) are controlled by proportional integral (PI) controllers in variable speed wind turbine generators (VSWTGs) equipped with Doubly Fed Induction Generators. Due to system complexity and nonlinearity, it is cumbersome to tune PI controllers and tune the PI gains optimally [20]. They used PSO to design optimal PI controllers on the rotor-side converter of DFIG using a new approach [20].

Valle [21] carried out comparison between GA and PSO and it was apparent that PSO was more suited for complex and high nonlinearity problems.

2.3 Literature Review for Frequency Stability:

Hansen et al. [22] examined modelling of control strategies for frequency controlling wind power in islanded power systems. They investigated the possibilities of primary frequency control of wind power plants. Their study results showed that significant improvements in islanding grid frequency performance may be achieved by use of power smoothing and frequency controlling wind power plants (WPP). They also discovered that variable delta control was a better power smoothing strategy than fixed delta control. From their grid frequency comparison between hydro only and a combination of both wind and hydro in normal wind produced with load steps of 24 MW at 100 second connection, gave 48.3Hz and 49Hz respectively. They found out that the limiting factor for successful transient inertia response and participation in primary frequency control is the amount of kinetic energy that could be extracted from the wind turbine without large excursions from the optimal energy operating point. They also observed that little research has been done on various ways of implementing frequency control in the overall wind turbine control architecture. Their research simulations assumed a constant consumer load but in practical situations the load keeps on varying. The simulations also were performed on one aggregated wind power plant model, hence a study on individual wind turbines would attract so much interest in terms of power computations and frequency control. A wind farm controller distributing signals to different wind turbines based on their present operational points is also required to efficiently distribute the signals for the control action needed.

Altin [16]studied dynamic frequency response of wind power plants. He investigated the system requirements for synchronising power support and inertial response of wind power plants (WPP) in high wind penetration scenarios. He considered a generic power system model and a generic WPP model with different wind power penetration percentage levels

implemented in RMS toolbox for wind integration studies. He proposed a new inertial response control for WPPs considering inertial response requirements of a generic power system.

The parameters of the simplified WPP and pre-designed inertial response are presented in Table 2.1.

Table 2.1: WPP and Pre-Designed Inertial Response Control.
Source: Altin [16]

Name of parameter	Measurement unit	Values	Remarks
R_{wpp}	Pu/s	0.1,0.5,1	Active power rate limiter
T_{wpp}	s	0.025,0.125, 0.25	Overall WPP performance
H_{wpp}	pu	5,7.5,10	Inertia constant similar to synchronous generator
K_{Droop}	pu	5,7.5,10	Gain of the variable droop
T_{Droop}	s	7,9,11	Variable droop duration

The sensitivity analysis of the inertial response gain (H_{wpp}) for 40% and 50% wind power penetration levels determined the amount of additional power from WPP in order not to trip the ROCOF relays in the distributed generation. The plots of frequency against time were done and it was realised 50% wind penetration from the graphs produced a worse frequency deviation compared to 40% wind penetration scenario.

Similarly, a sensitivity analysis was carried out for the variable droop gain from 5 pu value to 10 pu value for both 40% and 50% penetration scenario. It was found out that a value of 10 pu produced double dip in system frequency response for 50% penetration scenario. For all the droop gain values 5 pu to 10 pu for 40% penetration scenario, the minimum frequency value improved [16].

Applying the tuning methodology, the proposed control can be applied to any power system with high wind penetration. The proposed controller provides less energy and peak active power compared to the existing control concepts (derivative control and temporary frequency control) while achieving the performance criteria. The proposed new inertial control has also reduced the impact of the recovery period for operation below the rated wind speed [16].

Nguyen and Mitra [2] studied the effect of wind power on load frequency control. They developed one control area mathematical model in the presence of wind energy source and implemented load frequency control (LFC) in MATLAB/Simulink. The simulated results showed that increasing penetration levels of wind power into the grid in one control area increased maximum frequency deviation values from 0.14 Hz to 0.32 Hz due to reduced system inertia and higher frequency regulation constant that led to decreased area frequency response characteristic. In an interconnected system the maximum frequency deviation was from 0.075 Hz to 0.125 Hz where in both stand-alone and interconnected system, inertia reduction ranged from 0% to 60%. They also discovered that in addition to large frequency variation, the frequency recovery duration extended due to wind power presence. They also supported an interconnected system to assist control areas with large penetration of wind power in reducing frequency excursions. The study established that maximum tie-line power increased and maximum area control error (ACE) reduced [2]. Their analysis recommended maximum level of 30 % wind penetration in the grid based on system configuration, maximum predicted load disturbance of 0.04 Pu and frequency excursion safe range of ±0.2 Hz.

Hwang et al. [23] conducted a study of short-term frequency support (STFS) assuming Maximum Power Point Tracking (MPPT) mode while working with of wind turbine generators (WTG). He investigated the performance of STFS schemes with two cases of wind speeds and different generator trips as shown in Table 2.2 and Table 2.3. In case one, 10 m/s wind speed with 80MW synchronous generator trip was considered. The results were tabulated as follows in Table 2.2.

Table 2.2: Wind Speed of 10 m/s with 80 MW SG Trip-Case 1

Source: Hwang et al. [23]

	Without STFS	Scheme 1	Scheme 2	Proposed scheme
FN(Hz)	59.272	59.411	59.543	59.516
df/dt (Hz/s)	-0.445	-0.400	-0.341	-0.368

Table 2.3: Wind Speed of 8m/s with 110 MW SG Trip- Case 2.

Source: Hwang et al. [23]

	Without STFS	Scheme 1	Scheme 2	Proposed scheme
FN(Hz)	58.938	59.159	59.231	59.213
df/dt (Hz/s)	-0.646	-0.576	-0.554	-0.556

Scheme 1: Fixed-gain, uses df/dt loop and Δf loop

Scheme 2: Dynamic-gain and uses only Δf loop

In case two, frequency nadir (FN) of scheme 2 was greater than proposed scheme and max df/dt was the smallest as shown in Table 2.3. This is because scheme 2 released more kinetic energy during early stages of an event than scheme 1. Hence, less KE was left in scheme 2 than proposed scheme.

Using the EMTP-RV simulator, [23] demonstrated that the proposed scheme improved frequency nadir (minimum frequency) under various wind conditions even when the wind speed reduced, or successive event occurred. Its merits included supporting large release of kinetic energy during early stages of frequency event. It also retained the available kinetic energy for consecutive event by decreasing power output after frequency nadir [23]. In addition to ancillary service support, it provided steady operation of DFIG via reduction of control gain with rotor speed even with a significant reduction in wind speed. Their research did not consider long-term frequency support of Wind Turbine Generators (WTG) in relation to secondary frequency support.

Shang et al. [24] reviewed various inertial control methods of Variable-Speed Wind Turbines (VSWT) and listed the advantages and disadvantages of those methods. In his article, he gave the major characteristics of the wind turbine main inertia control as shown in Table 2.4:

Shang et al. [24] raised several challenges and future research areas which included the need to carry out further analysis of mechanical loading and stress to ensure safety of wind turbines and inertial response. Secondary frequency decline may be avoided by proper coordination between the inertia control and turbine control to ensure faster turbine control response. Cases of secondary frequency decline can be averted further by proper coordination between turbine control and primary frequency control of the entire network.

Table 2.4: Major Characteristics of the Wind Turbines Main Inertia Control.

Source: Shang et al. [24]

Control methods	**Response delay**	**Response characteristic**	**Implemented Complexity**	**Additional sensed variables**	**Main technical barriers and potential risks**
$\frac{df}{dt}$ method	Certain	Closed-loop feedback control	Medium	Grid frequency	Parameters setting is complicated Easily causes power fluctuations
Δf method	Certain	Closed-loop feedback control	Simple	Grid frequency	Wind turbine excessive inertial response Conflicts with primary frequency regulation of power system
Enercon IE	Certain	Closed-loop feedback control	Very simple	Grid frequency	Conflicts with primary frequency regulation of power system
Frequency deviation trigger	Certain	Open-loop feedback control	Very simple	Grid frequency	Excessive power support with large-scale integration of wind turbines. Conflict with primary frequency regulation of power system
Optimizing Phase-locked loop (PLL)	No	Open-loop feedback response	No modification	No	Easily causes power fluctuations. Influence the response of the other control loops. Wind turbine excessive inertial response
Virtual synchronous control	No	Open-loop feedback response	Complexity	No	Alters the control structure of the wind turbine. Fault tolerance. Excessive inertial response of the wind turbine.

Shang et al. [24] also proposed a comparative analysis of inertial response methods of wind turbines and conventional synchronous generators. He also encouraged further studies of the relationship and interactions between different inertial response control methods and grid frequency. They emphasized need to study the different inertial response control methods in the presence of system faults. He also advised study of the interactions and relations between inertial responses of multi-Wind Turbines themselves. Coordinated inertial response ought to be done to avoid competition between wind farm to wind farm, WT-to-WT, wind farm to synchronous generators in the presence of additional methods of supplementary signal. They proposed inertial control parameter analysis and optimization. A standardised grid code based on key inertial response characteristics and grid frequency should be formulated, revised and

developed for wind turbines. This is necessary for further investment in wind power generation and penetration in the grid.

Keung et al. [25] said that there was no reason to fear since wind has inertia constant comparable to that of conventional generators. Wind farm produce better performance over individual wind turbine generators (WTGs). Power electronic converters have fast response hence capable of providing kinetic energy as an alternative primary reserve in wind turbines. These controls require frequency threshold detector to trigger kinetic energy release and a soft strategy for kinetic energy recovery after discharge. It would also incorporate redesigning the controller gains for fast response and turbine blade pitch control to allow more wind power. His study addressed the kinetic energy recovery after discharge without triggering power dip in the system. He observed that wind speeds ranging 7.93m/s to 12 m/s would avail 19MW of power in normal operating mode. $T_{discharge}$ experiments showed that the wind farms could provide 36MW of power for 3 seconds. This was how they arrived at $T_{discharge}$ of 3s. The research gaps were coordination and timing and sizing of kinetic energy discharge with conventional plants. It also requires extensive research to design frequency threshold detector and trigger circuit to release kinetic energy from wind turbines [25].It requires signal processing, pattern recognition, adaptive strategies and intelligent features.

Li et al. [26] described various control strategies and outlined their merits and demerits. Some of the strategies listed for primary frequency control included droop, rotor speed and pitch angle control. Rate of change of frequency and steady-state deviation in electric power system grid could be reduced effectively by 1st scenario of combined inertia, speed and droop control.

The 2nd scenario incorporated only inertia and droop for primary frequency control. Inertia controller contributes to transient frequency response (ROCOF), droop- provide permanent response and affects only frequency deviation. Other methods include the kinetic energy control method and combined droop and pitch control method for primary frequency response.

Secondary frequency response refers to a situation where power increase or decrease of generators is realised by commands from transmission system operator (TSO). The methods applied are

(i) Rotor speed and pitch control method

(ii) Automatic Generation Control-frequency changing signal sent via PID controller feedback loop that produce control signal to operate pitch control.

Rotor speed absorbs energy from the grid to allow it to increase rotational speed that might lead to further frequency dip for the 1stscenario. When compared with pitch control in the 1st scenario, underspeeding decreases small signal stability while overspeeding improves small signal stability.

In the 2ndscenario, droop control affects only minimum allowable frequency (frequency nadir) and not transient frequency response. In addition to automatic generation control (AGC), he also said that rotor speed and pitch angle control were still suiTable for secondary frequency control. He stated that both pitch angle and rotor speed control run the VSWT in de-loaded mode to be able to offer frequency support in case of frequency excursions. The wind turbines standard methods of frequency control were absent and effective approaches for dealing with a specific system must be designed [26].

Erlich et al. [27] discussed primary frequency control with wind turbines. He employed both pitch angle control and kinetic energy extraction in his research. Pitch angle control participates in frequency control and reserve margin, if it is operated at a lower output power at a given wind speed. This necessitated generation and introduction of pitch angle β in the pitch controller to realise frequency support. Simulations for additional frequency support were realised using a proportional controller. The advantage of the proportional controller is that it is adapTable to the hydro power plant primary controller. The results showed a continuous improved output power. They also have potential for smoothing frequency dips and support until secondary frequency control is activated. Clearance of disturbance enables wind turbines to reduce power output and be ready to participate in frequency smoothing of future frequency events .This method results into lower energy yields and probably more CO_2-emissions due to mixed generation resources where thermal plants may be called upon to supplement power supply.

Erlich et al. [27] also proposed kinetic energy extraction. He pointed out that is suiTable only for short periods and kinetic energy was dependent on rotor speed and inertia of the rotor. He incorporated a lead lag compensator to improve frequency response to disturbances and named it kinetic energy I (KEC I). In his second method of approach KEC II, he delayed kinetic energy (KE) release and increased the rotor speed first by reducing wind turbine power output. When wind turbine increases power output, the rotor speed decelerates. Then wind turbine was controlled to operate optimally, and rotor re-accelerates. The main difference was the change in sign at the summation set point of power and lead/lag compensator parameters. KEC I raise

power output directly as opposed to KEC II that indirectly raises rotor speed first by de-loading wind turbine then loading (increasing power output) it later by deceleration of the rotor speed.

Zertek et al. [28] carried out a novel control strategy aimed at maximizing kinetic energy and optimising jointly the rotor speed and pitch angle using differential evolution. He also accounted for power reserve margin in the computations. They simulated four scenarios. The first case was where the pitch angle was maintained at zero degrees until maximum speed was reached. The minimum frequency was achieved 7 seconds after frequency drop. In the second case where an additional df/dt loop was introduced, it attained 10 seconds from the frequency-time plots. The proposed control approach as the third option, gave a 13 seconds frequency drop delay. Hence translating to almost 100% delay compared to the first method. He concluded that the new control strategy extracted more kinetic energy at same de-loaded power compared to existing approaches. He only considered a single line diagram consisting of an aggregated load, thermal plant and Doubly Fed Induction Generator wind turbine (DFIG WT). In real power system analysis, it would comprise of many system components like hydro and even PV.

2.4 Research Gaps

The design of an optimal frequency threshold detector and trigger to discharge kinetic energy from rotor mass of the WTGs with same conventional plants primary reserve capability is a challenge. The addition of supplementary signals complicates issues related to coordination of inertial response between wind turbine to wind turbine, wind farm to wind farm and wind farm to synchronous generators. The coordination, timing and amount of kinetic energy release with the conventional plants characteristics require extensive research. For instance, the kinetic energy discharge should not hinder hydro governor action [25].

The fundamental frequency control and regulation falls into 3 categories: Inertial frequency control, primary frequency, secondary frequency and tertiary frequency support. Inertial frequency controls concentrate on extraction and use of kinetic energy of the rotor to support and reduce transient frequency instability. There are several methods used in extraction of kinetic energy in this scheme and advantages and disadvantages have been summarised in Table 2.4. To mention just a few demerits is that some of these methods result in excessive extraction of kinetic energy and leads to slower recovery of the rotor speed to a stable operating range [27]- [24].

Primary frequency control provides instant frequency response to arrest frequency excursion using automatic droop control loop for a period of about twenty seconds. This normally steps in as a subsequent method to support inertial response. Droop control method does not participate in initial rate of frequency change (ROCOF) [27]. It is modelled on the governor-response characteristics. Speed control method only works below rated wind speed and when it approaches rated wind speed it becomes ineffective [27]. Lastly, the pitch angle control method has a slow-speed response to support frequency dips and works better under partly loaded-mode of the wind turbine [27].This becomes costly since power output is not maximized and therefore would result into under-utilization of the wind turbine that has an economic aspect and burden to other generators in the system.

2.5 Problem Formulation

Wind power generation is marked by variability and intermittency. In this research, it would address the problem of excessive extraction of kinetic energy by wind turbines, coordination with primary frequency control and restoration of frequency to the nominal value. This would be achieved by partial loading of the wind turbine to be able to participate in frequency control and provide power reserve margin as to emulate the current conventional power plants. The Kinetic energy extraction will be optimized using particle swarm optimization (PSO). This will apply to the rate of change method (df/dt), frequency deviation (Δf), rotor speed and pitch angle control methods. The test system will be IEEE 39 bus system. The simulations will be done in MATLAB-Simulink environment.

From the basics about wind power fundamentals [29], wind power depends on the following: Volume of wind, wind velocity and mass of wind (density) flowing in a given area or location. The derivation of wind-capture equation for Variable Speed Wind Turbines (VSWT) is given by [29]:

$$Kinetic\ Energy\ (KE)\ = \frac{1}{2}\ \mathrm{MV}^2 \tag{2.4}$$

Power is the kinetic energy per unit time.

$$\mathrm{P} = \frac{1}{2}\ \dot{\mathrm{M}}\mathrm{V}^2 \tag{2.5}$$

Mass flow rate is given by

$$\frac{\mathrm{dm}}{\mathrm{dt}} = \dot{\mathrm{M}} \tag{2.6}$$

Where,

M-mass of air.

V-wind velocity

Mass flow rate in fluid mechanics =density x Volume flux= $\rho * A * S$

Therefore,

$$\mathrm{P_w} = \frac{1}{2}\ \rho * A * S^3 \tag{2.7}$$

The blades swept area (A) is given by

$$A = \pi R^2 \tag{2.8}$$

Where,

$\mathrm{P_w}$-Wind power

ρ-Air density

S-wind velocity or speed.

The efficiency in extraction of power is given by the wind power coefficient (C_p), ratio of turbine power (P_t) to wind power (P_w).

$$C_p = \frac{\mathrm{Pt}}{\mathrm{P_w}} \tag{2.9}$$

$$P_t = \frac{1}{2}\ \rho * A * S^3\ * C_p \tag{2.10}$$

According to [26], [28] the wind power coefficient is given by:

$$C_p = C_1\left(\frac{C_2}{\lambda_i} - C_3\beta - C_4\right)e^{\frac{C_5}{\lambda_i}} + C_6\lambda_i \tag{2.11}$$

$$C_p = 0.5\left(\frac{116}{\lambda_i} - 0.4\beta - 5\right)e^{\frac{-21}{\lambda_i}} \tag{2.12}$$

$$\lambda = \frac{RW_r}{S} \tag{2.13}$$

$$\frac{1}{\lambda_i} = \frac{1}{\lambda + .08\beta} - \frac{0.035}{\beta^3 + 1} \tag{2.14}$$

Where

λ -tip speed ratio;W_r- wind turbine rotational speed; R- impeller(blade) radius; β-pitch angle.

C_1 -C_6 are constant representing the characteristics of specific wind turbines.

From swing equation [9],

$$\frac{\mathrm{H}}{\pi \mathrm{f}} \frac{d^2\partial}{dt^2} = \mathrm{Pm} - \mathrm{Pe} \quad \text{in pu} \tag{2.15}$$

P_m–Mechanical power input in pu

P_e-Electrical power output in pu

∂ -Rotor angular displacement from synchronously rotating reference frame called torque angle or power angle.

H- Inertia constant

f- System frequency.

The accelerating power P_a is given by [9],

$$2\mathrm{M}\dot{\mathrm{W}}/\mathrm{p} = \mathrm{Pa} \tag{2.16}$$

Where

M-Inertia constant

$\dot{W}$-electrical angular velocity in rads/second

P-number of poles

$$\mathrm{M=JW} \quad \text{joule. second} \tag{2.17}$$

$$\mathrm{KE= GH} = \frac{1}{2} J W_r{}^2 * 10^{-6} \text{ MJ} \tag{2.18}$$

KE-Kinetic Energy

G-Rated Capacity of the wind turbine (MVA)

H- Inertia Constant (MW-s/MVA)

J- Rotor Moment of Inertia in $\mathrm{Kg} - \mathrm{m}^2$

W_r- Mechanical synchronous speed in rads/sec

From Chamorro [13],

$$\frac{df}{dt} = \frac{1}{2} * \frac{\Delta P * f_0}{GH} \tag{2.19}$$

Therefore, to determine, the frequency deviations Δf, it is given by [12],

$$\Delta f = f_{nadir} - f_0 \tag{2.20}$$

For the Kenyan grid case 50 Hz is the normal system frequency and a constant, hence

$$\Delta \mathrm{f} = \left(\frac{2\mathrm{GH} * \frac{df}{dt}}{\Delta \mathrm{P}} \right) - 50 \tag{2.21}$$

$$f_{nadir} = \left(\frac{2\mathrm{GH} * \frac{df}{dt}}{\Delta \mathrm{P}} \right) \tag{2.22}$$

Where,

f_{nadir} -the minimum value of frequency (Hz) reached during transient period.

GH-Total Kinetic Energy.

ΔP- Change in power or power imbalance;f_0-nominal frequency (Hz);$\frac{df}{dt}$ -rate of change of frequency (ROCOF) in Hz/s.

To extract maximum kinetic energy, we should maximize the deceleration of the rotor speed.

Hence,

Min$\frac{df}{dt}$ and min Δf.

This implies that to reduce the frequency deviation, we must maximize the generation of kinetic energy to support frequency during disturbance. The power imbalance can be found from generation shortfall or the unit that has been de-committed.

From [30], the kinetic energy reserve margin is given by,

$$\Delta KE = 0.5J(w_{del}^2 - w_{opt}^2) \tag{2.23}$$

Where,

Wdel-De-loaded rotor speed

W Opt- Optimal rotor speed.

The W opt is a constant value determined from wind speed. Hence,

Max $\Delta KE = 0.5J(w_{del}^2)$ for a single wind turbine. When considering a wind farm, it becomes;

Max $\left[\sum_{k=1}^{n} 0.5J_k\left(w_{del,k}^2\right)\right]$

Considering kinetic energy reserve margin in the de-loaded mode, and loading the turbine at 85%, then,

$$\mathrm{P}_{opt} \geq 0.85P_{opt} + \Delta Pke \tag{2.24}$$

From [30], the accelerating power is given by,

$$\mathrm{J}W_h\dot{\mathrm{W}}_h = P_{in} - (P_{ref} + \Delta Pke) \tag{2.25}$$

W_h-Mechanical rotational speed

ΔPke- Accelerating power due to kinetic energy

P_{opt}– Maximum power of the generator in MW

P_{ref} – Reference Power

Pin-Mechanical input power

The power imbalance will be catered by the sum of power extraction from de-loaded mode due to deceleration of the rotor speed to counter frequency drop. Ignoring variable and fixed losses in the Variable Speed Wind Turbine, we obtain equation (2.26) as given by [30].

$$0.5JW_h\dot{W}_h = \sum_{k=1}^{n}\left(0.5JW_{del}\frac{W_{del}}{dt}\right) \tag{2.26}$$

Taking into consideration a wind farm with reference to equation (2.26), then maximize the extraction of accelerating power from the wind turbine. Since the reference power is a constant, Pref, then considering a maximum power point tracking (MPPT) curve has maximum and minimum rotor speeds in de-loaded mode.

$$Max\Delta Pke = \text{Max } \{\sum_{k=1}^{n}\left(P_{in} - JW_{del}\frac{W_{del}}{dt}\right)\} \tag{2.27}$$

$$\Delta Pke \leq 0.15P_{opt} \tag{2.28}$$

The wind farm power output, according to [30] is given by,

$$P_{ref,wf} = \sum_{k=1}^{n} P_{del,k} = \sum_{m=1}^{n} 0.85P_{opt,k} \tag{2.29}$$

Ignoring windage, iron and frictional losses,

$$\text{Total PG} = \text{Total Pt} \tag{2.30}$$

P_G- Total generated power in MW

Pt-Total turbine power =Total mechanical power

P_L −Power Demand

P_{del} – De-loaded Power derived from the wind turbine.

The objective function is

$$Max\Delta Pke = \text{Max } \{\sum_{k=1}^{n}\left(P_{in} - JW_{del,k}\frac{W_{del,k}}{dt}\right)\} \tag{2.31}$$

Subject to:

$$\text{Total } \Delta Pke \leq 0.15 \text{ Total } P_{opt} \tag{2.32}$$

$$P_{ref,wf} = \sum_{k=1}^{n} P_{del,k} = \sum_{k=1}^{n} 0.85 P_{opt,k} \tag{2.33}$$

$$P_{min} \leq P_{del} \leq P_{max} \tag{2.34}$$

$$W_{del,min} \leq W_{del} \leq W_{max} \tag{2.35}$$

$$\beta min, del \leq 0 \leq \beta\ max, del \tag{2.36}$$

$$C_p \leq 0.59 \tag{2.37}$$

2.6 Summary of Literature Review.

There are four frequency control methods: Inertial response, Primary, secondary and tertiary frequency control. Inertial frequency controls concentrate on extraction and use of kinetic energy of the rotor to support and reduce transient frequency instability. Primary frequency control utilizes automatic droop control loop to provide immediate frequency response and lasts about twenty seconds. This normally steps in as a subsequent method to support inertial response. Secondary frequency control employs the automatic generator control to restore nominal frequency value after the disturbance has ceased [26]. To get back to the reference frequency value, the secondary reserve is activated manually or automatically in a period of between 20s and 20 minutes. The rotor speed control method could be used if operated in de-loading condition. This could be attained by adjusting the rotor speed hence getting desired output power to meet the demand. Pitch angle could be altered by adjusting the windward area blades and operating in the de-loaded mode to increase or decrease power output by pitch control. Tertiary control involves use of economic dispatch and unit commitment to allocate load among generating plants and determine which units to operate within a plant to meet the load and realise economic operation [8]. For the purposes of this research, tertiary frequency control will not be considered.

2.7 Chapter Conclusion

It has been found out that integration of wind energy into the grid compromises power system stability. There are gaps that have been established in the course of the research. It results into excessive extraction of kinetic energy from the rotor of the wind turbine hence leads to challenges in the recovery of the rotor speed. Sometimes leading to the wind turbine behaving like a load by drawing current from the grid to ensure recovery of the rotor speed.

This research therefore addresses the issue of excessive extraction of kinetic energy from the rotor of the wind turbine by optimizing the extraction of power using both particle swarm optimization and simulation approach using power system analysis toolbox. It also utilizes rotor speed and pitch angle control in de-loaded mode of the wind turbine to enable its participation in frequency control of the power system.

CHAPTER THREE

RESEARCH METHODOLOGY

3.1 Introduction

The methodology covered research design, data collection, tools and instruments for data collection and analysis of data and presentation of results.

3.2 Research Design

This research work had two specific objectives. The first specific objective mainly focused on review of frequency control schemes in the presence of wind energy sources. The second specific objective was development of an enhanced frequency control scheme with wind energy using particle swarm optimization.

3.2.1 Previous Methods, Strengths and Weaknesses.

From literature, the methods used for frequency control and stability studies included inertial frequency controls. This method resulted into excessive extraction of kinetic energy and led to slower recovery of the rotor speed to a stable operating range [27]- [24].The only advantage was that it provided frequency support in case of a system frequency excursion to some degree. Primary frequency control using automatic droop control method does not participate in rate of change of frequency (ROCOF) [27]. Speed control only works below rated wind speed and when it approaches rated wind speed it becomes ineffective [27]. Pitch angle control method has slow-speed response to support frequency dips and works better under partly loaded-mode of the wind turbine [27].It promotes under-utilization of the wind turbine. The advantages of these methods were that they allowed use of the available kinetic energy to support system frequency. Secondary frequency control restores frequency nominal value of frequency after the disturbance has ceased [26]. To attain the reference frequency value, the secondary reserve was activated manually or automatically in a period of between 20s and 20 minutes.

3.2.2 Frequency Control Schemes with Wind Energy Using Simulation Approach

The objectives of this research were achieved by modelling IEEE 39 Bus test system in MATLAB/Simulink and by simulation using power system analysis toolbox (PSAT) [31],

[32]- [33].In scenario I: Without wind energy sources in the grid, scenario II: One Wind farm was introduced in the grid to determine the response of various parameters. Scenario III: Two wind farms were incorporated in the grid to determine the performance of various system parameters. Finally, scenario IV: Five wind farms were introduced in the grid to determine the system response. The simulations were done for three and four wind farms using PSAT as well but the results remained the same hence settling at five wind farms.

In this approach, the objective function was coded in particle swarm optimization and implemented to get the global best power and rotor speed which were used as inputs to Newton Raphson algorithm to determine the voltage and frequency profiles of the grid that informed stability of the power system.

(a) Choice of IEEE 39 bus System

The IEEE 39 Bus test system is a ten generator machine system that provides flexibility required to achieve the desired generation mix and conventional generator displacements for the study.

The Kenya Vision for energy demand envisages development of 5000 MW generation capacity in the near future which approximates with the IEEE real power generation of 6,297.87 MW hence suitable for the Kenyan case study.

The nodes were selected at random and could influence different results. This calls for further research on optimal placement or location of wind farms into the grid. This was beyond the scope of this research.

3.2.3 The Enhanced Frequency stability control Scheme using Particle Swarm Optimization

In the first instance, the power system stability was tested without integration of the wind farms by carrying out load flow. All power system stability studies start with load flow as the mandatory and basic requirement before other studies can be carried out such as time domain simulation.

Each wind farm basically had 8 wind turbines in this research when using particle swarm optimization, which were combined to make a large wind farms. In this method, the fitness function for extraction of power was formulated. At later stages of the study, the wind farms

were increased to 50 with a total of 400 wind turbines integrated into the network at different generating buses.

(a) Justification for use of Particle Swarm Optimization (PSO)

There are many population based algorithms that can be used in this study. The justification for use of PSO as derived from [34] is shown in Table 3.1.

Table 3.1: Table for Particle Swarm Optimisation Justification.

PSO	Genetic Algorithm (GA)	Other Techniques
Faster Convergence	Relatively slower convergence	Convergence dependent on initial values e.g. temperature and maximum number of iterations.
Relatively Faster	Time consuming	Long computational time.
Easy to implement and few parameters to adjust	Uses complex operators for selection and crossover and difficult encoding	Involves tuning parameters.

The particle swarm optimization algorithm was coded in MATLAB with a sole purpose of optimizing wind turbine rotor speed and also optimizing the global best power. The results obtained were then fed to Newton Raphson algorithm for load flow studies and graphs for voltage profile, active and reactive power injected profile plotted on a bar graph. The frequency response profile was also plotted using damping coefficients [35]. The calculation for active and reactive were apportioned as shown by [36]. The mapping of parameters to particle swarm optimization are shown in Table 3.2.

The proposed method was designed to ensure optimal extraction of kinetic energy to ensure the rotor speed maintain steady-state condition after a large system disturbance with minimal delays. It also maximized turbine power output by optimal adjustment of the pitch angle to follow the load changes. This method used a combination of two frequency control methods. To inject power into the grid, rotor speed control was used. To recover and achieve the nominal frequency pitch angle control was utilised.

Table 3.2: Mapping of the Problem to the Particle Swarm Algorithm

No	Parameter	Algorithm Representation	Values
1	Rotor speed in radians per second	Particle	7.2473 7.1065 6.6071 9.5386
2	Group of wind Turbines' inertial response	Swarm	100
3	Optimal Power due to kinetic energy released	Destination	2.5012MW 2.5275MW 2.6206MW 2.0741MW
4	Feasible region or region of the desirable Power injected.	Center of the swarm	Global Best -item 1 and 3 in this Table
5	Fitness function	Objective Function	

The research involved modelling the wind turbine power output and its frequency controls scheme by coding in MATLAB and tests carried out on IEEE 39 bus test system without incorporating wind energy sources. The second phase made use of wind energy sources. A large system disturbance was introduced in the system using coding of Newton Raphson in the absence of wind energy and in the presence wind energy using Particle Swarm Optimization. The grid frequency was modelled using damping coefficients, observed and plotted on graphs when a large disturbance was introduced into the test bus system [35]. The grid frequency response during an excursion from the graphs determined the performance of the new enhanced method. The wind energy penetration level was also increased to determine the grid frequency stability in the presence of large amount of wind energy sources. This was achieved by displacement of conventional energy sources by wind energy sources in MATLAB.The results of improved frequency stability with wind energy would be validated against the results obtained by [37] who carried out a multi-objective particle swarm optimization method with wind turbines to determine the validity of the results.

The advantage of particle swarm optimization method is that it is much faster than Artificial Neural Networks and Genetic algorithm hence preferred in this study because it reduces grid frequency response delays and it is also simple and does not require large memory for implementation.

3.3 Data Collection and Analysis

The research was carried out in line with and following the procedures carried out by earlier researches to ensure continuity of the flow of the research and built and improve the early work done by [30]- [37] and other researchers.

The system data was extracted from the IEEE 39 bus test system modelled into MATLAB/Simulink with respective system buses, synchronous generators, wind turbine generators and lines. The data was simulated in MATLAB/Simulink environment and results were captured in the form of graphs, Tables and comparative analysis and data interpretation carried out to ensure clarity and clear and concise explanation provided.

3.4 Achieved Results.

The particle swarm optimization method was used to optimize extraction of power due to kinetic energy, hence increase power injected into the grid and ensure frequency stability and controlled rotational speed of the rotor and pitch angle to ensure faster restoration of the system to steady-state condition after a system frequency excursion as shown in Figure 3.1. It also ensured the pitch angle adjustment led to optimal input power of the turbine and limited variations in the pitch angle that could lead to abrasions within the turbine or further damage to mechanical parts of the turbine leading to additional costs and a complete system breakdown.

3.5 Chapter Conclusion

The employed research methodology in this research provided results that were concurrent with the research objectives. The results showed that the percentage wind penetration was limited to 32.1 % and the ROCOF worsened from zero to 33.33% because of the intermittent nature of the wind energy resource.

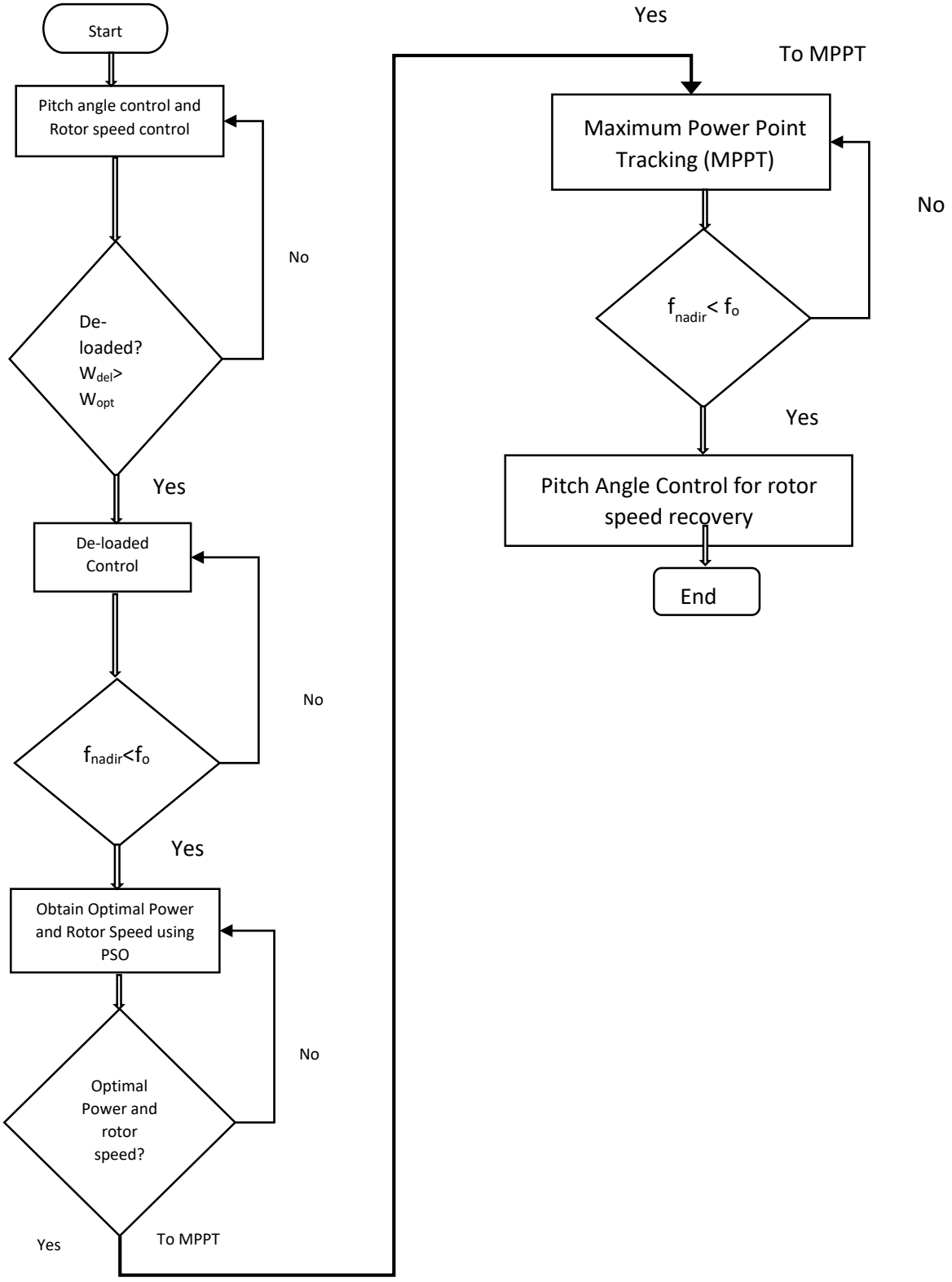

Figure 3.1: Flow Chart for Implementation of PSO Algorithm

CHAPTER FOUR

RESULTS AND ANALYSIS

4.1 Analysis and Statistics of Frequency Stability Control Schemes in the Presence of Wind Energy Sources.

4.1.1 Scenario I: Without Wind Farm connected to the Grid.

The IEEE 39 bus was modelled in MATLAB/Simulink environment and simulated in PSAT. The choice of simulation parameters were provided for as per IEEE 39 test bus data. The initial voltage guesses and lines power capacities were assumed. The PV bus parameter block was used and specifically power capacity in MVA was critical in the initialization of synchronous machines and Automatic voltage regulators (AVR).This parameter was gotten by trial and error and took a lot of time to guess the right value. The criteria used was to get a value that gives the least maximum error of convergence in the power flow iterations. In PSAT, power flow was executed first before time domain simulation was carried out. With the assumed values, the grid experienced voltage collapse in various buses and the Newton Raphson (NR) method did not converge and therefore carrying out time domain simulation was not achieved. This points to the fact that NR method fails to converge for large power system networks. There was also likely singular values pointing to infinity values during iteration. The base value for power was 100 MVA.

The statistics of the network were computed for the power flow using PSAT indicated in Table 4.1, Table 4.2 and Table 4.3.The power system layout in Simulink is displayed in Figure 4.1.

The NR has power mismatch calculations as shown in Table 4.1 and are quite small and falls outside tolerance values of 1E-05. I adjusted the power flow tolerance to 3E-05 but the NR did not converge. Therefore other methods have to be incorporated like using elements of the Jacobian matrix in normalized form [38]. The voltage values at various buses violated the limits and some buses had low voltages likely to trigger voltage collapse (total system blackout). Voltage collapse signals a system that is highly unstable in relation to voltage stability and overall power system stability.

The active power system loss accounted for 86.18% showing that the system was inefficient in Table 4.3. The line capacities need to be improved and more reactive power introduced into the grid to stabilize it. The reactive power losses accounted for 99.7%, quite a high value, explaining the need to add extra reactive power to compensate for active power losses. The

determinants of loading and losses should also be investigated to achieve optimal loading and minimize losses. This work was published as a paper [39].

Table 4.1: Scenario I - Output Results without a Wind Farm Connected to the Grid Using Simulation Approach

Network Statistics	Number
Buses:	39
Lines:	34
Transformers:	12
Generators:	10
Loads:	19
Solution Statistics	
Number of Iterations:	9
Maximum P mismatch [p.u.]	2.07096E-05
Maximum Q mismatch [p.u.]	2.97945E-05
Power rate [MVA]-Base Value	100

4.1.2 Scenario II: With one Wind Farm in the Grid.

The wind farm composed of 30 wind turbines with a capacity of 600 MVA while carrying out simulations using power system analysis toolbox. The power mismatch values increased marginally worsening the convergence criterion as shown in Table 4.4. The voltage profile showed changes in voltage magnitude at some buses to an improved value or a much lesser value while others remained constant values as shown in Table 4.5. It showed that wind turbine was a source of reactive power and hence helps inject some reactive power in the grid. The voltage at different buses increased to a higher value because of the presence of increased reactive power in the grid. The active power loss increased marginally to 88.6% while the reactive power loss remained constant at 99.7% when Table 4.3 and Table 4.6 were compared. Over extraction of energy from the rotating mass of wind turbines could cause it to become a load instead of a generator when it recovers to normal operation. The wind turbine therefore draws more current from the grid causing the voltage drop and increased losses.

Table 4.2: Magnitude and Phase Angle Profile of Power Parameters without a Wind Farm connected to the Grid

Bus	V	Phase	P Gen	Q Gen	P Load	Q Load
	[P.U.]	[Rad]	[P.U.]	[P.U.]	[P.U.]	[P.U.]
22	0.00	-67579.11	-2.86e-05	1.40e-05	0	0
24	0.60	-176.51	-36.26	24.11	1.02	-0.31
30	1.05	-350.14	0.26	5.21	0	0
31	0.98	0	1.41	8.07	0.37	0.18
32	0.91	-500.61	-3.10	2.25	0	0
33	1.00	-338763.66	3.39	18.04	0	0
34	1.01	-1.09e+12	1.13	19.04	0	0
35	1.05	-482588.19	0.78	15.68	0	0
36	0.98	-350.48	-0.05	4.13	0	0
37	1.03	-294.55	0.25	5.01	0	0
38	1.03	122.00	-4.25	0.11	0	0
1	0.00	-142.34	-2.43e-05	-3.32e-05	0	0
10	0.83	-72.23	-222.85	450.00	0	0

Table 4.3: Generation, Load and Losses from Power Flow without a Wind Farm

Total Generation	Quantity	Percent (%)
Real Power [P.U.]	346.59	
Reactive Power [P.U.]	3899.01	
Total Load		
Real Power [P.U.]	47.89	13.82
Reactive Power [P.U.]	11.56	0.30
Total Losses		
Real Power [P.U.]	298.69	86.18
Reactive Power [P.U.]	3887.45	99.70

The energy imbalance between generation and demand could also cause voltage drop and system losses in the system during displacement of conventional generators with wind farms in the grid. The tripping of wind farms during frequency events reduce generation causing an imbalance between generation and demand causing voltage drops and losses. The IEEE 39 bus

has fixed or constant loads in the network, the study focused on displacement of conventional generators only.

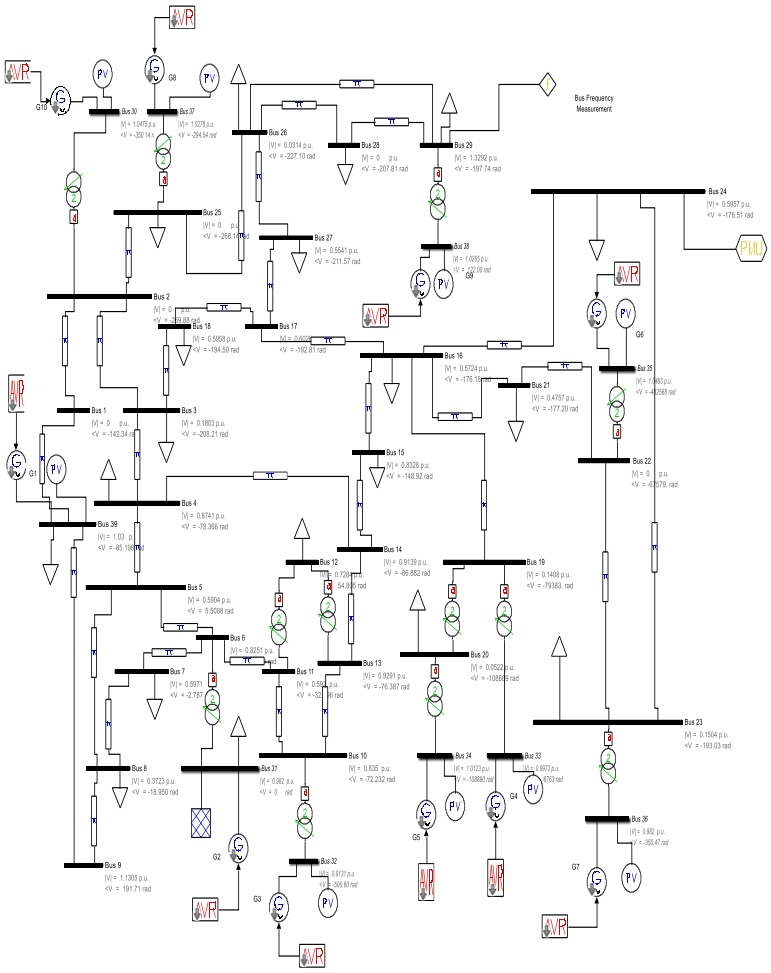

Figure 4.1: The Simulink diagram for IEEE 39 bus without a wind Farm.

The non-optimal and random placement of wind farms in the grid are also known to cause voltage drops and power losses in the grid. This requires further study on optimal placement of the wind farms in the grid to evaluate the performance on voltage profile and system losses.

The other major observations were that active power generated increased almost twice as reactive power generation. Active power generated increased by 34.7% while the reactive power generated increased by 17.8% when Table 4.3 and Table 4.6 were compared. The total active load reduced from 13.82% to 11.40% while reactive load reduced minimally from 30% to 29%. This points to the fact that the wind generator injects both active and reactive power

boosting the system voltage hence the active and reactive load drawn from the system drops. The Simulink power system layout is shown in Figure 4.2.

Table 4.4: Scenario II - Output Results for One Wind Farm Integrated in the Grid Using Simulation Approach

Network Statistics	Number
Buses:	39
Lines:	34
Transformers:	12
Generators:	9
Loads:	19
Solution Statistics	
Number of Iterations:	8
Maximum P mismatch [p.u.]	7.21584E-05
Maximum Q mismatch [p.u.]	7.5171E-05
Power rate [MVA]-Base value	100

Table 4.5: Magnitude and Phase Angle Profile of Power Parameters with One Wind Farm connected to the Grid

Bus	V	phase	P gen	Q gen	P load	Q load
	[p.u.]	[rad]	[p.u.]	[p.u.]	[p.u.]	[p.u.]
22	1.14	22.14	-20.50	118.26	0	0
24	0.00	30.99	2.27E-05	2.14E-05	0.00	-0.00
30	1.05	-35.66	-5.44	18.53	0	0
31	0.98	0	2.04	6.57	0.367	0.18
32	0.91	-176.06	-1.47	-0.55	0	0
33	1.00	18.58	0.87	17.33	0	0
34	1.01	45.84	2.34	-4.10	0	0
35	1.05	6.14	6.74	32.20	0	0
36	0.98	-108.22	5.47	3.66	0	0
37	1.03	0.81	14.26	9.72	0	0
38	1.03	131.83	2.98	5.20	0	0
1	0.00	6405843.33	-8.56E-05	-2.20E-05	0	0
10	1.05	81.87	333.33	496.97	0	0

4.1.3 Scenario III: With Two Wind Farms Integrated in the Grid.

The power mismatch values in Table 4.7 did not meet the convergence criterion of 1E-05 and were much worse compared to values in both Table 4.1 and 4.4. The wind farm located at bus 36 had a capacity of 600 MVA with 30 wind turbines while wind farm at bus 32 had 630 MVA with 30 wind turbines.

Table 4.6: Generation, Load and Losses from Power Flow with One Wind Farm.

Total Generation	Quantity	Percent (%)
Real Power [p.u.]	466.75	
Reactive Power [p.u.]	4593.08	
Total Load		
Real Power [p.u.]	53.23	11.40
Reactive Power [p.u.]	13.54	0.29
Total Losses		
Real Power [p.u.]	413.52	88.60
Reactive Power [p.u.]	4579.53	99.71

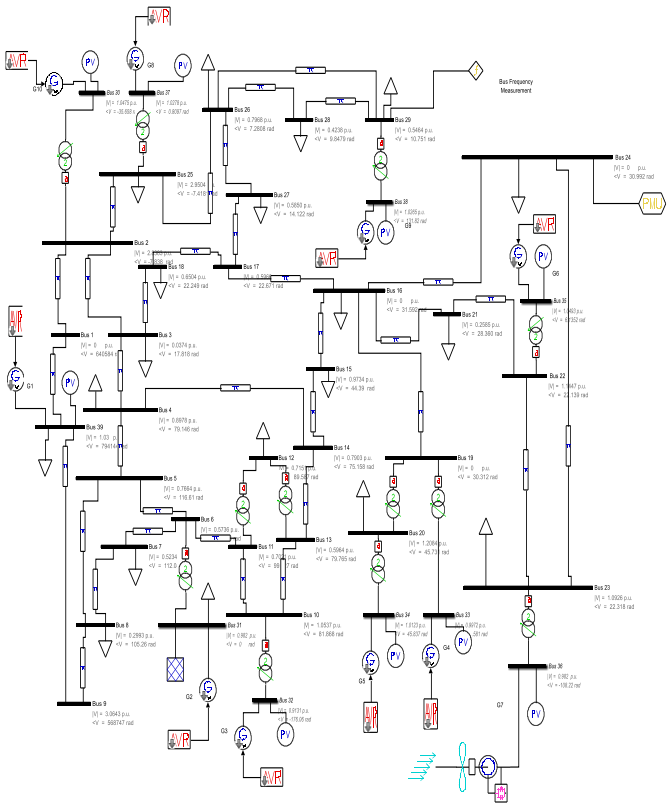

Figure 4.2: The Simulink diagram for IEEE 39 bus with one wind Farm.

Integrating individual wind turbines was not feasible because it was not possible to control the response required from each wind turbine. It is also complex to design controls for individual wind turbines and coordinate with others in the grid. Some buses like 10 and 24 in Table 4.8 had voltage overshoots while other buses the voltages were zero as others recorded normal voltage profiles within the tolerance limits. It implies there was over-generation at some buses while others experienced substantial voltage drops due to line limitations or excessive loading at the buses.

The total power generated, total losses increased to high values to orders 1*10^10 which were much worse and recorded values beyond the capability of the system to handle as shown in Table 4.9. However, the active power losses reduced to 72.85% while reactive power dropped marginally to 99.50%. It implies the wind turbines introduced extra reactive power into the grid thus reducing the system power losses. The Simulink power system layout is shown in Figure 4.3.

Table 4.7: Scenario III - Output Results for Two Wind Farms Integrated in Grid Using Simulation Approach.

Network Statistics	Number
Buses:	39
Lines:	34
Transformers:	12
Generators:	8
Loads:	19
Solution Statistics	
Number of Iterations:	7
Maximum P mismatch [p.u.]	1.253926881
Maximum Q mismatch [p.u.]	5.078144908
Power rate [MVA]-Base value	100

4.1.4 Scenario IV: With Five Wind Farms connected to the Grid

A total of five wind farms were connected one at a time until they reached five to ensure proper initialization of the DFIG because fixing the PV parameters would be complicated if done all at once and their rated capacities are shown in Table 4.10.

The active power mismatch values in Table 4.11 were higher compared to the previous values in Table 4.7. The reactive power mismatch was minimal. This is explained by the capability of wind turbines to consume or add extra reactive power into the grid thus compensating for the mismatch. The voltage profile for the sampled buses shows that bus 22 and 24 changed values as shown in Table 4.12. These buses could be weak buses as shown by their continuously high voltage volatility. The other buses relatively had constant values hence least affected by the wind integration.

Table 4.8: Magnitude and Phase Angle Profile of Power Parameters with Two Wind Farms connected to the Grid

Bus	V	phase	P gen	Q gen	P load	Q load
	[p.u.]	[rad]	[p.u.]	[p.u.]	[p.u.]	[p.u.]
22	0.02	91074618.93	0.24	1.39	0	0
24	2.10	91074621.54	279.43	-164.96	5.67	-1.69
30	1.05	15571672.78	-61.34	21.12	0	0
31	0.98	0	0.58	4.38	0.37	0.18
32	0.91	91074300.47	5.44	28.64	0	0
33	1.00	91074621.67	-1.86	45.74	0	0
34	1.01	91074627.34	4.86	11.71	0	0
35	1.05	91074619.72	1.04	15.40	0	0
36	1.00	91074536.13	0.25	4.96	0	0
37	1.03	15571526.4	0.25	5.01	0	0
38	1.03	4.38E+11	-1.09	7.39	0	0
1	0.00	293161383	0.00	-5.80E-05	0	0
10	6.00	91074743.6	11319.94	-778.61	0	0

The active power losses increased to 77.62% while reactive power losses reduced marginally to 99.46% as indicated in Table 4.13. This implies the wind turbines could be becoming loads drawing more current from the network thus increasing active power losses. As said earlier, they have reactive power production capabilities thus maintains the percentage of reactive power loss almost constant. The power system layout in MATLAB/Simulink is displayed in Figure 4.4.

Table 4.9: Generation, Load And Losses From Power Flow With Two Wind Farms Connected To The Grid.

Total Generation	Quantity	Percent (%)
Real Power [p.u.]	1.78E+11	
Reactive Power [p.u.]	1.41E+12	
Total Load		
Real Power [p.u.]	48363500829	27.15
Reactive Power [p.u.]	6479770651	0.46
Total Losses		
Real Power [p.u.]	1.30E+11	72.85
Reactive Power [p.u.]	1.40E+12	99.54

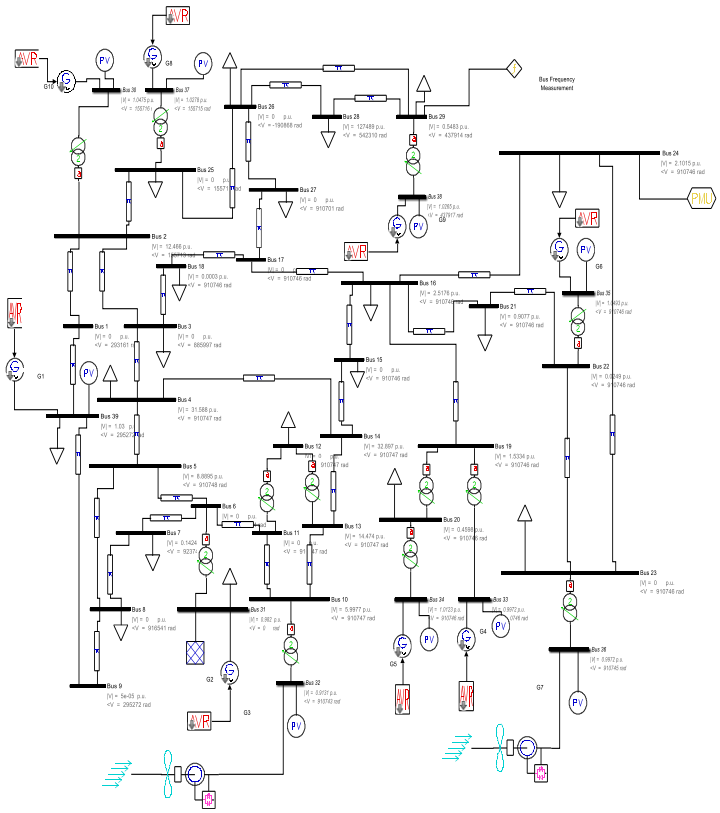

Figure 4.3: The Simulink diagram for IEEE 39 bus with two wind farms.

Table 4.10: Five Wind Farms with Rated Capacities and Number of Wind Turbines in Each Wind Farm.

Bus No	Wind Farm Capacity(MVA)	No of Wind Turbines in the Farm
32	630	30
36	600	30
37	500	30
38	900	60
39	100	30

4.2 Enhanced Frequency Stability Control Scheme using Particle Swarm Optimization Algorithm.

4.2.1 Case 1: Without Wind Farm Integrated in the Grid

The Newton Raphson algorithm was coded to run the load flow. The load flow and subsequent plotting of frequency response was done without connection of wind farms in the grid. It was presumed that bus 1 was the slack bus. While bus 31 to 39 were generator or PV buses. Solar generator was at bus 31. Steam turbine generators were found at buses 32, 33 and 34. Gas turbines were at bus 35, 36, 37 and Hydro Generators were at bus 38, 39 to portray the energy mix of an assumed power grid and the equivalent average system inertia. The assumed average inertia parameters were solar-0, steam turbine-6.5, Gas turbine-3.5, Hydro-3 and Wind-3.5 as tabulated by [12].

This inertia parameters were manually adjusted before running the particle swarm algorithm and newton Raphson pointing to the difficult in coding to automatically update the equivalent system inertia of each generator. The damping coefficient was set at 2 to minimize the oscillations in the rotor of the turbine before it settles [35].The voltage profile and frequency response results are shown in Figure 4.5 and 4.6. The other results for the active, reactive power injected profiles and voltage angle profiles are displayed in appendix B part 1 indicated in Figure 4.15, Figure 4.16 and Figure 4.17 respectively.

The voltage profile falls within the limits of 1±0.1 pu. Hence no violations of voltages were realised when a disturbance was introduced in the grid. The system frequency response also falls within 50±0.5 Hz, hence the system frequency is relatively stable. The other system parameters are as follows: settling time of 0.91673 sec, total system inertia H of 36 seconds and rate of change of frequency (ROCOF) had a value of 0.030389 Hz/sec.

From the results above, the system responded fast enough to address the dip in system frequency. The frequency nadir was 49.9963 Hz and fell within frequency threshold range.

The real and reactive power injected at bus 20 was -40 MW and -800 MVARs respectively. This implies that the demand exceeds the generation at this buses and excess demand must be met from other buses otherwise the grid might experience instability

Table 4.11: Scenario IV - Output Results for Five Wind Farm Integrated in Grid Using Simulation Approach

Network Statistics	Number
Buses:	39
Lines:	34
Transformers:	12
Generators:	6
Loads:	19
Solution Statistics	
Number of Iterations:	8
Maximum P mismatch [p.u.]	128.8572411
Maximum Q mismatch [p.u.]	2.4057E-05

The total active and reactive lines losses are 0.913 MW and 57.049 MVARs. This shows that the system is efficient in power delivery with active power losses accounting for less than 0.015% of the total active power generation and reactive losses at 0.1% of the total reactive power generation.

4.2.2 Case 2: With One Wind Farm Integrated in the Grid Using PSO

One wind farm consisting of 400 wind turbines was introduced at bus 39 to displace the 1000 MW hydro plant with randomly generated power of 1083.3214 MW without using the wind farm placement index. A disturbance was introduced in the system by changing the wind turbine rotor angle. The rotor speed of the wind turbine was optimized using particle swarm optimization algorithm. The voltage profile did not violate the limits as indicated in Figure 4.7. The optimal power coefficient point was set at 0.4535 within the Betz law limit of 0.59. The accompanying system parameters were settling time of 0.92946 sec, total system Inertia H of 36.5 sec and rate of change of frequency (ROCOF) was 0.029972 Hz/sec. The settling time increased because of increased system inertia and thus the ROCOF reduced by a small value

compared to the case without a wind farm of 0.030389 Hz/sec. It implies the wind turbine improved the system frequency response to the disturbance.

Table 4.12: Magnitude and Phase Angle Profile of Power Parameters with Five Wind Farms connected to the Grid

Bus	V	phase	P gen	Q gen	P load	Q load
	[p.u.]	[rad]	[p.u.]	[p.u.]	[p.u.]	[p.u.]
22	0.01	4540337.13	0.03	-0.07	0	0
24	0.00	4540284.63	3.53E-10	5.08E-10	1.42E-07	-4.24E-08
30	1.05	-525.23	-0.34	6.87	0	0
31	0.98	0	0.62	4.41	0.37	0.18
32	0.91	24638278.82	0.18	3.63	0	0
33	1.00	394741.47	6.37	23.05	0	0
34	1.01	394779.81	5.06	8.04	0	0
35	1.05	4540324.10	0.74	15.61	0	0
36	0.982	4540308.06	0.24	4.81	0	0
37	1.03	-505.29	0.25	5.01	0	0
38	1.03	-16592014.06	6.55	0.45	0	0
1	0.75	-252.33	27.42	12.87	0	0
10	0.00	307959.72	9.49E-08	-0.00	0	0

Table 4.13: Generation, Load And Losses From Power Flow With Five Wind Farms Connected To The Grid.

Total Generation	Quantity	Percent (%)
Real Power [p.u.]	263.51	
Reactive Power [p.u.]	3154.20	
Total Load		
Real Power [p.u.]	58.97	22.38
Reactive Power [p.u.]	17.18	0.54
Total Losses		
Real Power [p.u.]	204.54	77.62
Reactive Power [p.u.]	3137.01	99.46

The change in power which was the power consumed by infinite bus was calculated by setting power coefficients at 0.3617 and 0.4535.The difference in the resultant global best power determined the net power added by de-loaded wind farm with optimization of the rotor speed and pitch angle adjustment from 1 degree to zero degree at tip speed ratio of 7 and 8 respectively. The power coefficient values were derived from the function for calculating power coefficient as coded in MATLAB.

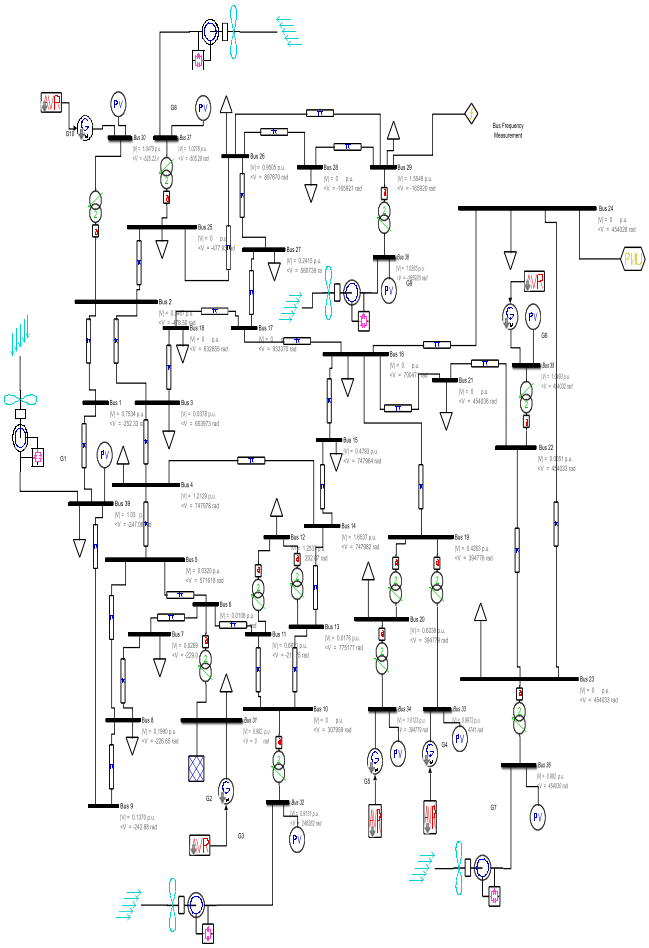

Figure 4.4: The Simulink diagram for IEEE 39 bus with five wind farms.

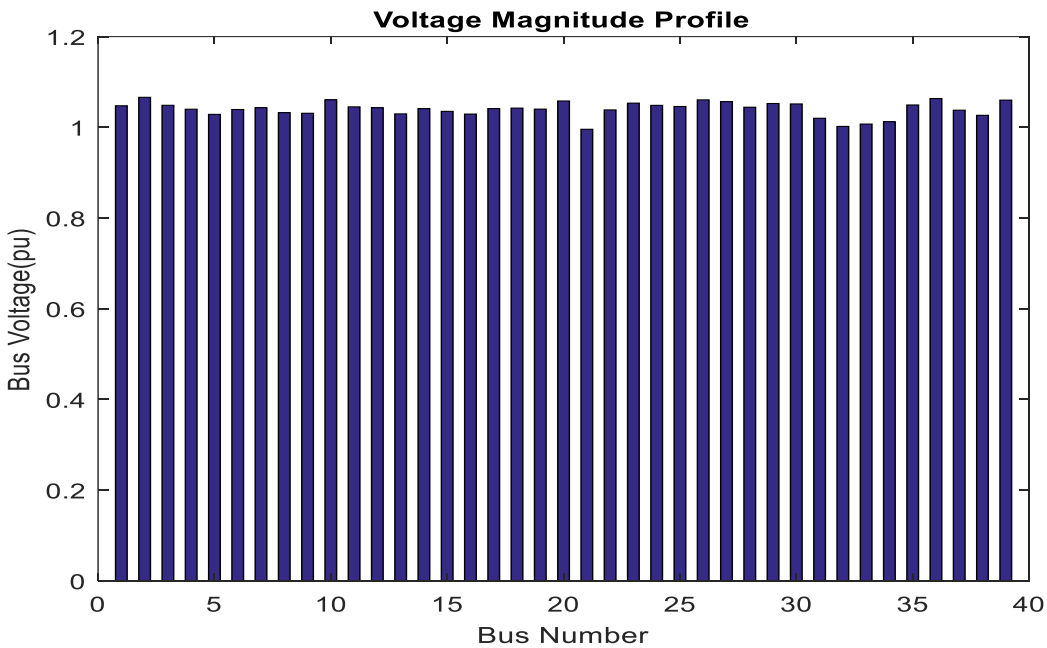

Figure 4.5: Voltage Magnitude Profile without Wind Farm in the Grid.

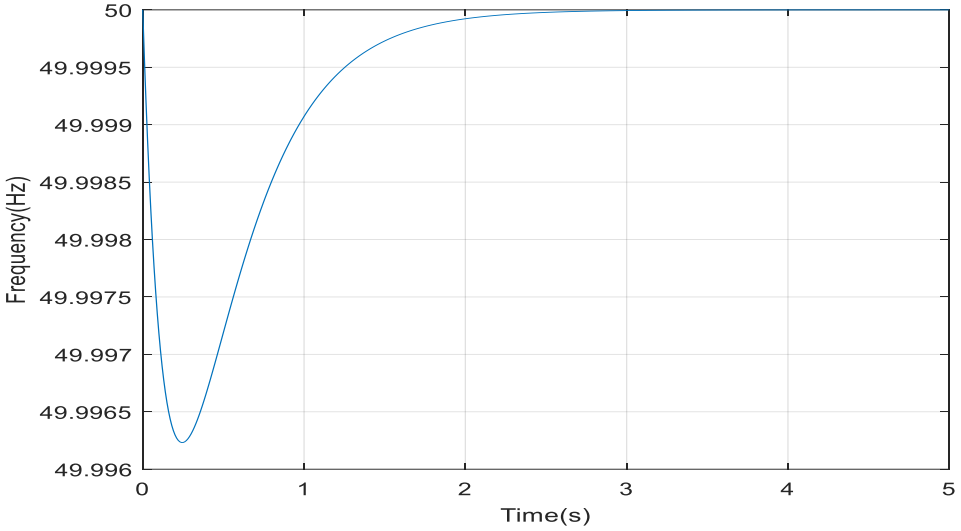

Figure 4.6: Frequency Plot with Disturbance without a Wind Farm.

In the de-loaded mode with power coefficient of 0.3617, the best global power was 917.2406 MW and running at maximum power point tracking with power coefficient of 0.4535 was 1083.3214MW. The percentage of wind power penetration in de-loaded mode was 15.24% of the total system generated power of 6018.7166 MW. This provided a power reserve margin of approximately 20.24 % based on de-loaded and optimal mode ratios which violates the standard practice of 15% of most utilities globally. This is because setting parameters such as the tip speed ratio to achieve 15% power reserve margin requires complex extrapolation calculations compromising accuracy of the derived values. The active power output from the wind farm keeps on fluctuating and this values are just a representative values that fall within a range of 1000±300 MW. The difference in power was 166.0808MW used as input to change in power to the infinite bus for plotting the frequency response curve as displayed in Figure 4.8. The frequency nadir was 49.9966 Hz showing an improved response from a previous case without a wind farm of 49.9963 Hz. The frequency response is also within the limits of 50±0.5Hz.

The system load was constant hence the total active and reactive power injections were also constant consequently losses as shown in Appendix B part 2 in Figures 4.18 and Figure 4.19. The voltage phase angle profile is shown in Figure 4.20.

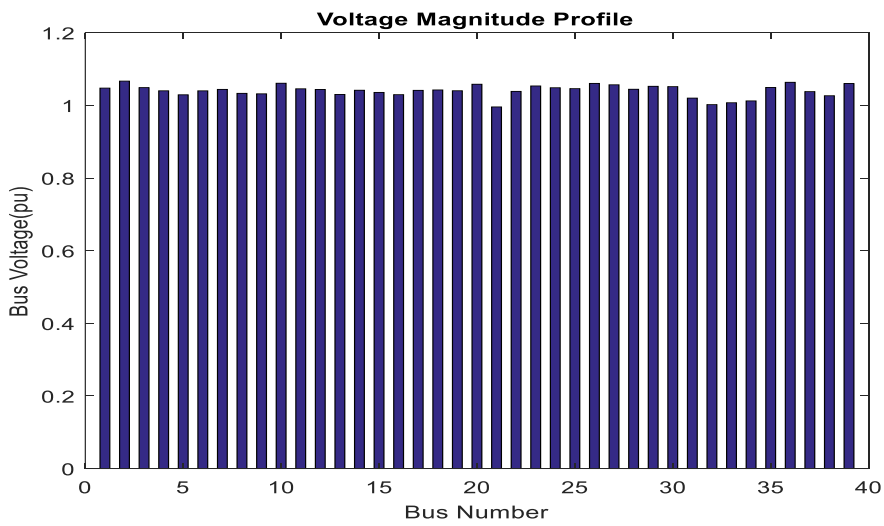

Figure 4.7: Voltage Profile with One Wind Farm in the Grid Using PSO

4.2.3 Case 3: With Two Wind Farms Integrated in the Grid Using PSO

Two wind farms were introduced at bus 39 and bus 34 at random. The wind farms had a total of 200 wind turbines at each bus The 508 MW generation of steam turbine at bus 34 was replaced with the second wind farm of total generation 539.0675 MW with optimal power coefficient of 0.4535. At power coefficient of 0.3617, the generated power was 463.8749 MW. Hence, the power injected into the grid was 75.1926 MW on system disturbance.

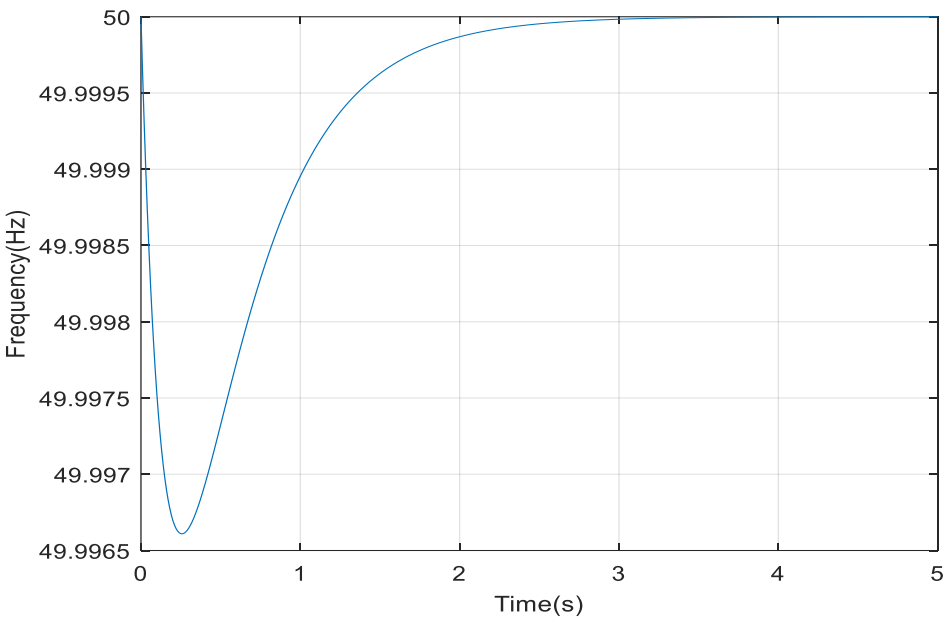

Figure 4.8: Frequency Response with One Wind Farm in the Grid Using PSO

Hence summing the net power injection from the two wind farms results to 150.3852 MW of power injected into infinite bus. The total power generated constitutes sum of wind power generated and conventional connected generating stations of 5521.2258 MW. The net wind power penetration in de-loaded mode integrated in the grid accounted for 16.80 % of the total generated power.

The voltage profile did not violate the limits as displayed in Figure 4.9. The active and reactive power injected and losses were constant because the loads were constant as in the previous cases. The other system parameters were settling time of 0.85307sec, total system inertia H of 33.5sec and rate of change of frequency (ROCOF) was 0.032656Hz/sec or 7.46%. The system inertia reduced because of the introduction of the two wind farms but the ROCOF increased marginally though the system still remained stable. The system frequency response increased to frequency nadir of 49.9965 Hz as shown in Figure 4.10. This implies that replacement of synchronous generators with wind turbines by introducing rotor angle disturbances, the system is able to overcome and stabilize as long as the capacities of the wind farms displacing conventional sources are closely matched.

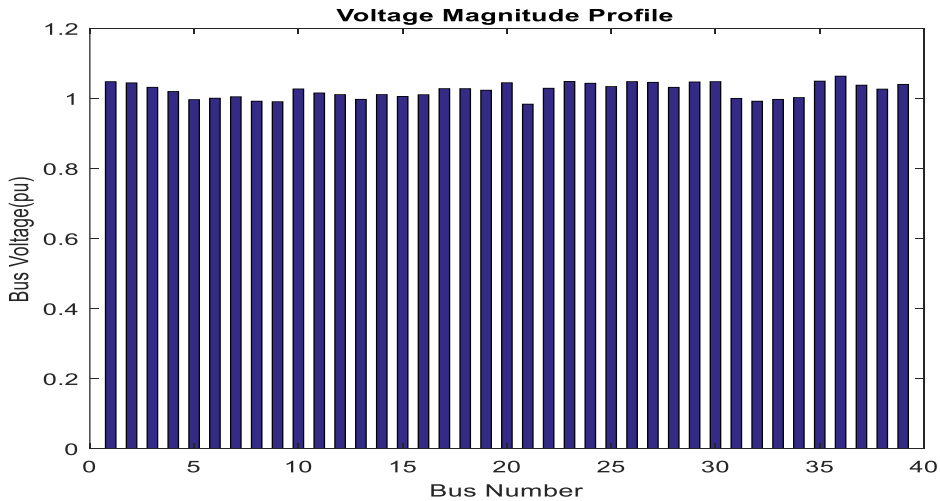

Figure 4.9: Voltage Profile with Two Wind Farms in the Grid Using PSO

4.2.4 Case 4: With Two Wind farms Integrated in the Grid and generator at bus 39 Tripped

Two wind farms with 200 wind turbines in each farm were introduced at bus 34 and 35 with each having total generation of 740.8843 MW with a maximum power coefficient of 0.4535 replacing the available steam and gas generators of capacities 508 MW and 650 MW

respectively. A power coefficient of 0.3617 gave 619.3998 MW of wind power output. The conventional displaced total generation was 1158 MW. This implied total generation increased to 6182.2756 MW. Hence the percentage penetration of wind accounted for 20.04 %.

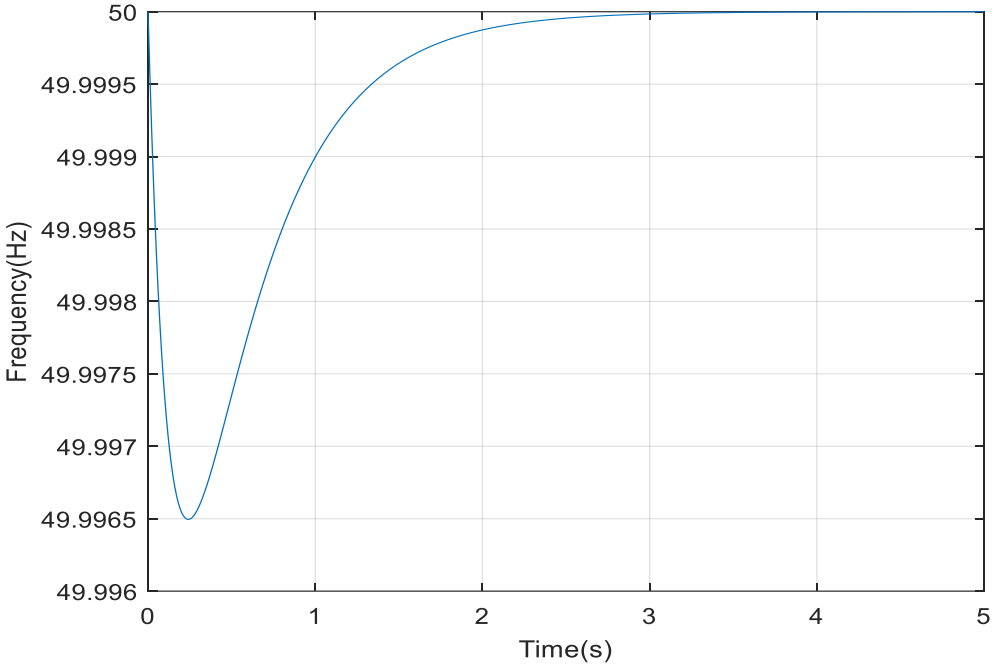

Figure 4.10: Frequency Response with Two Wind Farms Displacing Conventional Sources and Closely Matched Active Power Using PSO

The hydro turbine at bus 39 was tripped. The net injected power on a disturbance was 242.969 MW of wind power. The results showed that the voltage profile met the limits as found in Figure 4.11. The frequency response was within limits having a frequency nadir of 49.9971 Hz given an operating range of 50±0.5Hz shown in Figure 4.12. The system parameters were found to have settling time of 0.76394 sec, total system inertia H of 30 sec and rate of change of frequency (ROCOF) was 0.036466Hz/sec or 20%. The ROCOF increased marginally compared to case 3 with a ROCOF of 0.032656Hz/sec or 7.46%.

4.2.5 Case 5: With Two Wind farms Integrated in the Grid and generators at bus 38 and 39 Tripped.

The power wind farm was run using de-loaded method having power coefficient of 0.3617, the power system collapsed completely and the algorithm failed to run. In the optimal mode, with power coefficient of 0.4535 the system parameters were settling time of 0.68755sec, total

system inertia H of 27 sec and rate of change of frequency (ROCOF) was 0.040518Hz/sec or 33.33% and an active power generated from each wind farm of 756.45MW.

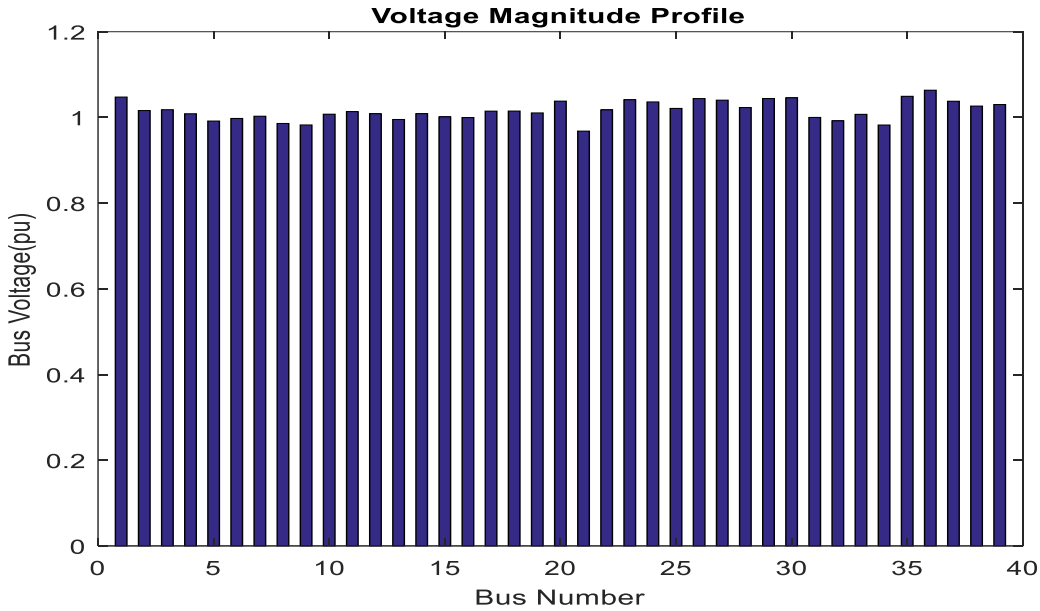

Figure 4.11: Voltage Profile with Two Wind Farms and bus 39 Generator Tripped

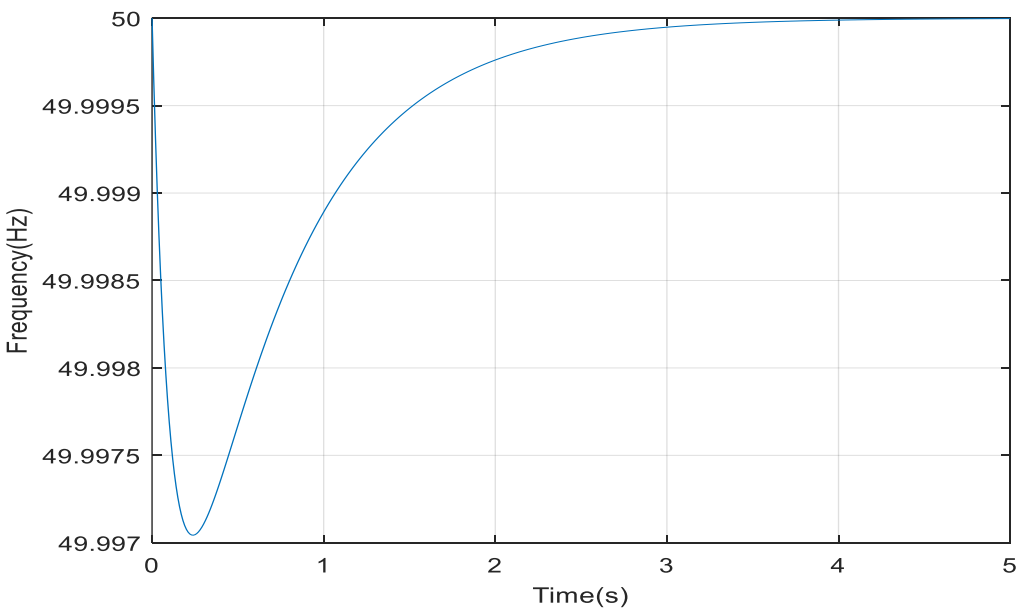

Figure 4.12: Frequency Response with Two Wind Farms and bus 39 Generator Tripped.

The active power output increased from 740.88 to 756.45 MW because of the wind intermittency. The voltage profile violated the limits as shown in Figure 4.13. Buses 5, 6,7,8,9 and 13 recorded values below 0.9 per unit voltage as in appendix C part 5. The power delivered

to the infinite bus was maintained at 222.8908 MW because the de-loaded mode did not operate. The total active power output was 1512.90 MW. The total generated power was 4716.376 MW. The percentage of wind penetration accounted for 32.08%. This points to the fact that wind farm penetration should not exceed 32.08 % of the total active power generation from conventional sources. The frequency response was stagnant with reduced generation from conventional sources as shown in Figure 4.14. The frequency nadir rose to 49.9968 Hz and the ROCOF increased to 0.040518Hz/sec as opposed to only one generator switched off with a ROCOF of 0.036466Hz/sec.

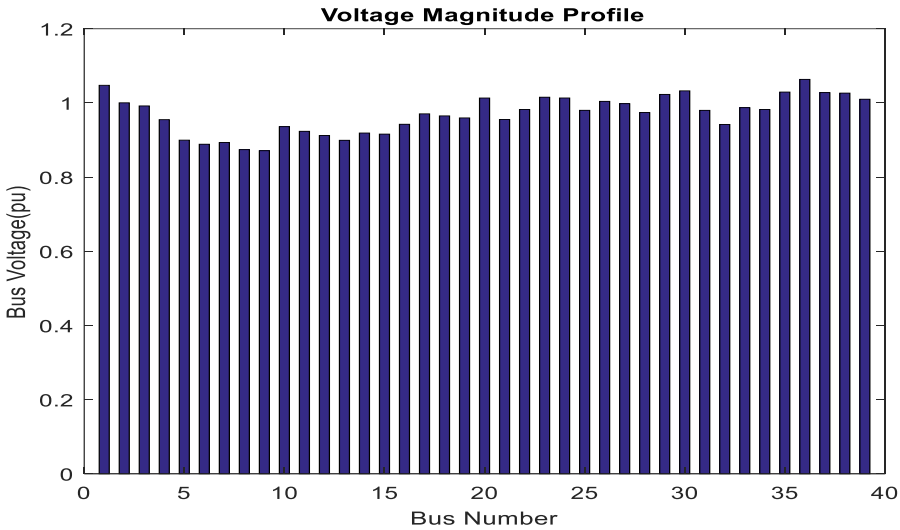

Figure 4.13: Two Wind Farms in the Grid with Two Generators at bus 38 And 39 Tripped.

The results in Table 4.14 show that the particle swarm improved the minimum frequency from 49.9963 Hz to 49.9971 Hz. The ROCOF however worsened from 0.030389 Hz/s to 0.040518 Hz/s an indicator of an unstable power system due to the uncertainty of the wind energy resource.

4.3 Validation of Particle Swarm Optimization with other existing Methods

There was a research done on a micro-grid which would not suffice as comparable results because of the type of grid that was selected in the study [37]. A grid is largely an expansive network compared to a micro-grid thus the results are incomparable. However, basic comparisons can be made on the methods employed during study of the two grids. Similar studies conducted on the grid before October 2019 could not be found but further research could establish comparable results for the study.

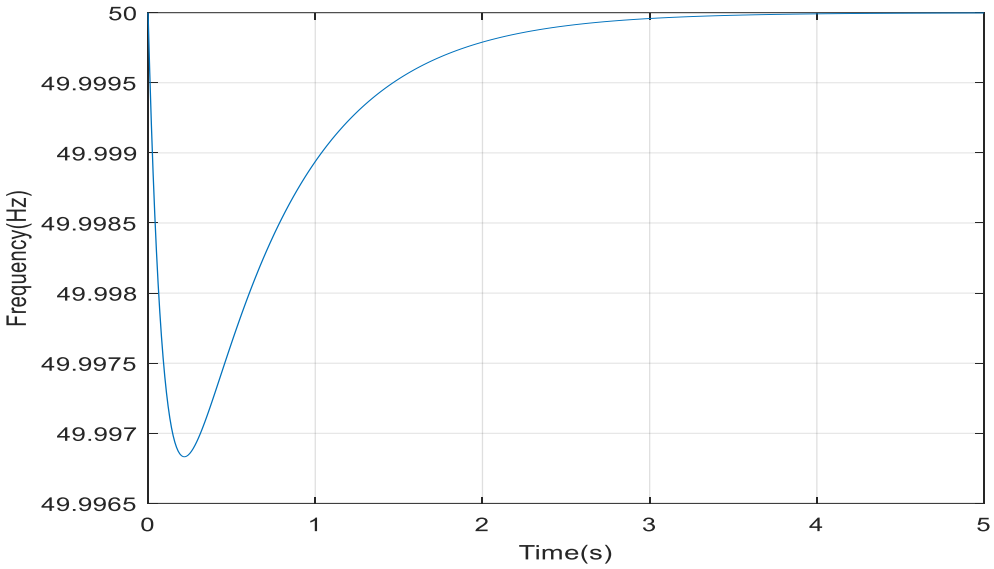

Figure 4.14: Frequency response of two wind farms with two generators at bus 38 and bus 39 Tripped.

He performed studies on a micro grid using pareto-dominance Multi-Objective PSO and attained a minimum frequency of 49.01 Hz from 48.31 Hz where there was no support to the system as shown in Table 4.14. He assumed a 20% wind penetration ratio in his study [37].From Table 4.14, it shows that frequency is more stable in a grid than a micro-grid based on the f_{nadir} values of 49.9963 Hz and 49.9963 Hz for the respective networks.

4.4 Chapter Conclusion

The Particle swarm optimization improved the grid frequency from 49.9963 Hz to 49.9971 Hz. The rate of change of frequency worsened from 0.030389 Hz/s to 0.040518 Hz/s due uncertainty of the wind energy sources.

The maximum percentage of wind power penetration was 32.08% beyond which the grid becomes unstable. The micro-grid is a weaker grid compared to the grid based on the minimum frequencies in both hence require an aggressive inertial response as opposed to the grid. In both the micro-grid and grid, inertial response and support is critical for the stability of the grid.

Table 4.14: PSO Results.

Case	No of Wind farms	Frequency (Hz)	ROCOF (Hz/s)	Voltage (pu)	Inertia (s)	Displaced Generators At Buses	Tripped generator	Settling time	Remarks
1	0	49.9963	0.030389	1±0.1	36	None	None	0.91673	Stable
2	1	49.9966	0.029972	1±0.1	36.5	39	None	0.92946	Relatively Stable
3	2	49.9965	0.032656	1±0.1	33.5	39,34	None	0.85307	Slightly Unstable
4	2	49.9971	0.036466	1±0.1	30	34,35	39	0.76394	System unstable
5	2	49.9968	0.040518	violated	27	34,35	38,39	0.68755	In optimal mode unstable/ In de-loaded mode does not operate.

Table 4.15: PSO Validation with other methods.

Micro-grid						**Grid**	
Parameter description	No Support	PD-1	PD-2	PD-3	PD-4	No Support	PSO
f_{nadir}(Hz)	48.31	49.01	48.90	48.57	48.83	49.9963	49.9971
ROCOF(Hz/s)	0.9016	0.9014	0.9014	0.9016	0.9017	0.030389	0.040518

CHAPTER FIVE

CONCLUSION AND RECOMMENDATIONS

The particle swarm optimization improved frequency response from frequency nadir of 49.9963 Hz without a wind farm in case 1 to 49.9971 Hz in case 4 by use of de-loaded mode but failed to execute in case 5 in the presence of wind energy sources. The ROCOF deteriorated from 0.030389 Hz/sec to 0.040518 Hz/sec. Hence, the rate of change of frequency (ROCOF) as a percentage was 33.33%. This shows that wind energy beyond the allowable penetration levels introduces instability in the grid even when optimized using particle swarm optimization. It was also established that when wind generation from wind farms exceeds the generation of conventional sources as a result of displacement at specific buses and hence the total load demand, the stability of the grid is maintained. The only hindrance is the cost of maintaining high reserve power that is idle on the grid as shown in case 2 and case 3.

This thesis also reviewed frequency stability control schemes with wind turbines integration using PSAT simulation tool in MATLAB/Simulink and has established that the tool is not sufficient to provide accurate results for IEEE 39 Bus system using time domain simulation. This therefore calls for further research using other simulation tools so as be able to provide more accurate results. It also points out that Newton Raphson method easily gets trapped in local optima and hence other methods either metaheuristic or numerical methods or IEEE 39 Bus data needs to be re-organized to overcome inability of Newton Raphson in conducting time domain simulation of wind farms in the grid.

The factors determining system inertia are influenced by the type of generator being displaced in the system as well for example steam turbines have average inertia of 6.5 seconds as opposed to wind turbines with average inertia of 3.5 seconds.

5.1 Further Research Work

There is need to develop algorithms to automate the compilation and coordination of wind power plants with the occurrence of disturbances in the grid. For example calculation of the power coefficient from rotor speed of the wind turbine and pitch angle should be done automatically without manual intervention. There is also a need to develop advanced methods for determining the tip speed ratio other than numerical methods to achieve accuracy in the results.

The intermittent nature of wind require optimization techniques to mimic uncertainty and predict variability and wind speed to develop sufficient and accurate algorithms for its operation and control to support frequency response.

The participation of wind turbines is tied to two parameters that are competing: faster frequency response and optimal power that seem to be competing parameters hence meeting the two objectives at the same time without compromise using the current technologies limits their efficiency and performance. For example, operating the wind turbine in de-loaded mode in order to support frequency response defeats the purpose for optimizing power.

The determinants of loading and losses to achieve optimal loading and minimize losses should be investigated. The optimal placement of wind farms in the grid need to be established to achieve an efficient and balanced generation-demand system.

A frequency detector needs to be developed to coordinate timing and extraction of power from the rotor of the wind turbine. It requires a complex algorithm to meet these requirements.

There is need for designing control methods suitable for making wind farms emulate synchronous generators in supporting frequency stability. The method used for calculation of equivalent system inertia used average values which may not be accurate in calculation of ROCOF and frequency response. There is need to develop methods for determining the sum contribution of system inertia from each wind farm.

The correlation between frequency and power imbalance seems to be at a lower level hence deriving the fish hook-shaped response is not straight forward and other advanced relationships must be developed to provide accurate results. The central finite difference method was used to estimate the change of rotor speed with time, there could be other available and better methods for differentiating the function.

REFERENCES

[1] G. Lalor, A. Mullane and M. O'Malley, "Frequency Control and Wind Turbine Technologies," *IEEE Transactions on Power Systems,* vol. 20, no. 4, 2005.

[2] N. Nguyen and J. Mitra, "Effect of Wind Power on Load Frequency Control," *IEEE Power and Energy Society General Meeting(PESGM),* pp. 1-5, 2016.

[3] H. T. Nguyen, G. Yang, A. H. Nielson and P. H. Jensen, "Frequency Stability Improvement of Low Inertia Systems Using Synchronous Condensers," *IEEE International Conference on Smart Grid Communications (SmartGridComm),* 2016.

[4] K. M. Abo-Al-Ez and R. Tzoneva, "Active Power Control(APC) of PMSG Wind Farm Using Emulated Inertia and Droop Control".

[5] N. Nguyen and J. Mitra, "An Analysis of the Effects and Dependency of Wind Power Penetration on System Frequency Regulation," *IEEE Transactions on Sustainable Energy,* vol. 7, no. 1, 2016.

[6] Y. Zhang, X. Liu and B. Qu, "Distributed Model Predictive Load Frequency Control of Multi-area Power System with DFIG," *IEEE/CAA Jounal of Automatica Sinica,* vol. 4, no. 1, 2017.

[7] W. M. S. P. Limited, "Wind Sector Prospectus-Kenya," Nairobi, 2013.

[8] W. Stevenson, Elements of Power System Analysis, 4th ed., I. S. Edition, Ed., London: Mcgraw-Hill Publishing Company, 1982.

[9] D. P. Kothari and I. J. Nagrath, Modern Power System Analysis, New Delhi: Tata Mcgraw Hill Education Private Ltd, 2003.

[10] A. M. Garcia, I. Munoz-Benavente, A. D. Hansen and E. G. Lazaro, "Demand-Side Contribution to Primary Frequency Control with Wind Farm Auxiliary Control," *IEEE Transactions on Power Systems,* vol. 29, no. 5, 2014.

[11] M. F. Arani and Y. A.-R. I. Mohamed, "Analysis and Impacts of Implementing Droop Control in DFIG-Based Wind Turbines on Microgrid/Weak-Grid Stability," *IEEE Transactions on Power Systems,* vol. 30, no. 1, 2015.

[12] L. Shang, J. Hu, X. Yuan and Y. Chi, "Understanding Inertial Response of Variable-Speed Wind Turbines by Defined Internal Potential Vector," *Energies,* December 2016.

[13] M. P. Musau and T. L. Chepkania, "Under Frequency Under Voltage Load Shedding with Renewable Energy Storage:A Proposed Case Study of the Kenyan Grid," *IEEE PES AFRICA ,* 2017.

[14] H. Chamorro, M. Ghandhari and R. Eriksson, “Wind Power Impact on Power System Frequency Response,” *North American Power Symposium,* 2013.

[15] L. o. Kenya, “Energy Act,” National Council for Law Reporting, Nairobi, 2006.

[16] K. e. al, “Definition and Classification of Power System Stability,” *IEEE/CIGRE Joint Task Force on Stability Terms and Definitions, IEEE Transactions on Power Systems,* vol. 19, no. 2, 2004.

[17] M. Altin, "Dynamic Frequency Response of Wind Power Plants," *Ph.D. Dissertation,Dept.Energy.Tech,Aalbg Univ.,* November 2012.

[18] Z. Ya-Min and X. Jia-Dong, “Application of particle swarm optimization for the design of a broadband microstrip antenna,” *International Conference on Computer Application and System Modeling,* 2010.

[19] M. R. AlRashid, M. F. AlHajri and A. K. Al-Othman, “Particle Swarm optimization and its Applications in Power Systems,” in *Computational Intelligence in Power Engineering,* Kuwait, 2010, pp. 295-324.

[20] M. R. AlRashidi and M. E. El-Hawary, “A survey of Particle Swarm Optimization Applications in Electric Power Systems,” *IEEE Transactions on Evolutionary Computation,* 2006.

[21] W. Qiao, G. K. Venayagamoorthy and R. G. Harley, “Design of Optimal PI Controllers for Doubly Fed Induction Generators Driven by Wind Turbines Using Particle Swarm Optimization,” *International Joint Conference on Neural Networks,* 2006.

[22] Y. d. Valle, G. K. Venayagamoorthy, S. Mohagheghi, J.-c. Hernandez and R. G. Harley, “Particle Swarm Optimization: Basic concepts,Variants and Applications in Power Systems,” *IEEE Transactions on Evolutionary Computation,* vol. 12, no. 2, 2008.

[23] M. W. Hansen, R. Josefsson and H. Mehmedovic, *Frequency Controlling Wind Power,Modelling of Control Strategies,* Stockholm: Unpublished, 2012.

[24] M. Hwang, E. Muljadi, G. Jang and Y. C. Kang, “Disturbance-Adaptive Short-Term Frequency Support of a DFIG Associated with the Variable Gain Based on ROCOF and Rotor Speed,” *IEEE Transactions on Power Systems,* vol. 32, no. 3, May 2017.

[25] P.-K. Keung, P. Li, H. Banakar and B. T. Ooi, “Kinetic Energy of Wind-Turbine Generators for System Frequency Support,” *IEEE Transactions on Power Systems,* vol. 24, no. 1, February 2009.

[26] P. Li, W. Hu and Z. Chen, “Review on Integrated-Control Method of Variable Speed Wind Turbines Participation in Primary and Secondary Frequency,” *Industrial Electronics Society,,* 2016.

[27] I. Erlich and M. Wilch, “Primary Frequency Control by Wind Turbines,” *IEEE PES General Meeting,* 2010.

[28] A. Zertek, G. Verbic and M. Pantos, “Optimised Control Approach for Frequency Control Contribution of Variable Speed Wind Turbines,” *Institution of Engineering and Technology Renewable Power Generation,* 2011.

[29] A. Kalmikov, K. Dykes and K. Araujo, “Wind Power Fundamentals,” Massachusettes.

[30] M.-K. Kim, “Optimal Control & Operational Strategy for Wind Turbines Contributing to Grid Primary Frequency Regulation,” *Applied Sciences,* 2017.

[31] F. Milano, Power System Analysis Toolbox, Genova: Free Software Foundation, 2008.

[32] F. Milano, “A Brief Introduction to the Power System Analysis Toolbox (PSAT) for Power System Analysis Undergraduate Courses,” [Online]. Available: http://faraday1.ucd.ie/archive/psat/brieftutorial.pdf.

[33] F. Milano, “An Open Source Power System Analysis Toolbox,” *IEEE Transactions on Power Systems.*

[34] Z. Beheshti and S. M. Shamsuddin, “A Review of Population-based Meta-Heuristic algorithm,” *International Journal of Advanced Software Computing and Applications,* vol. 5, no. 1, 2013.

[35] P. M. Musau, B. O. Ojwang and M. Kiprotich, “Improving Frequency Stability for Renewable Energy Power Plants with Disturbances,” in *IEEE PES GTD Asia,* Asia, 2019.

[36] Y. Wang, G. Li and Y. Lai, “Calculating of Reactive Power Compensation Capacity in Wind Farms Based on Chance Constrained Programming,” *IEEE,* 2013.

[37] F. Hafiz, A. K. Swain, N. Patel and A. K. Kar, “Shaping Inertial Response from Wind Turbines: A Multi-Objective Approach,” *IEEE Transactions,* 2016.

[38] D. P. Kothari and I. J. Nagrath, Modern Power system Analysis, New Delhi: Tata McGraw Hill Education Private Ltd, 2003.

[39] T. L. Chepkania, M. P. Musau and C. W. Wekesa, “Review of Frequency Stability Control Schemes in the Presence of Wind Energy Sources,” in *IEEE AFRICON,* Accra, 2019.

[40] G. Lalor, A. Mullane and M. O'Malley, “Frequency Control and Wind Turbine Technologies,” *IEEE Transactions on Power Systems,* vol. 20, no. 4, 2005.

[41] Z. Chen, “Issues of Connecting Wind Farms into Power systems,” *IEEE/PES Transmission and Distribution Conference & Exhibition:Asia and Pacific,* 2005.

[42] H. Chamorro, M. Ghandhari and R. Eriksson, “Wind Power Impact on Power System Frequency Response,” *North American Power Symposium,* 2013..

[43] P. Li, W. Hu and Z. Chen, “Review on Integrated-Control Method of Variable Speed Wind Turbines Participation in Primary and Secondary Frequency,” *Industrial Electronics Society,,* 2016.

[44] P. M. Anderson and A. A. Fouad, Power System Control and Stability, IOWA: Galgotia Publications, 1984.

[45] J. Zhao, X. Lyu, Y. Fu, X. Hu and F. Li, "Coordinated Microgrid Frequency Regulation Based on DFIG Variable Coefficient Using Virtual Inertia and Primary Frequency Control," *IEEE Transactions on Energy Conversion,* vol. 31, no. 3, 2016.

[46] I. Erlich and M. Wilch, "Primary Frequency Control by Wind Turbines," in *IEEE PES General Meeting,* 2010.

[47] Mathworks, "Matlab," Matlab, 2019. [Online]. Available: https://www.mathworks.com/help/matlab/ref/function.html. [Accessed 10 July 2019].

APPENDIX B

Published Works.

Review of Frequency Stability Control Schemes in the Presence of Wind Energy Sources

Terry .L. Chepkania[1], Peter .M. Musau[2], Cyrus .W. Wekesa[3]
Department of Electrical and Information Engineering
The University of Nairobi
Nairobi, Kenya
tchepkania@students.uonbi.ac.ke[1],pemosmusa@uonbi.ac.ke[2],cwekesa@uonbi.ac.ke[3]

***Abstract*—Renewable energy sources have become a major area of interest for governments and utilities world-wide. They not only promote use of clean energy but also ensure a friendly and healthy living environment. As a result, large integration of renewable energy into the grid has become common and is growing fast. However, this rapid development has realized drastic and insurmountable challenges. The stability of the power system is compromised because renewable energy sources do not provide system inertia. The inadequacy or lack of system inertia lead to increased system frequency excursions and henceforth frequency instability. Wind energy resource development has seen unprecedented scales of growth and has also been adversely affected by frequency instability especially in isolated power systems. Research has shown that isolated or weak grids not supported by system inertia experience more instability. Most researchers therefore concentrated on finding solutions to the isolated power systems. However, large scale integration of renewables imply conventional sources of energy will be displaced and frequency instability problems would also occur in the grid. There are many frequency control methods utilized at different levels to stabilize the power system. The three levels are inertia, primary and secondary frequency response based on time of the response. This research paper investigates frequency stability with wind energy sources using IEEE 39 bus test system. It is modelled in MATLAB/Simulink and simulated by power system analysis toolbox. The results show huge power system losses and power mismatch values. In conclusion the toolbox is not sufficient to simulate and analyze the grid with the provided IEEE 39 bus data.**

***Index Terms* - frequency instability, renewable energy sources, and power system stability.**

I. INTRODUCTION

The continued interest in the development of renewable energy has seen unprecedented growth in the energy sector. Renewable energy has innumerable benefits with accompanying economic, social, environmental and technical challenges. Renewable energy has been touted as the most economical source of energy compared with fossil-fuelled generators. It is relatively less costly compared to conventional energy sources and does not support carbon emissions, promotes fuel security and energy diversity [40].The use and depletion of fossil-fuel reserves has rekindled interest in renewable energy that would offer a long-term solution to the biting pollution problems and consequent health related complications. It has been found that reduction of carbon dioxide emissions decreases effects of global warming [41].

The benefits accrue with reminiscent problems. On the economic front, it has been found that most of these renewable energy sources occur in areas that are less or least densely populated. As a result, the cost of evacuation of power by constructing long transmission overhead lines or offshore submarine cables to the on shore has been a challenge. Socially, areas inhabited by population are forced to relocate to pave way for transmission line construction and even establishment of the plants. It has also resulted in death of some rare birds in locations where wind turbines have been installed. Environmentalists have even initiated legal actions against setting up of plants of these nature that have killed the rare species of birds in some countries.

The main focus has been the technical constraints related to tapping of renewable energy. Many researchers have said that renewable energy sources contribute less or do not support the system inertia and affect frequency stability after large system disturbances, hence the stability of the power system is compromised [40]- [41]. They have also delved further and concluded that islanded grids would suffer most in terms of frequency instability where conventional power plants are not many enough to contribute to total system inertia [40]- [3].

The area of research interest has been how to provide the system inertia either synthetically or naturally. There are various methods that have been proposed to address the problem of system inertia. External mechanisms have been proposed such as renewable energy storage systems. These are methods where the deficiency in demand or loss of generation is met by use of remedial energy storage systems [4]. The methods have been found viable only that they increase investment cost in establishment of the renewable energy plants.

Internal or natural methods have also been proposed and seem more viable to address the issue with more challenges related to operation and control, system stability and quality of power [4]. They eliminate the additional cost of setting up storage systems more like a parallel plant to support system inertia.

The power system frequency control has three stages: Inertial response, primary control and secondary control. Inertial frequency response extracts kinetic energy from rotating masses to limit frequency excursion from the scheduled frequency value. Primary frequency control activates the generator governors to keep frequency deviation within acceptable levels. Secondary frequency control, on its part restores the frequency to its scheduled frequency and restores used reserves to their initial values [41].

The methods used for frequency control and stability studies included inertial frequency controls. This method resulted into excessive extraction of kinetic energy and led to slower recovery of the rotor speed to a stable operating range [5]- [6].The only advantage is that it provided frequency support in case of a system frequency excursion to some degree. Primary frequency control using automatic droop control method does not participate in rate of change of frequency (ROCOF) [7].

Doubly-fed induction generators, full power converter wind turbines and permanent magnet synchronous generators are the common variable speed wind turbines currently in use on large scale [45]. The single functional control methods utilized in these turbines include rotor speed control that only operates within the designed and rated wind speed range. The pitch angle control has a slow-speed response to support frequency dips and works better under partly loaded-mode of the wind turbine [5].

This paper is organised as follows: Section II delves into frequency control schemes with wind energy, problem formulation of power extraction from wind turbine is covered in Section III. Section IV provides the IEEE 39 Bus test system model in MATLAB/Simulink environment and simulated by Power System Analysis Toolbox (PSAT). Result Analysis and Discussions are done in section V and finally conclusion is given in section VI.

II. FREQUENCY CONTROL SCHEMES WITH WIND ENERGY

A. Inertial Frequency Control

Altin [9] investigated the requirements for synchronised power support and inertial response of wind power plants in high wind penetration scenarios. He considered a generic power system model and a generic wind power plant model implemented in RMS toolbox with different percentage levels of wind power penetration. He proposed a new inertial response control for wind power plants considering the inertial requirements for the generic power system. He carried out sensitivity analysis of the inertial response gain for 40% and 50% penetration levels and found reduced frequency deviation for penetration levels below 40%. He also did sensitivity analysis for variable droop gain from 5-10 p.u. value at 40%-50% penetration levels and found out that 40% penetration level produced an improved minimum frequency value.

Erlich et al. [7] proposed two methods for kinetic energy extraction control strategy. He said it was only suitable for short periods and kinetic energy was dependent on rotor speed and inertia of the rotor. He introduced a lead lag compensator to improve frequency response and named it KEC I. in the second method KEC II, he delayed release of kinetic energy and increased the rotor speed by reducing power output of the wind turbine. The deceleration of rotor speed implies increase power output from the wind turbine. Then the wind turbine was set to operate optimally and rotor re-accelerates.

B. Primary Frequency Control

Nguyen and Mitra [11] studied the effect of wind power on load frequency control. They implemented a mathematical model for one area control in MATLAB/Simulink for load frequency control in the presence of wind energy. Their simulated results showed that increasing wind penetration levels worsened frequency deviation from 0.14 Hz to 0.32Hz due to reduced system inertia and higher frequency regulation constant. In an interconnected system the maximum frequency deviation was from 0.075Hz to 0.125 Hz where in both stand-alone and interconnected system inertia reduction ranged between 0% and 60%. The frequency recovery also worsened with presence of wind energy sources in the grid. They established that maximum tie line power increased and area control error (ACE) reduced in an interconnected system. They recommended a 30% wind penetration level based on system configuration, maximum predicted load

level of 0.04 p.u. and safe frequency deviation range of ±0.2 Hz.

Zertek et al. [12] came up with a novel control strategy aimed at maximizing kinetic energy and optimising jointly the rotor speed and pitch angle using differential evolution. They simulated four scenarios while accounting for power reserve margins in the computations. The first case was where the pitch angle was maintained at zero degrees until maximum speed was reached. The minimum frequency was achieved 7 seconds after frequency drop. In the second case where an additional df/dt loop was introduced, it attained 10 seconds from the frequency-time plots. The proposed control approach as the third option, gave a 13 seconds frequency drop delay. Hence translating to almost 100% delay compared to the first method. He concluded that the new control strategy extracted more kinetic energy at same de-loaded power compared to existing approaches. He only considered a single line diagram consisting of an aggregated load, thermal plant and Doubly Fed Induction Generator wind turbine (DFIG WT).

C. Secondary Frequency Control.

Secondary frequency response refers to a situation where power increase or decrease of generators is realised by commands from transmission system operator (TSO).In addition to automatic generation control (AGC), Li et al. [26] also said that rotor speed and pitch angle control were still suitable for secondary frequency control. He stated that both pitch angle and rotor speed control run the VSWT in de-loaded mode to be able to offer frequency support in case of frequency excursions. The wind turbines standard methods of frequency control were absent and effective approaches for dealing with a specific system must be designed [26].

In summary, the frequency control methods for variable speed wind turbines are many and vary depending on desired power output of the wind turbines. These methods also indicate that researchers are yet to develop a robust, optimal and standardised method for supporting system inertia of the grid in the event of frequency excursions.

III. PROBLEM FORMULATION

From the swing equation, the accelerating torque T_a is given by [14],

$$J\dot{W} = T_a \tag{1}$$

Where:

$\dot{W}$ is average angular acceleration in radians/second squared (rad/s^2), J is rotor moment of inertia in Kg-m^2, Ta is accelerating torque in N.M.

$$T_m - T_e = T_a \tag{2}$$

T_m is the driving mechanical torque and T_e is the retarding electrical torque.

We also know that Power, P is given by

$$P = TW \tag{3}$$

Where:

T is torque in N.M and W is angular velocity in rad/s.

However, kinetic energy is given by

$$GH = \left(\frac{1}{2}\right)(J * W^2) \tag{4}$$

Hence,

$$\Delta P = Ta * W = J\dot{W} * W. \tag{5}$$

$$\Delta P = (2GH * \dot{W})/W \tag{6}$$

Inertia response is achieved by extraction of kinetic energy

$$GH = \frac{0.5\Delta P * W}{\dot{W}} \tag{7}$$

Then,

$$\frac{dW}{dt} = \frac{0.5\Delta P * W}{GH} \tag{8}$$

Similarly,

For a synchronous machine as derived from [15],

$$\frac{df}{dt} = \frac{\Delta P * f_0}{2 * GH} \tag{9}$$

Where:

ΔP is the change in power, f_0 refers to the nominal frequency, $\frac{df}{dt}$ is the rate of change of frequency (ROCOF), G is rated apparent power, H is inertia time constant, K is number of machine poles. Therefore, to determine, the frequency deviations Δf, it is given by,

$$\Delta f = f_0 - f_{nadir} \tag{10}$$

$$\Delta f = f_0 - [(2GH * \frac{df}{dt})/\Delta P] \tag{11}$$

To extract maximum kinetic energy, we should maximize the deceleration of the rotor. Hence, min $\frac{df}{dt}$ and min Δf.

The wind power of the wind turbine is derived as shown in equation 12 from [16].

$$P_w = \frac{1}{2}\rho * A * V^3 \quad (12)$$

The blades swept area is given by

$$A = \pi R^2 \quad (13)$$

Where:

P_w is wind power, ρ is air density and V is wind speed in metres/second (m/s).

The efficiency in extraction of power is given by the wind power coefficient (C_p), ratio of power extracted by the turbine (P_t) to the total wind power (P_w).

$$C_p = \frac{Pt}{P_w} \quad (14)$$

Where:

$$P_t = \frac{1}{2} * \rho * A * V^3 * C_p \quad (15)$$

According to [45], [12] the wind power coefficient is given by:

$$C_p = C_1\left(\frac{C_2}{\lambda_i} - C_3\beta - C_4\right)e^{\frac{C_5}{\lambda_i}} + C_6\lambda_i \quad (16)$$

$$C_p = 0.5 * (\frac{116}{\lambda_i} - 0.4\beta - 5)e^{\frac{-21}{\lambda_i}} \quad (17)$$

Where:

$$\lambda = \frac{RW_r}{V} \quad (18)$$

$$\frac{1}{\lambda_i} = \frac{1}{\lambda + .08\beta} - \frac{0.035}{\beta^3 + 1} \quad (19)$$

Where λ is the tip speed ratio of variable speed wind turbine (VSWT);W_r is the rotational speed of wind turbine; R is radius of the impeller; β is the pitch angle.

C_1 -C_6 are constants representing the characteristics of specific wind turbines.

Considering primary power reserve margin, and loading the turbine at 85%, then

$$P_{opt} \geq 0.85P_{opt} + \Delta Pke \quad (20)$$

$$\Delta Pke \leq 0.15P_{opt} \quad (21)$$

Ignoring windage, iron and frictional losses,

$$P_G = P_t \quad (22)$$

P_G is total generated electrical power in MW,Pt is total turbine power equal to total mechanical power

According to [17], the accelerating power is given by

$$JW_r\dot{W}_r = P_{in} - (P_{ref} + \Delta Pke) \quad (23)$$

W_r is mechanical rotational speed,ΔPke is change in power due to kinetic energy, P_{opt} is optimal power of the generator in MW,
P_{ref} is reference power and P_{in} is mechanical input power.

The power imbalance will be catered by the difference between the input power and power extraction from de-loaded mode due to deceleration of the rotor speed to counter frequency drop. Ignoring variable and fixed losses in the Variable Speed Wind Turbine

$$\Delta Pke = P_{in} - \sum_{k=1}^{n}(JW_{del}\frac{\dot{W}_{del}}{dt}) \quad (24)$$

Taking into consideration a wind farm with reference to equation (25), then maximize the extraction of accelerating power from the wind turbine. Since the reference power is a constant, P_{ref}, then considering a maximum power point tracking (MPPT) curve has maximum and minimum rotor speeds in de-loaded mode.

$$Max\ \Delta Pke = Max\ \{\sum_{k=1}^{n}(P_{in} - JW_{del}\frac{\dot{W}_{del}}{dt})\} \quad (25)$$

The wind farm power output, according to [17] is given by,

$$P_{ref,wf} = \sum_{k=1}^{n} P_{del,k} = \sum_{m=1}^{n} 0.85P_{opt,k} \quad (26)$$

The objective function will be

$$Max\ \Delta Pke = Max\ \left\{\sum_{k=1}^{n}\left(P_{in,k} - JW_{del,k}\frac{\dot{W}_{del,k}}{dt}\right)\right\} \quad (27)$$

Subject to the constraints:

$$\text{Total } \Delta Pke \leq 0.15 \text{ Total } P_{opt}$$

$$P_{ref,wf} = \sum_{k=1}^{n} P_{del,k} = \sum_{k=1}^{n} 0.85P_{opt,k}$$

$$P_{min} \leq P_{del} \leq P_{max}$$

$$W_{del,min} \leq W_{del} \leq W_{max}$$

$$\beta min \leq 0 \leq \beta\ max$$

$$C_p \leq 0.59$$

IV. SIMULATION APPROACH

In order to achieve the objectives of this research, IEEE 39 Bus test system was modelled in MATLAB/Simulink and simulated by power system analysis toolbox (PSAT).In scenario I: Without wind energy sources in the grid, scenario II: One Wind farm will be introduced in the grid to determine the response of various parameters. Scenario III: Two wind farms will be incorporated in the grid to determine the performance of various system parameters. Finally, scenario IV: Five wind farms will be introduced in the grid to determine the system response.

V. RESULTS AND DISCUSSIONS

I. Scenario I: Without Wind Farm connected to the Grid.

In this case, IEEE 39 Bus was modelled in MATLAB/Simulink environment and simulated in PSAT. The choice of simulation parameters are provided for as per IEEE 39 test bus data. The initial voltage guesses and lines power capacities are assumed. The PV bus parameter block was used and specifically power capacity in MVA was critical in the initialization of synchronous machines and Automatic voltage regulators (AVR).This parameter was gotten by trial and error and took a lot of time to guess the right value. The criteria used was to get a value that gives the least maximum error of convergence in the power flow iterations. In PSAT, power flow must be executed first before time domain simulation is carried out. With the assumed values, the grid experienced voltage collapse in various buses and the Newton Raphson method did not converge. The Newton Raphson (NR) did not converge and therefore carrying out time domain simulation was not achieved. This points to the fact that this NR method fails to converge for large power system networks. There was also likely singular values pointing to infinity values in the process of iteration.

The network data computed for the power flow using PSAT was as shown in Table I, and appendix A in Table II and III.

TABLE I. OUTPUT RESULTS WITHOUT A WIND FARM CONNECTED TO THE GRID

NETWORK STATISTICS	
Buses:	39
Lines:	34
Transformers:	12
Generators:	10
Loads:	19
SOLUTION STATISTICS	
Number of Iterations:	9
Maximum P mismatch [p.u.]	2.07096E-05
Maximum Q mismatch [p.u.]	2.97945E-05
Power rate [MVA]	100

The NR has power mismatch calculations as shown in Table I and are quite small and falls outside tolerance values of 1E-05. I adjusted the power flow tolerance to 3E-05 but the NR did not converge. Therefore other methods have to be incorporated like using elements of the Jacobian matrix in normalized form [15]. The voltage values at various buses violated the limits and some buses have low voltages likely to trigger voltage collapse (total system blackout). Voltage collapse signals a system that is highly unstable in terms of voltage stability and overall power system stability.

The active power system loss accounts for 86.18% showing that the system is very inefficient. The line capacities need to be improved and more reactive power injected into the network to stabilize the network. The reactive power losses account for 99.7%, quite a high value, explaining the need to inject more reactive power to compensate for active power losses.

II. Scenario II: With one Wind Farm in the Grid.

The wind farm was composed of 30 wind turbines with a total capacity of 600 MVA. The power mismatch values increased marginally worsening the convergence criterion as shown in Table IV. The voltage profile showed changes in voltage magnitude at some buses to an improved value or a much lesser value while others remained constant values as shown in Table V. It shows that wind turbine is a source of reactive power and hence helps inject some reactive power in the network. The active power loss increased marginally to 88.6% while the reactive power loss remained constant at 99.7% when Table III and Table IV are compared in appendix A. The major observation is that active generated increased almost twice as reactive power generation. Active power generated increased by 34.7% while the reactive power generated increased by 17.8%.The total load power also increased as well as total losses. This points to the fact that the wind generator at one time acts as a generator and other instances as a load due its variable output power causing increased power system losses. The voltage levels at various buses also increased to a higher value due to the presence of increased reactive power in the grid.

TABLE IV. OUTPUT RESULTS FOR ONE WIND FARM CONNECTED TO THE GRID

NETWORK STATISTICS	
Buses:	39
Lines:	34
Transformers:	12
Generators:	9
Loads:	19

SOLUTION STATISTICS	
Number of Iterations:	8
Maximum P mismatch [p.u.]	7.21584E-05
Maximum Q mismatch [p.u.]	7.5171E-05
Power rate [MVA]	100

III. Scenario III: With Two Wind Farms connected to the Grid.

The power mismatch values in Table VII did not meet the convergence criterion of 1E-05 and were much worse compared to values in both Table I and IV. Wind farm at bus 36 had a capacity of 600 MVA with 30 wind turbines while wind farm at bus 32 had 630 MVA with 30 wind turbines. Integrating individual wind turbines is not feasible because it may not be possible to control the response required. It is also complex to design controls for individual wind turbines and coordinate with others in the grid. Some buses like 10 and 24 in Table VIII had voltage overshoots while other buses the voltages were zero as others recorded normal voltage profiles within the tolerance limits. It implies there was over-generation at some buses while others experienced substantial voltage drops due to line limitations or excessive loading at the buses.

The total power generated, total losses increased to high values to orders 1*10^10 which were much worse and recorded values beyond the capability of the system to handle as shown in Table IX. However, the active power losses reduced to 72.85% while reactive power dropped marginally to 99.50%. It implies the wind turbines injected reactive power into the network thus reducing the power losses.

TABLE VII. OUTPUT RESULTS FOR TWO WIND FARMS CONNECTED TO THE GRID

NETWORK STATISTICS	
Buses:	39
Lines:	34
Transformers:	12
Generators:	8
Loads:	19
SOLUTION STATISTICS	
Number of Iterations:	7
Maximum P mismatch [p.u.]	1.253926881
Maximum Q mismatch [p.u.]	5.078144908
Power rate [MVA]	100

IV. Scenario IV: With Five Wind Farms connected to the Grid

The wind farms were connected one at a time until they reached five to ensure proper initialization of the DFIG because fixing the PV parameters would be complicated if done all at once and their rated capacities are shown in Table X.

TABLE XI. OUTPUT RESULTS FOR FIVE WIND FARM CONNECTED TO THE GRID

NETWORK STATISTICS	
Buses:	39
Lines:	34
Transformers:	12
Generators:	6
Loads:	19
SOLUTION STATISTICS	
Number of Iterations:	8
Maximum P mismatch [p.u.]	128.8572411
Maximum Q mismatch [p.u.]	2.4057E-05

The active power mismatch was higher compared to the previous values as shown in Table XI. The reactive power mismatch was minimal. This is explained by the capability of wind turbines to absorb or inject more reactive power into the grid thus compensating for the mismatch. The voltage profile for the sampled buses shows that bus 22 and 24 changed values as shown in Table XII. These buses could be weak buses as shown by their continuity high voltage volatility. The other buses relatively have constant values hence least affected by the wind integration.

The active power losses increased to 77.62% while reactive power losses reduced marginally to 99.46%. This implies the wind turbines could be becoming loads drawing more current from the network thus increasing active power losses. As said earlier, they have reactive power production capabilities thus maintains the reactive almost constant.

VI. CONCLUSION

This paper has reviewed frequency stability control schemes with wind turbines integration using PSAT simulation tool in MATLAB/Simulink and has established that the tool is not sufficient to provide accurate results for IEEE 39 Bus system using time domain simulation. This therefore calls for further research using other simulation tools so as be able to provide more accurate results. It also points out that Newton Raphson method easily gets trapped in local optima and hence other methods either metaheuristic or numerical methods or IEEE 39 Bus data needs to be re-organized to overcome inability of Newton Raphson in conducting time domain simulation of wind farms in the grid.

REFERENCES

[1] G. Lalor, A. Mullane and M. O'Malley, "Frequency Control and Wind Turbine Technologies," *IEEE Transactions on Power Systems*, vol. 20, no. 4, 2005.

[2] H. Chamorro, M. Ghandhari and R. Eriksson, "Wind Power Impact on Power System Frequency Response," *North American Power Symposium*, 2013..

[3] J. Zhao, X. Lyu, Y. Fu, X. Hu and F. Li, "Coordinated Microgrid Frequency Regulation Based on DFIG Variable Coefficient Using Virtual Inertia and Primary Frequency

Control," *IEEE Transactions on Energy Conversion,* vol. 31, no. 3, 2016.

[4] Z. Chen, "Issues of Connecting Wind Farms into Power systems," *IEEE/PES Transmission and Distribution Conference & Exhibition:Asia and Pacific,* 2005.

[5] I. Erlich and M. Wilch, "Primary Frequency Control by Wind Turbines," in *IEEE PES General Meeting,* 2010.

[6] L. Shang, J. Hu, X. Yuan and Y. Chi, "Understanding Inertial Response of Variable-Speed Wind Turbines by Defined Internal Potential Vector," *Energies,* December 2016.

[7] I. Erlich and M. Wilch, "Primary Frequency Control by Wind Turbines," *IEEE PES General Meeting,* 2010.

[8] P. Li, W. Hu and Z. Chen, "Review on Integrated-Control Method of Variable Speed Wind Turbines Participation in Primary and Secondary Frequency," *Industrial Electronics Society,,* 2016.

[9] M. Altin, "Dynamic Frequency Response of Wind Power Plants," *Ph.D. Dissertation,Dept.Energy.Tech,Aalbg Univ.,* November 2012.

[10] M. W. Hansen, R. Josefsson and H. Mehmedovic, *Frequency Controlling Wind Power,Modelling of Control Strategies,* Stockholm: Unpublished, 2012.

[11] N. Nguyen and J. Mitra, "Effect of Wind Power on Load Frequency Control," *IEEE Power and Energy Society General Meeting(PESGM),* pp. 1-5, 2016.

[12] A. Zertek, G. Verbic and M. Pantos, "Optimised Control Approach for Frequency Control Contribution of Variable Speed Wind Turbines," *Institution of Engineering and Technology Renewable Power Generation,* 2011.

[13] P. Li, W. Hu and Z. Chen, "Review on Integrated-Control Method of Variable Speed Wind Turbines Participation in Primary and Secondary Frequency," *Industrial Electronics Society,,* 2016.

[14] P. M. Anderson and A. A. Fouad, Power System Control and Stability, IOWA: Galgotia Publications, 1984.

[15] D. P. Kothari and I. J. Nagrath, Modern Power system Analysis, New Delhi: Tata McGraw Hill Education Private Ltd, 2003.

[16] A. Kalmikov, K. Dykes and K. Araujo, "Wind Power Fundamentals," Massachusettes.

[17] M.-K. Kim, "Optimal Control & Operational Strategy for Wind Turbines Contributing to Grid Primary Frequency Regulation," *Applied Sciences,* 2017.

[18] Mathworks, "Matlab," Matlab, 2019. [Online]. Available: https://www.mathworks.com/help/matlab/ref/function.html. [Accessed 10 July 2019].

Appendix A

TABLE II. MAGNITUDE AND PHASE ANGLE PROFILE OF POWER PARAMETERS WITHOUT A WIND FARM CONNECTED TO THE GRID

Bus	V	phase	P gen	Q gen	P load	Q load
	[p.u.]	[rad]	[p.u.]	[p.u.]	[p.u.]	[p.u.]
22	0.00	-67579.11	-2.86E-05	1.40E-05	0	0
24	0.60	-176.51	-36.26	24.11	1.02	-0.31
30	1.05	-350.14	0.26	5.21	0	0
31	0.98	0	1.41	8.07	0.37	0.18
32	0.91	-500.61	-3.10	2.25	0	0
33	1.00	-338763.66	3.39	18.04	0	0
34	1.01	-1.09E+12	1.13	19.04	0	0
35	1.05	-482588.19	0.78	15.68	0	0
36	0.98	-350.48	-0.05	4.13	0	0
37	1.03	-294.55	0.25	5.01	0	0
38	1.03	122.00	-4.25	0.11	0	0
1	0.00	-142.34	-2.43E-05	-3.32E-05	0	0
10	0.83	-72.23	-222.85	450.00	0	0

TABLE III. GENERATION, LOAD AND LOSSES FROM POWER FLOW WITHOUT A WIND FARM

TOTAL GENERATION		PERCENT (%)
REAL POWER [p.u.]	346.59	
REACTIVE POWER [p.u.]	3899.01	
TOTAL LOAD		
REAL POWER [p.u.]	47.89	13.82
REACTIVE POWER [p.u.]	11.56	0.30
TOTAL LOSSES		
REAL POWER [p.u.]	298.69	86.18
REACTIVE POWER [p.u.]	3887.45	99.70

TABLE V. MAGNITUDE AND PHASE ANGLE PROFILE OF POWER PARAMETERS WITH ONE WIND FARM CONNECTED TO THE GRID

Bus	V	phase	P gen	Q gen	P load	Q load
	[p.u.]	[rad]	[p.u.]	[p.u.]	[p.u.]	[p.u.]
22	1.14	22.14	-20.50	118.26	0	0
24	0.00	30.99	2.27E-05	2.14E-05	0.00	-0.00
30	1.05	-35.66	-5.44	18.53	0	0
31	0.98	0	2.04	6.57	0.367	0.18
32	0.91	-176.06	-1.47	-0.55	0	0

33	1.00	18.58	0.87	17.33	0	0
34	1.01	45.84	2.34	-4.10	0	0
35	1.05	6.14	6.74	32.20	0	0
36	0.98	-108.22	5.47	3.66	0	0
37	1.03	0.81	14.26	9.72	0	0
38	1.03	131.83	2.98	5.20	0	0
1	0.00	6405843.33	-8.56E-05	-2.20E-05	0	0
10	1.05	81.87	333.33	496.97	0	0

TABLE VI. GENERATION, LOAD AND LOSSES FROM POWER FLOW WITH ONE WIND FARM.

TOTAL GENERATION		PERCENT (%)
REAL POWER [p.u.]	466.75	
REACTIVE POWER [p.u.]	4593.08	
TOTAL LOAD		
REAL POWER [p.u.]	53.23	11.40
REACTIVE POWER [p.u.]	13.54	0.29
TOTAL LOSSES		
REAL POWER [p.u.]	413.52	88.60
REACTIVE POWER [p.u.]	4579.53	99.71

TABLE VIII. MAGNITUDE AND PHASE ANGLE PROFILE OF POWER PARAMETERS WITH TWO WIND FARMS CONNECTED TO THE GRID

Bus	V	phase	P gen	Q gen	P load	Q load
	[p.u.]	[rad]	[p.u.]	[p.u.]	[p.u.]	[p.u.]
22	0.02	91074618.93	0.24	1.39	0	0
24	2.10	91074621.54	279.43	-164.96	5.67	-1.69
30	1.05	15571672.78	-61.34	21.12	0	0
31	0.98	0	0.58	4.38	0.37	0.18
32	0.91	91074300.47	5.44	28.64	0	0
33	1.00	91074621.67	-1.86	45.74	0	0
34	1.01	91074627.34	4.86	11.71	0	0
35	1.05	91074619.72	1.04	15.40	0	0
36	1.00	91074536.13	0.25	4.96	0	0
37	1.03	15571526.4	0.25	5.01	0	0
38	1.03	4.38E+11	-1.09	7.39	0	0
1	0.00	293161383	0.00	-5.80E-05	0	0
10	6.00	91074743.6	11319.94	-778.61	0	0

Bus	V	phase	P gen	Q gen	P load	Q load
	[p.u.]	[rad]	[p.u.]	[p.u.]	[p.u.]	[p.u.]
22	0.01	4540337.13	0.03	-0.07	0	0
24	0.00	4540284.63	3.53E-10	5.08E-10	1.42E-07	-4.24E-08
30	1.05	-525.23	-0.34	6.87	0	0
31	0.98	0	0.62	4.41	0.37	0.18
32	0.91	24638278.82	0.18	3.63	0	0
33	1.00	394741.47	6.37	23.05	0	0
34	1.01	394779.81	5.06	8.04	0	0
35	1.05	4540324.10	0.74	15.61	0	0
36	0.982	4540308.06	0.24	4.81	0	0
37	1.03	-505.29	0.25	5.01	0	0
38	1.03	-16592014.06	6.55	0.45	0	0
1	0.75	-252.33	27.42	12.87	0	0
10	0.00	307959.72	9.49E-08	-0.00	0	0

TABLE IX. GENERATION, LOAD AND LOSSES FROM POWER FLOW WITH TWO WIND FARMS CONNECTED TO THE GRID.

TOTAL GENERATION		PERCENT (%)
REAL POWER [p.u.]	1.78E+11	
REACTIVE POWER [p.u.]	1.41E+12	
TOTAL LOAD		
REAL POWER [p.u.]	48363500829	27.15
REACTIVE POWER [p.u.]	6479770651	0.46
TOTAL LOSSES		
REAL POWER [p.u.]	1.30E+11	72.85
REACTIVE POWER [p.u.]	1.40E+12	99.54

TABLE X. FIVE WIND FARMS WITH RATED CAPACITIES AND NUMBER OF WIND TURBINES IN EACH WIND FARM.

Bus No	Wind Farm Capacity(MVA)	No of Wind Turbines in the Farm
32	630	30
36	600	30
37	500	30
38	900	60
39	100	30

TABLE XII. MAGNITUDE AND PHASE ANGLE PROFILE OF POWER PARAMETERS WITH FIVE WIND FARMS CONNECTED TO THE GRID

TABLE XIII. GENERATION, LOAD AND LOSSES FROM POWER FLOW WITH FIVE WIND FARMS CONNECTED TO THE GRID.

TOTAL GENERATION		PERCENT (%)
REAL POWER [p.u.]	263.51	
REACTIVE POWER [p.u.]	3154.20	
TOTAL LOAD		
REAL POWER [p.u.]	58.97	22.38
REACTIVE POWER [p.u.]	17.18	0.54
TOTAL LOSSES		
REAL POWER [p.u.]	204.54	77.62
REACTIVE POWER [p.u.]	3137.01	99.46

Particle Swarm Optimized Power Grid Frequency Stability Control Scheme in the Presence of Wind Energy Sources.

Terry .L. Chepkania[1], Moses .P. Musau[2],
Department of Electrical and Information Engineering
The University of Nairobi
Nairobi, Kenya
lumbasit@gmail.com[1],pemosmusa@uonbi.ac.ke[2]

Cyrus .W. Wekesa[3]
School of Engineering
University of Eldoret
Eldoret, Kenya
cyrus.wekesa@gmail.com[3]

***Abstract* - Renewable energy sources (RES) have become a subject of interest world-wide, including in Kenya where recently a 310 MW Wind Power plant was commissioned. They are clean energy technologies and relatively cheaper compared to fossil-fuels. They do not inherently provide system inertia from rotating masses of the rotor of the wind turbine hence when integrated into the grid pose electrical power system frequency instability. The optimization and load flow were conducted using particle swarm optimization algorithm and Newton Raphson algorithm. Results showed that the voltage profile and frequency response profile improved significantly as the percentage of wind penetration increased in the grid. For the test system considered, the maximum wind penetration was 32.1%. Notably, as the percentage of wind penetration increased, the rate of change of frequency worsened because of the intermittent nature of wind energy source.**

***Index Terms:* Frequency instability, system inertia, particle swarm optimization.**

I. INTRODUCTION

Renewable energy sources are clean energy technologies and in some cases occur in abundance and mitigate against sustained depletion of fossil-fuels and support energy diversification [40].These sources reduce carbon dioxide emissions and hence the effects of global warming [41]. Some of the common challenges are the rare species of birds have become victims of the windmills and wind turbines world-wide. The beauty of the land is destroyed in using some of the wind turbines to generate electrical power and cost of land drops as result of their establishment.

Wind energy conversion systems are known to offer less or no support at all to system frequency stability due to lack of system inertia because of the presence power electronic converters employed for constant power output during generation [40]- [41]. For example, islanded grids suffer severe frequency instabilities in the presence of these technologies because of lack of support from conventional sources of energy [40]- [3]. Research has proposed use of natural or synthetic methods to provide system inertia. This includes use of renewable energy storage systems (RESS) [4], [5].This is a noble idea but increases investment cost because it supports setting up more like parallel plants to stabilise grid system frequency in the event of transient disturbances.

Natural methods of providing system inertia avoid establishment of parallel plants but have dire consequences related to operation, control and support of frequency stability. The power system frequency control has three stages [6], [45], [8]- [9].

This paper is organised as follows: Section II delves into particle swarm optimization in the presence of wind energy sources, problem formulation of power extraction from wind turbine is covered in Section III. Section IV provides the IEEE 39 Bus test system model in MATLAB environment and coded using particle swarm optimization (PSO) algorithm approach. Result analysis and discussions are done in section V and finally conclusion is given in section VI.

II. PARTICLE SWARM OPTIMIZATION (PSO) IN THE PRESENCE OF WIND ENERGY SOURCES

This paper is not the first one to use PSO in optimization of either energy or power from the Variable Speed Wind Turbines (VSWT). Pareto-Dominance was used with Multi-objective PSO to select emulated inertial response control parameters on a micro grid [10].Parameters of the inertial controller and those that satisfy multiple and conflicting power system objectives were selected for the test system. In conclusion, design preference influences parameter selection for example weaker grid require aggressive inertial response because frequency stability is a major concern. In post disturbance support, inertial response demand is limited hence parameter settings will change. Pitch angle and rotor speed

optimization in VSWT were also tested using differential evolution [11]. The effect of wind power penetration on frequency stability and frequency regulation capability were examined [50]. The results showed that the integration of wind power leads to reduced frequency stability because of reduced overall system inertia.

III. PROBLEM FORMULATION

From the swing equation, the accelerating torque T_a is given by [6], [13].

$$J\dot{W} = T_a \tag{1}$$

Where:

$\dot{W}$ is average angular acceleration in radians/second squared (rad/s^2), J is rotor moment of inertia in Kg-m^2, T_a is accelerating torque in N.m.

$$T_m - T_e = T_a \tag{2}$$

T_m is the driving mechanical torque and T_e is the retarding electrical torque.

Similarly,

For a synchronous machine as derived from [14],

$$\frac{df}{dt} = \frac{\Delta P * f_0}{2 * GH} \tag{3}$$

ΔP is the change in power, f_0 refers to the nominal frequency in Hz, $\frac{df}{dt}$ is the rate of change of frequency (ROCOF), G is rated apparent power, H is inertia time constant. Therefore, to determine, the frequency deviations Δf, it is given by,

$$\Delta f = f_0 - f_{nadir} \tag{4}$$

$$\Delta f = f_0 - [(2GH * \frac{df}{dt})/\Delta P] \tag{5}$$

f_{nadir} is the minimum frequency value in Hz.To extract maximum kinetic energy, we should maximize the deceleration of the rotor. Hence, min $\frac{df}{dt}$ and min Δf.

The equations for extraction of wind power from the wind turbine are derived from [6], [51].

Considering primary power reserve margin, and loading the turbine at 85%, then

$$P_{opt} \geq 0.85P_{opt} + \Delta Pke \tag{6}$$

$$\Delta Pke \leq 0.15P_{opt} \tag{7}$$

ΔPke is change in power due to kinetic energy, P_{opt} is optimal power of the generator in MW

Ignoring windage, iron and frictional losses,

$$P_G = P_t \tag{8}$$

P_G is total generated electrical power in MW, Pt is total turbine power equal to total mechanical power

According to [16], the accelerating power is given by

$$JW_r\dot{W}_r = P_{in} - (P_{ref} + \Delta Pke) \tag{9}$$

W_r is mechanical rotational speed, P_{ref} is reference power and P_{in} is mechanical input power of the wind turbine.

The power imbalance will be catered by the difference between the input power and power extraction from de-loaded mode due to deceleration of the rotor speed to counter frequency drop. Ignoring variable and fixed losses in the Variable Speed Wind Turbine

$$\Delta Pke = P_{in} - \sum_{k=1}^{n} (JW_{del}\frac{W_{del}}{dt}) \tag{10}$$

W_{del} is the de-loaded rotor speed in radians per second (rad/s).Taking into consideration a wind farm with n wind turbines with reference to equation (10), then maximize the extraction of accelerating power from the wind turbine. Since the reference power is a constant, P_{ref}, then considering a maximum power point tracking (MPPT) curve has maximum and minimum rotor speeds in de-loaded mode.

$$Max\ \Delta Pke = Max\ \{\sum_{k=1}^{n} (P_{in} - JW_{del}\frac{W_{del}}{dt})\} \tag{11}$$

The wind farm power output, according to [16] is given by,

$$P_{ref,wf} = \sum_{k=1}^{n} P_{del,k} = \sum_{k=1}^{n} 0.85P_{opt,k} \tag{12}$$

$P_{ref,wf}$ is the system operator's output command, $P_{del,k}$ is the de-loaded power reference. The objective function is

$$Max\ \Delta Pke = Max\ \left\{\sum_{k=1}^{n} \left(P_{in,k} - JW_{del,k}\frac{\dot{W}_{del,k}}{dt}\right)\right\}$$

(13)

Subject to the constraints:

$$\text{Total } \Delta Pke \leq 0.15 \text{ Total } P_{opt} \tag{14}$$

$$P_{min} \leq P_{del} \leq P_{max} \tag{15}$$

$$W_{del,min} \leq W_{del} \leq W_{max} \tag{16}$$

$$\beta min \leq 0 \leq \beta\ max \tag{17}$$

$$C_p \leq 0.59 \tag{18}$$

β is the pitch angle in degrees, C_p is the power coefficient.

IV. PARTICLE SWARM (PSO) APPROACH

In this case, the objective function was coded using PSO and the output power was the best global power and optimal rotor speed. The derived power was used as an input in the load flow using Newton Raphson algorithm for IEEE 39 Bus test system to display the voltage profile and frequency response when a disturbance was introduced in the grid. The mapping of the problem to particle swarm optimization (PSO) is shown in Table I. The power coefficient is derived from wind velocity (m/s) inputs of 4,7,8,9,10,11,12,14 with judiciously selected tip speed ratio range of 1-8,and beta (β) values of 0,0.5,1,2,3,4,5 and 6 degrees and wind turbine blade radius of 35.25 metres.

There were five scenarios in total. Scenario I: Without wind energy sources in the grid. Scenario II: With one wind energy source in the grid. Scenario III: With two wind energy sources in the grid. Scenario IV: With two wind energy sources and Bus 39 generator tripped. Scenario V: With two wind energy sources and Buses 38 and 39 tripped. In the first 3 instances, rotor angle disturbance was introduced after displacement of the conventional generators by wind generators. In the fourth and fifth instances, generators at buses 39 and 38-39 buses were tripped respectively.

TABLE I. MAPPING OF THE PROBLEM TO PARTICLE SWARM OPTIMIZATION ALGORITHM.

No	**Parameter description**	**Algorithm Representation**
1	Rotor speed in radians per second	Particle
2	Group of wind Turbines' inertial response	Swarm
3	Optimal Power due to kinetic energy released	Destination
4	Feasible region or region of the desirable Power injected.	Center of the swarm
5	Fitness function	Objective Function

V. RESULTS AND DISCUSSIONS

A. Scenario I: Without Wind Farm Integrated in the Grid

The grid system frequency achieved was 49.9963 Hz and without PSO optimization. The rate of change of frequency (ROCOF) was 0.030389 Hz/s and system inertia of 36 seconds and the voltage profile was 1±0.1 per unit within the limits and the grid was stable.

B. Scenario II: With One Wind Farm Integrated in the Grid

In this case the grid system frequency achieved was 49.9966 Hz with PSO optimization. The ROCOF was 0.029972 Hz/s with system inertia of 36.5 seconds and voltage profile of 1±0.1 per unit. The hydro generator at Bus 39 rated at 1000 MW was displaced by one wind farm consisting of 400 wind turbines and none of the units was tripped in the IEEE 39 Bus test system. The wind farm produced 1083.32 MW based on a Doubly Fed Induction Generator (DFIG) model in optimal mode at 0.4535 power coefficient. The de-loaded mode power coefficient was set at 0.3617 with tip speed ratio of 7 at one degree pitch angle and power generated was 917.24 MW. On disturbance introduction, the power coefficient was set at 0.4535 with a value of 8 for tip ratio speed and zero degree pitch angle. The grid was relatively stable compared to scenario I.

C. Scenario III: With Two Wind Farms Integrated in the Grid

Two wind farms each with 200 wind turbines were placed at Buses 34 and 39 randomly. This displaced steam and hydro turbines with initial power generations of 508 MW and 1000 MW respectively. The two wind farms initially operated in de-loaded mode with a power coefficient of 0.3617 at one degree pitch angle and a value of 7 tip speed ratio that produced power of 463.87 MW each. In the optimal mode, at 8 tip speed ratio and zero degree pitch angle with power coefficient of 0.4535 power produced was 539.07 MW. In de-loaded mode, total power generated in the grid was 5521.23 MW. Power generated from wind was 927.74 MW which accounted for 16.80 % of the total power generated. The system frequency dropped to 49.9965 Hz with a ROCOF of 0.032656 Hz/s. The voltage profile was within the limits of 1±0.1 per unit. The system inertia dropped to 33.5 seconds. Hence the grid became relatively unstable though with minimal impact on the grid.

D. Scenario IV: With Two Wind Farms Integrated in the Grid and Bus 39 Generator Tripped

Buses 34 and 35 generators were replaced with two wind farms with 200 wind turbines at each bus. They displaced both steam and gas turbines of 508 MW and 650 MW capacities respectively. In de-loaded mode, a power coefficient of 0.3617 produced 619.4 MW at each bus. The percentage of wind penetration was 20.04 % because the total generation increased to 6182.28 MW from 6101.48 MW. In optimal mode, Bus 39 generator was tripped and settings of the wind turbine set to zero degree pitch angle and a value of 8 for tip speed ratio with a power coefficient of 0.4535 producing 740.88 MW of power. The system frequency was 49.9971 Hz with a ROCOF of 0.036466Hz/s. The system inertia was 30 seconds. The voltage profile remained within the limits of 1±0.1 per unit. Reduction in system inertia and a worse value of ROCOF compared to scenario III indicates the electrical power system is unstable.

E. Scenario V: With Two Wind Farms Integrated in the Grid and Buses 38 and 39 Generators Tripped

Buses 34 and 35 generators were replaced with wind two wind farms as in scenario IV, but generators 38 and 39 were both tripped. In the de-loaded mode, the PSO algorithm failed to run and give any results. In the optimal mode, with a power

coefficient of 0.4535 for zero degree pitch angle and tip speed ratio of 8, power produced was 756.45 MW.The system inertia was 27 seconds. The voltage profile limits were violated recording values below 0.9 per unit. The system frequency dropped to 49.9968 Hz with a ROCOF of 0.040518 Hz/s. The grid was unstable with maximum wind penetration of 32.08%.

Generally, scenarios I-III recorded positive frequency improvement and voltage profile was relatively stable when rotor angle disturbance was introduced as shown in appendix A, Table II. The voltage and frequency responses for scenarios II and V are also displayed in appendix A: Fig. 1 and Fig. 2.

The results obtained from this study are more superior when frequencies from [10] are compared. The post support minimum frequency value was 49.37 Hz while this study obtained 49.9971 Hz. However, the systems are different because this study focussed on the grid while the former [10] on micro grid which is weaker compared to grid stability.

VI. CONCLUSION.

The PSO improved frequency response in de-loaded mode from 49.9963Hz to 49.9971 Hz in case 4 but case 5 failed to execute.The ROCOF deteriorated from 0.030389 Hz/sec to 0.040518 Hz/sec.

This paper established that wind energy penetration percentage was limited to 32.08% beyond which frequency instability occurs. It also found out that displacement of conventional sources of power should consider the system inertia of specific generator being replaced. Some replacements could reduce the inertia by a large value and destabilise the grid.

REFERENCES

[1] G. Lalor, A. Mullane and M. O'Malley, "Frequency Control and Wind Turbine Technologies," *IEEE Transactions on Power Systems,* vol. 20, no. 4, 2005.

[2] H. Chamorro, M. Ghandhari and R. Eriksson, "Wind Power Impact on Power System Frequency Response," *North American Power Symposium,* 2013..

[3] J. Zhao, X. Lyu, Y. Fu, X. Hu and F. Li, "Coordinated Microgrid Frequency Regulation Based on DFIG Variable Coefficient Using Virtual Inertia and Primary Frequency Control," *IEEE Transactions on Energy Conversion,* vol. 31, no. 3, 2016.

[4] Z. Chen, "Issues of Connecting Wind Farms into Power systems," *IEEE/PES Transmission and Distribution Conference & Exhibition:Asia and Pacific,* 2005.

[5] M. P. Musau and T. L. Chepkania, "Under Frequency Under Voltage Load Shedding with Renewable Energy Storage:A Proposed Case Study of the Kenyan Grid," *IEEE PES AFRICA* , 2017.

[6] T. L. Chepkania, M. P. Musau and C. W. Wekesa, "Review of Frequency Stability Control Schemes in the Presence of Wind Energy Sources," in *IEEE AFRICON,* Accra, 2019.

[7] P. Li, W. Hu and Z. Chen, "Review on Integrated-Control Method of Variable Speed Wind Turbines Participation in Primary and Secondary Frequency," *Industrial Electronics Society,,* 2016.

[8] L. Shang, J. Hu, X. Yuan and Y. Chi, "Understanding Inertial Response of Variable-Speed Wind Turbines by Defined Internal Potential Vector," *Energies,* December 2016.

[9] I. Erlich and M. Wilch, "Primary Frequency Control by Wind Turbines," in *IEEE PES General Meeting,* 2010.

[10] F. Hafiz, A. K. Swain, N. Patel and A. K. Kar, "Shaping Inertial Response from Wind Turbines: A Multi-objective Approach," in *IEEE 2nd Annual Southern Power Electronics Conference (SPEC),* Aukland, 2016.

[11] A. Zertek, G. Verbic and M. Pantos, "Optimised Control Approach for Frequency-Control contribution of Variable Speed Wind Turbines," *IET Renewable Power Generation,* vol. 6, no. 1, p. 6, 2012.

[12] N. Nguyen and J. Mitra, "An Analysis of the Effects and Dependency of Wind Power Penetration on System Frequency Regulation," *IEEE Transactions on Sustainable Energy* , vol. 7, no. 1, 2016.

[13] P. M. Anderson and A. A. Fouad, Power System Control and Stability, IOWA: Galgotia Publications, 1984.

[14] D. P. Kothari and I. J. Nagrath, Modern Power system Analysis, New Delhi: Tata McGraw Hill Education Private Ltd, 2003.

[15] A. Kalmikov, K. Dykes and K. Araujo, *Wind Power Fundamentals,* Massachusettes: Massachusettes Institute of Technology, 2010.

[16] M.-K. Kim, "Optimal Control & Operational Strategy for Wind Turbines Contributing to Grid Primary Frequency Regulation," *Applied Sciences,* 2017.

APPENDIX A

TABLE II. RESULTS OF THE PSO APPROACH.

SCENARIO	WIND FARMS (No.)	FREQUENCY (Hz)	ROCOF (Hz/s)	V (pu)	INERTIA(s)	DISPLACED GENERATOR BUS No.	GEN-TRIPPED BUS No.	SETTLING TIME (s)	STATUS OF THE GRID
I	0	49.9963	0.030389	1±0.1	36	None	None	0.91673	Stable
II	1	49.9966	0.029972	1±0.1	36.5	39	None	0.92946	Relatively stable compared to scenario I
III	2	49.9965	0.032656	1±0.1	33.5	39,34	None	0.85307	Relatively Unstable
IV	2	49.9971	0.036466	1±0.1	30	34,35	39	0.76394	Unstable
V	2	49.9968	0.040518	violated	27	34,35	38,39	0.68755	In optimal mode unstable/De-loaded mode does not operate

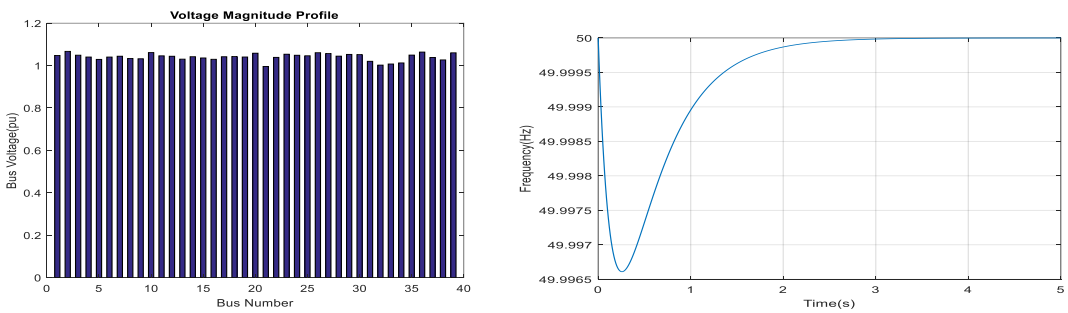

Fig. 1. Voltage Profile and Frequency Response of one Wind Farm integrated in the Grid

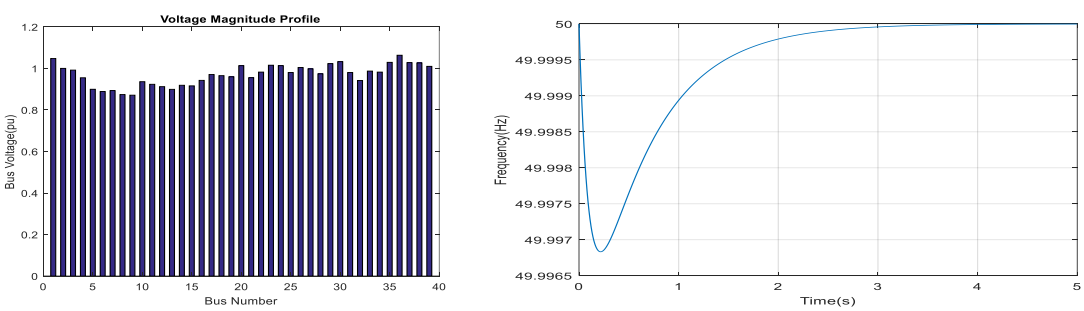

Fig. 2. Voltage Profile and Frequency Response of two Wind Farms integrated in the Grid with two Generators at Buses 38 and 39 trip

IEEE 39 Bus using Particle Swarm Optimization Algorithm Results

Part 1: Results of the Load Flow without Wind Farm Integrated in the Grid

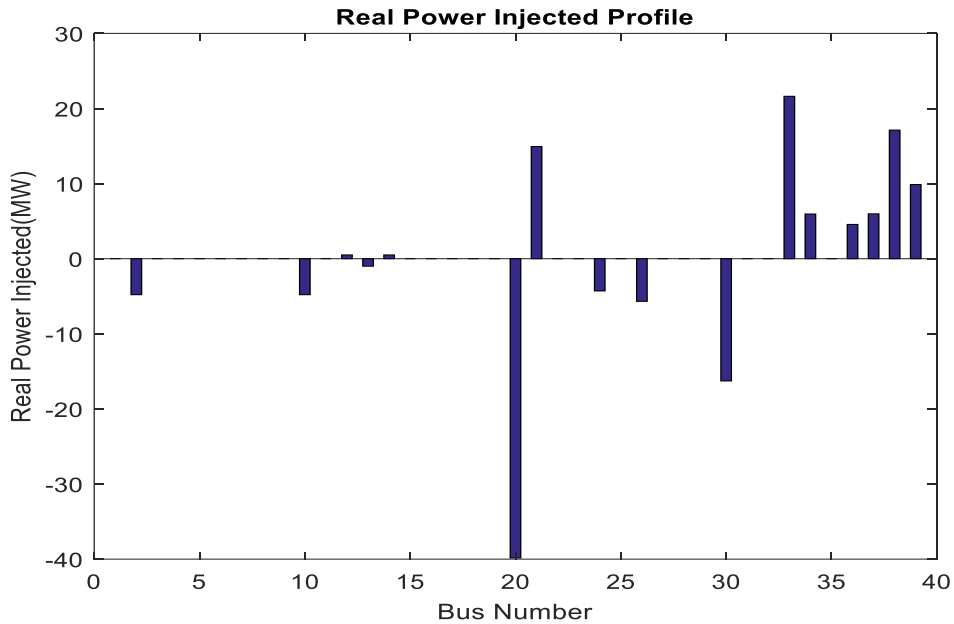

Figure 4.15: Real Power injected in the grid without a wind farm

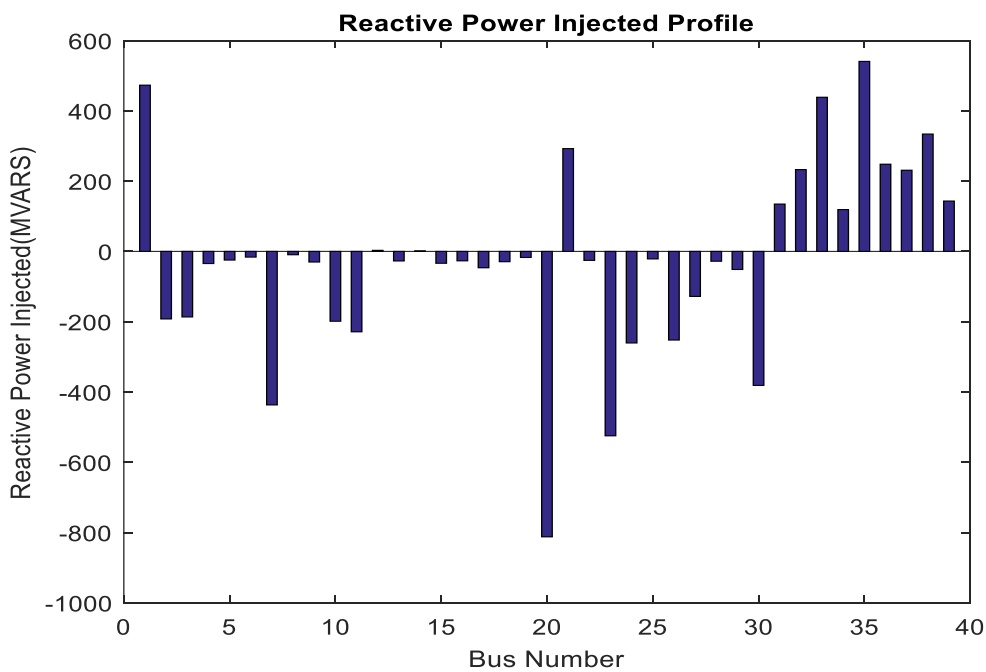

Figure 4.16: Reactive power injected in the grid without a wind farm in the grid.

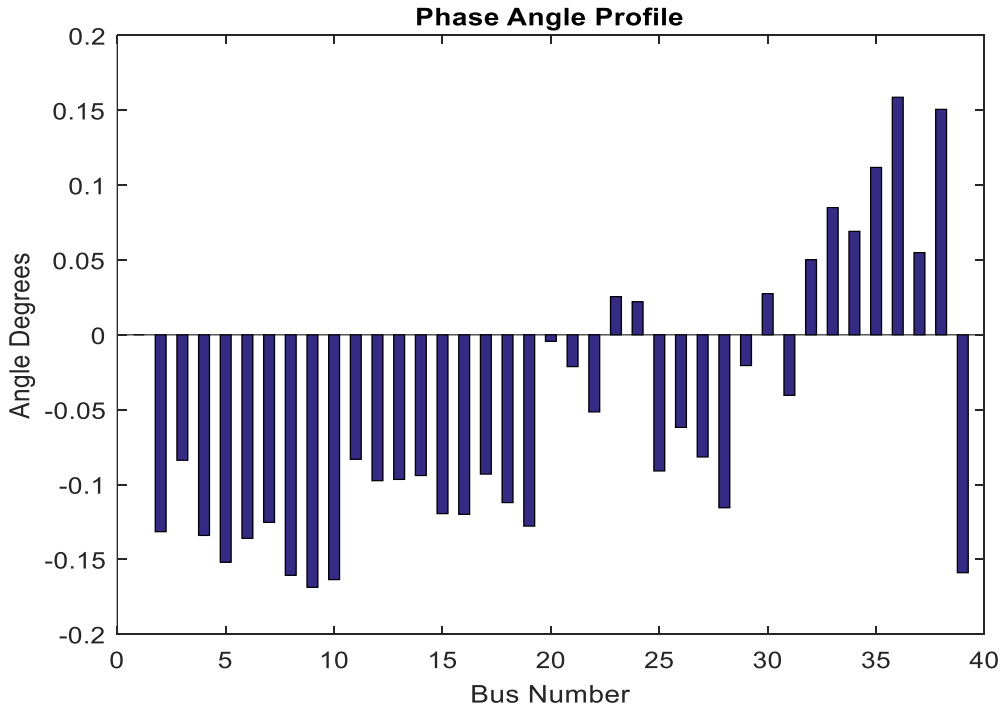

Figure 4.17: Phase angle profile without a wind farm in the grid.

| Network Statistics |

|No. of Buses | Lines |Generators |Loads |

39.0000 46.0000 10.0000 19.0000

| Solution Statistics |

|P mismatch | Q mismatch|No of Iterations |

-0.0000 -0.0000 10

Newton Raphson Load flow Analysis

| Bus | V | Angle | Injection | Generation | Load |

| No | pu | Degree | MW | MVar | MW | Mvar | MW | MVar |

---

1 1.0475 0.0000 0.000 473.137 9.200 477.737 9.200 4.600

---

2 1.0662 -7.5366 -4.792 -192.248 -4.792 -192.248 0.000 0.000

3	1.0486	-4.8016	0.000	-186.566	0.000	-186.566	0.000	0.000
4	1.0400	-7.6796	0.000	-34.620	322.000	-32.220	322.000	2.400
5	1.0285	-8.7017	0.000	-24.690	500.000	159.310	500.000	184.000
6	1.0393	-7.7880	-0.000	-16.260	-0.000	-16.260	0.000	0.000
7	1.0433	-7.1760	-0.000	-436.903	-0.000	-436.903	0.000	0.000
8	1.0323	-9.2021	-0.000	-9.550	233.800	74.450	233.800	84.000
9	1.0310	-9.6592	0.000	-30.300	522.000	145.700	522.000	176.000
10	1.0606	-9.3703	-4.792	-198.828	-4.792	-198.828	0.000	0.000
11	1.0452	-4.7595	0.000	-228.891	0.000	-228.891	0.000	0.000
12	1.0433	-5.5845	0.504	3.092	0.504	3.092	0.000	0.000
13	1.0296	-5.5352	-1.001	-27.221	6.499	60.779	7.500	88.000
14	1.0412	-5.3860	0.504	1.422	0.504	1.422	0.000	0.000
15	1.0352	-6.8446	0.000	-33.830	0.000	-33.830	0.000	0.000
16	1.0293	-6.8705	0.000	-26.850	320.000	126.150	320.000	153.000
17	1.0412	-5.3315	-0.000	-46.600	329.000	-14.300	329.000	32.300
18	1.0424	-6.4222	-0.000	-29.390	-0.000	-29.390	0.000	0.000
19	1.0402	-7.3224	0.000	-17.290	158.000	12.710	158.000	30.000
20	1.0581	-0.2478	-39.845	-812.303	-39.845	-812.303	0.000	0.000

21	0.9957	-1.2174	14.925	292.575	642.925	395.575	628.000	103.000
22	1.0384	-2.9520	0.000	-25.570	274.000	89.430	274.000	115.000
23	1.0534	1.4631	0.000	-524.808	0.000	-524.808	0.000	0.000
24	1.0485	1.2660	-4.290	-260.657	243.210	-176.057	247.500	84.600
25	1.0459	-5.2117	0.000	-21.450	308.600	-113.450	308.600	-92.000
26	1.0606	-3.5414	-5.672	-252.274	218.328	-205.074	224.000	47.200
27	1.0567	-4.6757	-0.000	-128.090	139.000	-111.090	139.000	17.000
28	1.0444	-6.6201	0.000	-28.060	281.000	47.440	281.000	75.500
29	1.0525	-1.1774	0.000	-51.460	206.000	-23.860	206.000	27.600
30	1.0516	1.5746	-16.278	-381.328	267.222	-354.428	283.500	26.900
31	1.0200	-2.3162	0.000	134.753	0.000	134.753	0.000	0.000
32	1.0020	2.8731	0.000	232.835	0.000	232.835	0.000	0.000
33	1.0072	4.8705	21.626	438.689	21.626	438.689	0.000	0.000
34	1.0123	3.9617	5.952	119.040	5.952	119.040	0.000	0.000
35	1.0493	6.4080	0.000	540.721	0.000	540.721	0.000	0.000
36	1.0635	9.0949	4.562	248.196	4.562	248.196	0.000	0.000
37	1.0378	3.1482	5.976	231.057	5.976	231.057	0.000	0.000
38	1.0265	8.6315	17.127	333.986	17.127	333.986	0.000	0.000

39	1.0600	-9.1061	9.872	143.367	1113.872	393.367	1104.000	250.000
Total			4.376	-833.167	6101.476	575.933	6097.100	1409.100

Line Flow and Losses

From Bus	To Bus	P MW	Q MVar	From Bus	To Bus	P MW	Q MVar	Line Loss MW	Line Loss MVar
2	3	0.000	0.000	3	2	-0.000	0.000	0.000	0.000
2	39	-4.792	-119.808	39	2	4.936	123.403	0.144	3.594
3	4	0.000	0.000	4	3	-0.000	0.000	0.000	0.000
3	26	0.000	0.000	26	3	-0.000	0.000	0.000	0.000
4	5	0.000	0.000	5	4	-0.000	0.000	0.000	0.000
4	19	0.000	0.000	19	4	-0.000	0.000	0.000	0.000
5	6	0.000	0.000	6	5	-0.000	0.000	0.000	0.000
5	15	0.000	0.000	15	5	-0.000	0.000	0.000	0.000
6	7	0.000	0.000	7	6	-0.000	0.000	0.000	0.000
6	9	0.000	0.000	9	6	-0.000	0.000	0.000	0.000
7	8	0.000	0.000	8	7	-0.000	0.000	0.000	0.000
7	12	0.000	0.000	12	7	-0.000	0.000	0.000	0.000
8	9	0.000	0.000	9	8	-0.000	0.000	0.000	0.000

9	10	0.000	0.000	10	9	-0.000	0.000	0.000	0.000
10	39	-4.792	-119.808	39	10	4.936	123.403	0.144	3.594
11	12	0.000	0.000	12	11	-0.000	0.000	0.000	0.000
11	14	0.000	0.000	14	11	-0.000	0.000	0.000	0.000
14	15	0.000	0.000	15	14	-0.000	0.000	0.000	0.000
15	16	0.000	0.000	16	15	-0.000	0.000	0.000	0.000
16	17	0.000	0.000	17	16	-0.000	0.000	0.000	0.000
17	18	0.000	0.000	18	17	-0.000	0.000	0.000	0.000
17	20	0.000	0.000	20	17	-0.000	0.000	0.000	0.000
17	22	0.000	0.000	22	17	-0.000	0.000	0.000	0.000
17	25	0.000	0.000	25	17	-0.000	0.000	0.000	0.000
18	19	0.000	0.000	19	18	-0.000	0.000	0.000	0.000
18	28	0.000	0.000	28	18	-0.000	0.000	0.000	0.000
22	23	0.000	0.000	23	22	-0.000	0.000	0.000	0.000
23	24	0.000	0.000	24	23	-0.000	0.000	0.000	0.000
24	25	0.000	0.000	25	24	-0.000	0.000	0.000	0.000
26	27	0.000	0.000	27	26	-0.000	0.000	0.000	0.000
27	28	0.000	0.000	28	27	-0.000	0.000	0.000	0.000

27	29	0.000	0.000	29	27	-0.000	0.000	0.000	0.000
27	30	0.000	0.000	30	27	-0.000	0.000	0.000	0.000
29	30	0.000	0.000	30	29	-0.000	0.000	0.000	0.000
13	12	0.000	0.000	12	13	-0.000	0.000	0.000	0.000
13	14	0.000	0.000	14	13	-0.000	0.000	0.000	0.000
7	1	0.000	-177.570	1	7	-0.000	186.005	0.000	8.435
11	32	-0.000	84.112	32	11	0.000	-82.598	0.000	1.514
20	33	0.906	18.384	33	20	-0.904	-18.332	0.003	0.051
21	34	-3.378	-67.555	34	21	3.419	68.386	0.042	0.831
23	35	0.000	-336.347	35	23	-0.000	352.928	0.000	16.582
24	36	-4.290	-233.377	36	24	4.562	248.196	0.272	14.819
26	37	-3.021	-116.827	37	26	3.105	120.075	0.084	3.248
3	31	-0.000	0.000	31	3	0.000	0.000	0.000	0.000
30	38	-8.477	-165.294	38	30	8.701	169.674	0.225	4.380
20	21	0.000	0.000	21	20	-0.000	0.000	0.000	0.000
Total Loss							0.913	57.049	

Settling time = 0.91673sec

Total system Inertia H = 36sec

Rate of Change of Frequency (ROCOF)= 0.030389Hz/sec

Part 2: Results of the Load Flow with one Wind Farm Integrated in the Grid

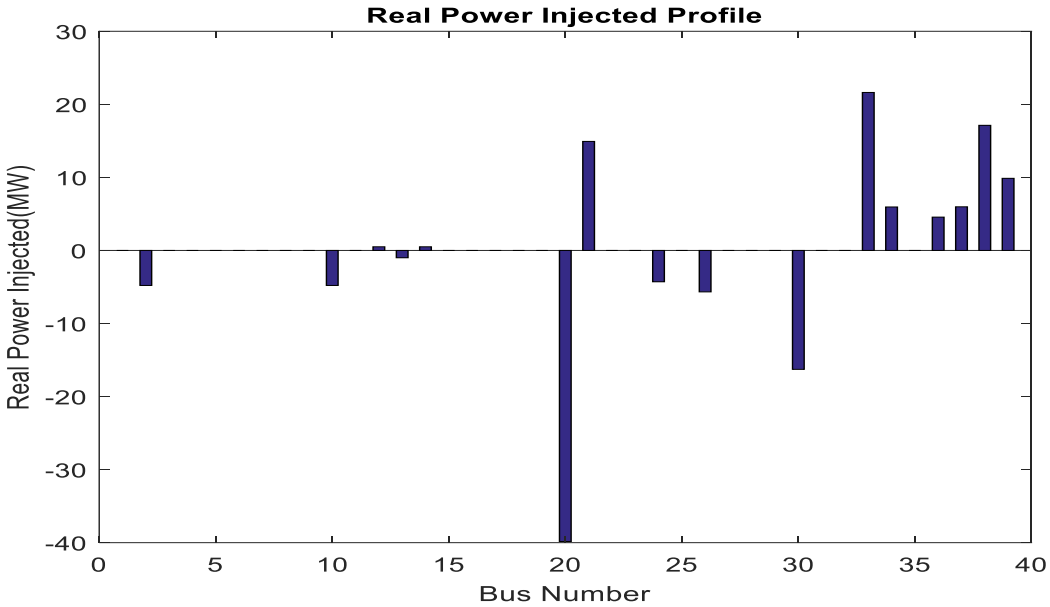

Figure 4.18: Real Power Profile with one wind farm integrated in the grid

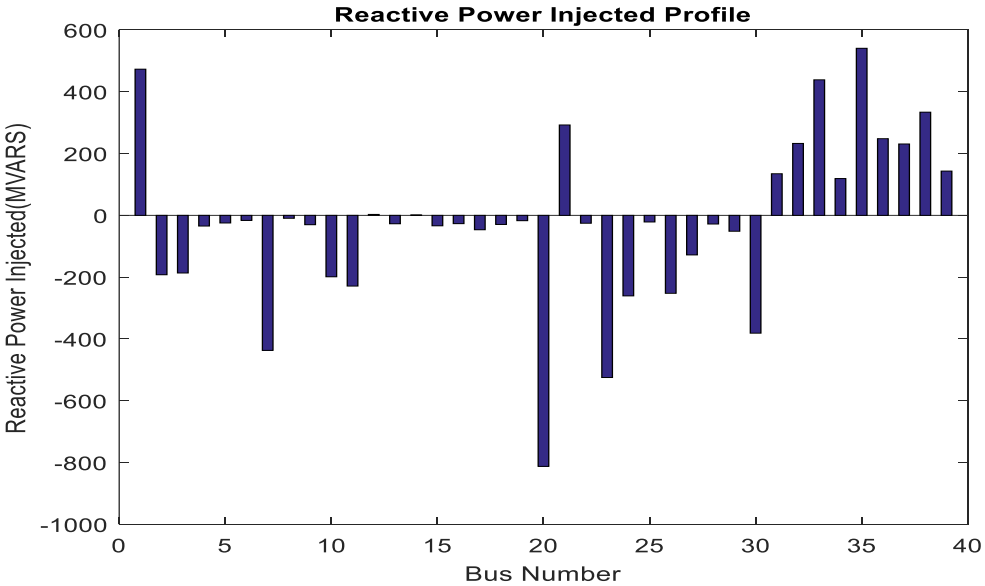

Figure 4.19: Reactive Power Profile with one wind farm in the grid

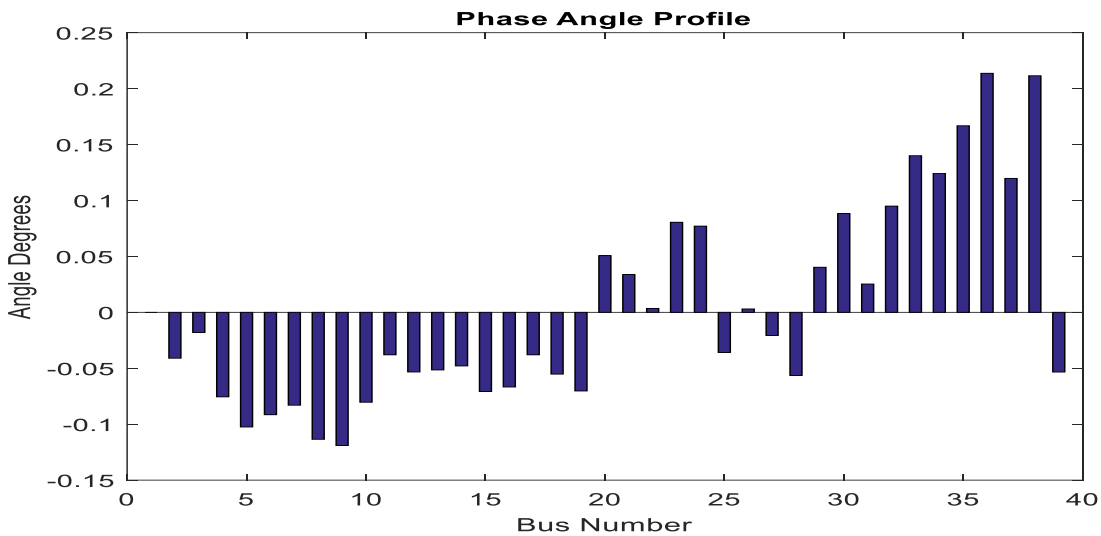

Figure 4.20: Voltage phase angle profile with one wind farm in the grid

---

| Network Statistics |

|No. of Buses | Lines |Generators |Loads |

39.0000 46.0000 10.0000 19.0000

| Solution Statistics |

|P mismatch | Q mismatch|No of Iterations |

-0.0000 -0.0000 10

Newton Raphson Loadflow Analysis

| Bus | V | Angle | Injection | Generation | Load |

| No | pu | Degree | MW | MVar | MW | Mvar | MW | MVar |

---

1 1.0475 0.0000 0.000 473.137 9.200 477.737 9.200 4.600

---

2 1.0668 -4.9712 -4.792 -192.248 -4.792 -192.248 0.000 0.000

---

3 1.0488 -2.9424 0.000 -186.566 0.000 -186.566 0.000 0.000

---

4 1.0401 -6.0331 0.000 -34.620 322.000 -32.220 322.000 2.400

---

5 1.0290 -7.3144 0.000 -24.690 500.000 159.310 500.000 184.000

6	1.0400	-6.5414	-0.000	-16.260	-0.000	-16.260	0.000	0.000
7	1.0440	-5.9902	-0.000	-436.903	-0.000	-436.903	0.000	0.000
8	1.0331	-7.8810	-0.000	-9.550	233.800	74.450	233.800	84.000
9	1.0318	-8.2703	0.000	-30.300	522.000	145.700	522.000	176.000
10	1.0610	-7.0235	-4.792	-198.828	-4.792	-198.828	0.000	0.000
11	1.0456	-3.4909	0.000	-228.891	0.000	-228.891	0.000	0.000
12	1.0438	-4.3428	0.504	3.092	0.504	3.092	0.000	0.000
13	1.0301	-4.2661	-1.001	-27.221	6.499	60.779	7.500	88.000
14	1.0416	-4.0896	0.504	1.422	0.504	1.422	0.000	0.000
15	1.0357	-5.4757	0.000	-33.830	0.000	-33.830	0.000	0.000
16	1.0294	-5.3753	0.000	-26.850	320.000	126.150	320.000	153.000
17	1.0413	-3.7821	-0.000	-46.600	329.000	-14.300	329.000	32.300
18	1.0424	-4.8219	-0.000	-29.390	-0.000	-29.390	0.000	0.000
19	1.0402	-5.7045	0.000	-17.290	158.000	12.710	158.000	30.000
20	1.0582	1.3012	-39.845	-812.303	-39.845	-812.303	0.000	0.000
21	0.9957	0.3317	14.925	292.575	642.925	395.575	628.000	103.000
22	1.0385	-1.4029	0.000	-25.570	274.000	89.430	274.000	115.000
23	1.0534	3.0119	0.000	-524.808	0.000	-524.808	0.000	0.000

24	1.0485	2.8148	-4.290	-260.657	243.210	-176.057	247.500	84.600
25	1.0460	-3.6623	0.000	-21.450	308.600	-113.450	308.600	-92.000
26	1.0605	-1.7161	-5.672	-252.274	218.328	-205.074	224.000	47.200
27	1.0566	-2.9625	-0.000	-128.090	139.000	-111.090	139.000	17.000
28	1.0443	-4.9586	0.000	-28.060	281.000	47.440	281.000	75.500
29	1.0525	0.5361	0.000	-51.460	206.000	-23.860	206.000	27.600
30	1.0516	3.2883	-16.278	-381.328	267.222	-354.428	283.500	26.900
31	1.0200	-0.4575	0.000	134.753	0.000	134.753	0.000	0.000
32	1.0020	4.1385	0.000	232.835	0.000	232.835	0.000	0.000
33	1.0072	6.4195	21.626	438.689	21.626	438.689	0.000	0.000
34	1.0123	5.5108	5.952	119.040	5.952	119.040	0.000	0.000
35	1.0493	7.9567	0.000	540.721	0.000	540.721	0.000	0.000
36	1.0635	10.6434	4.562	248.196	4.562	248.196	0.000	0.000
37	1.0378	4.9741	5.976	231.057	5.976	231.057	0.000	0.000
38	1.0265	10.3453	17.127	333.986	17.127	333.986	0.000	0.000
39	1.0600	-6.1181	9.872	143.367	1113.872	393.367	1104.000	250.000
Total			4.376	-833.167	6101.476	575.933	6097.100	1409.100

Line FLow and Losses

From Bus	To Bus	P MW	Q MVar	From Bus	To Bus	P MW	Q MVar	Line Loss MW	Line Loss MVar
2	3	0.000	0.000	3	2	-0.000	0.000	0.000	0.000
2	39	-4.792	-119.808	39	2	4.936	123.403	0.144	3.594
3	4	0.000	0.000	4	3	-0.000	0.000	0.000	0.000
3	26	0.000	0.000	26	3	-0.000	0.000	0.000	0.000
4	5	0.000	0.000	5	4	-0.000	0.000	0.000	0.000
4	19	0.000	0.000	19	4	-0.000	0.000	0.000	0.000
5	6	0.000	0.000	6	5	-0.000	0.000	0.000	0.000
5	15	0.000	0.000	15	5	-0.000	0.000	0.000	0.000
6	7	0.000	0.000	7	6	-0.000	0.000	0.000	0.000
6	9	0.000	0.000	9	6	-0.000	0.000	0.000	0.000
7	8	0.000	0.000	8	7	-0.000	0.000	0.000	0.000
7	12	0.000	0.000	12	7	-0.000	0.000	0.000	0.000
8	9	0.000	0.000	9	8	-0.000	0.000	0.000	0.000
9	10	0.000	0.000	10	9	-0.000	0.000	0.000	0.000
10	39	-4.792	-119.808	39	10	4.936	123.403	0.144	3.594

11	12	0.000	0.000	12	11	-0.000	0.000	0.000	0.000
11	14	0.000	0.000	14	11	-0.000	0.000	0.000	0.000
14	15	0.000	0.000	15	14	-0.000	0.000	0.000	0.000
15	16	0.000	0.000	16	15	-0.000	0.000	0.000	0.000
16	17	0.000	0.000	17	16	-0.000	0.000	0.000	0.000
17	18	0.000	0.000	18	17	-0.000	0.000	0.000	0.000
17	20	0.000	0.000	20	17	-0.000	0.000	0.000	0.000
17	22	0.000	0.000	22	17	-0.000	0.000	0.000	0.000
17	25	0.000	0.000	25	17	-0.000	0.000	0.000	0.000
18	19	0.000	0.000	19	18	-0.000	0.000	0.000	0.000
18	28	0.000	0.000	28	18	-0.000	0.000	0.000	0.000
22	23	0.000	0.000	23	22	-0.000	0.000	0.000	0.000
23	24	0.000	0.000	24	23	-0.000	0.000	0.000	0.000
24	25	0.000	0.000	25	24	-0.000	0.000	0.000	0.000
26	27	0.000	0.000	27	26	-0.000	0.000	0.000	0.000
27	28	0.000	0.000	28	27	-0.000	0.000	0.000	0.000
27	29	0.000	0.000	29	27	-0.000	0.000	0.000	0.000
27	30	0.000	0.000	30	27	-0.000	0.000	0.000	0.000

29	30	0.000	0.000	30	29	-0.000	0.000	0.000	0.000
13	12	0.000	0.000	12	13	-0.000	0.000	0.000	0.000
13	14	0.000	0.000	14	13	-0.000	0.000	0.000	0.000
7	1	0.000	-177.570	1	7	-0.000	186.005	0.000	8.435
11	32	-0.000	84.112	32	11	0.000	-82.598	0.000	1.514
20	33	0.906	18.384	33	20	-0.904	-18.332	0.003	0.051
21	34	-3.378	-67.555	34	21	3.419	68.386	0.042	0.831
23	35	0.000	-336.347	35	23	-0.000	352.928	0.000	16.582
24	36	-4.290	-233.377	36	24	4.562	248.196	0.272	14.819
26	37	-3.021	-116.827	37	26	3.105	120.075	0.084	3.248
3	31	-0.000	0.000	31	3	0.000	0.000	0.000	0.000
30	38	-8.477	-165.294	38	30	8.701	169.674	0.225	4.380
20	21	0.000	0.000	21	20	-0.000	0.000	0.000	0.000
Total Loss							0.913	57.049	

Settling time = 0.92946sec

Total system Inertia H = 36.5sec

Rate of Change of Frequency (ROCOF)= 0.029972Hz/sec

Best Global Power = 1083.3214MW

Part 3: Results of the Load Flow with two Wind Farms Integrated in the Grid

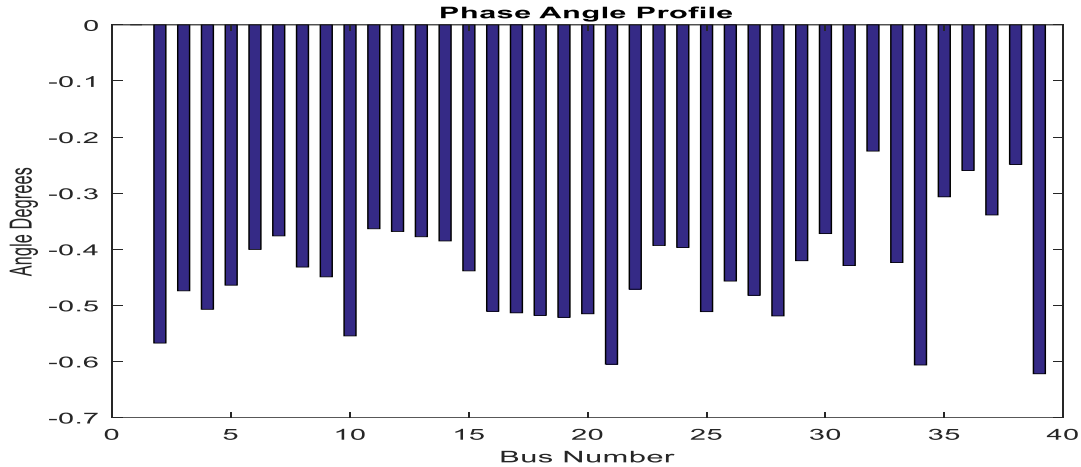

Figure 4.21: Voltage phase angle profile with two wind farms in the grid.

| Network Statistics |

|No. of Buses | Lines |Generators |Loads |

39.0000 46.0000 10.0000 19.0000

| Solution Statistics |

|P mismatch | Q mismatch|No of Iterations |

-0.0000 -0.0000 10

Newton Raphson Loadflow Analysis

| Bus | V | Angle | Injection | Generation | Load |

| No | pu | Degree | MW | MVar | MW | Mvar | MW | MVar |

---

1 1.0475 0.0000 0.000 473.137 9.200 477.737 9.200 4.600

---

2 1.0444 -32.5067 -4.792 -192.248 -4.792 -192.248 0.000 0.000

---

3 1.0318 -27.1712 0.000 -186.566 0.000 -186.566 0.000 0.000

---

4 1.0199 -29.0557 0.000 -34.620 322.000 -32.220 322.000 2.400

5	0.9969	-26.5932	0.000	-24.690	500.000	159.310	500.000	184.000
6	1.0014	-22.9380	-0.000	-16.260	-0.000	-16.260	0.000	0.000
7	1.0054	-21.5594	-0.000	-436.903	-0.000	-436.903	0.000	0.000
8	0.9929	-24.7429	-0.000	-9.550	233.800	74.450	233.800	84.000
9	0.9913	-25.7432	0.000	-30.300	522.000	145.700	522.000	176.000
10	1.0276	-31.7757	-4.792	-198.828	-4.792	-198.828	0.000	0.000
11	1.0160	-20.8338	0.000	-228.891	0.000	-228.891	0.000	0.000
12	1.0113	-21.1125	0.504	3.092	0.504	3.092	0.000	0.000
13	0.9980	-21.6477	-1.001	-27.221	6.499	60.779	7.500	88.000
14	1.0115	-22.0768	0.504	1.422	0.504	1.422	0.000	0.000
15	1.0062	-25.1331	0.000	-33.830	0.000	-33.830	0.000	0.000
16	1.0108	-29.2630	0.000	-26.850	320.000	126.150	320.000	153.000
17	1.0280	-29.4201	-0.000	-46.600	329.000	-14.300	329.000	32.300
18	1.0280	-29.6780	-0.000	-29.390	-0.000	-29.390	0.000	0.000
19	1.0236	-29.8765	0.000	-17.290	158.000	12.710	158.000	30.000
20	1.0447	-29.5178	-39.845	-812.303	-39.845	-812.303	0.000	0.000
21	0.9836	-34.6676	14.925	292.575	642.925	395.575	628.000	103.000
22	1.0291	-27.0021	0.000	-25.570	274.000	89.430	274.000	115.000

23	1.0484	-22.5398	0.000	-524.808	0.000	-524.808	0.000	0.000
24	1.0433	-22.7385	-4.290	-260.657	243.210	-176.057	247.500	84.600
25	1.0339	-29.3006	0.000	-21.450	308.600	-113.450	308.600	-92.000
26	1.0480	-26.1759	-5.672	-252.274	218.328	-205.074	224.000	47.200
27	1.0460	-27.6276	-0.000	-128.090	139.000	-111.090	139.000	17.000
28	1.0318	-29.7355	0.000	-28.060	281.000	47.440	281.000	75.500
29	1.0470	-24.0979	0.000	-51.460	206.000	-23.860	206.000	27.600
30	1.0478	-21.3292	-16.278	-381.328	267.222	-354.428	283.500	26.900
31	1.0000	-24.5949	0.000	134.753	0.000	134.753	0.000	0.000
32	0.9920	-12.9011	0.000	232.835	0.000	232.835	0.000	0.000
33	0.9972	-24.2885	21.626	438.689	21.626	438.689	0.000	0.000
34	1.0023	-34.7484	5.952	119.040	5.952	119.040	0.000	0.000
35	1.0493	-17.5714	0.000	540.721	0.000	540.721	0.000	0.000
36	1.0635	-14.8761	4.562	248.196	4.562	248.196	0.000	0.000
37	1.0378	-19.4233	5.976	231.057	5.976	231.057	0.000	0.000
38	1.0265	-14.2573	17.127	333.986	17.127	333.986	0.000	0.000
39	1.0400	-35.6441	9.872	143.367	1113.872	393.367	1104.000	250.000
Total			4.376	-833.167	6101.476	575.933	6097.100	1409.100

Line FLow and Losses

From Bus	To Bus	P MW	Q MVar	From Bus	To Bus	P MW	Q MVar	Line Loss MW	Line Loss MVar
2	3	0.000	0.000	3	2	-0.000	0.000	0.000	0.000
2	39	-4.792	-119.808	39	2	4.936	123.403	0.144	3.594
3	4	0.000	0.000	4	3	-0.000	0.000	0.000	0.000
3	26	0.000	0.000	26	3	-0.000	0.000	0.000	0.000
4	5	0.000	0.000	5	4	-0.000	0.000	0.000	0.000
4	19	0.000	0.000	19	4	-0.000	0.000	0.000	0.000
5	6	0.000	0.000	6	5	-0.000	0.000	0.000	0.000
5	15	0.000	0.000	15	5	-0.000	0.000	0.000	0.000
6	7	0.000	0.000	7	6	-0.000	0.000	0.000	0.000
6	9	0.000	0.000	9	6	-0.000	0.000	0.000	0.000
7	8	0.000	0.000	8	7	-0.000	0.000	0.000	0.000
7	12	0.000	0.000	12	7	-0.000	0.000	0.000	0.000
8	9	0.000	0.000	9	8	-0.000	0.000	0.000	0.000
9	10	0.000	0.000	10	9	-0.000	0.000	0.000	0.000

10	39	-4.792	-119.808	39	10	4.936	123.403	0.144	3.594
11	12	0.000	0.000	12	11	-0.000	0.000	0.000	0.000
11	14	0.000	0.000	14	11	-0.000	0.000	0.000	0.000
14	15	0.000	0.000	15	14	-0.000	0.000	0.000	0.000
15	16	0.000	0.000	16	15	-0.000	0.000	0.000	0.000
16	17	0.000	0.000	17	16	-0.000	0.000	0.000	0.000
17	18	0.000	0.000	18	17	-0.000	0.000	0.000	0.000
17	20	0.000	0.000	20	17	-0.000	0.000	0.000	0.000
17	22	0.000	0.000	22	17	-0.000	0.000	0.000	0.000
17	25	0.000	0.000	25	17	-0.000	0.000	0.000	0.000
18	19	0.000	0.000	19	18	-0.000	0.000	0.000	0.000
18	28	0.000	0.000	28	18	-0.000	0.000	0.000	0.000
22	23	0.000	0.000	23	22	-0.000	0.000	0.000	0.000
23	24	0.000	0.000	24	23	-0.000	0.000	0.000	0.000
24	25	0.000	0.000	25	24	-0.000	0.000	0.000	0.000
26	27	0.000	0.000	27	26	-0.000	0.000	0.000	0.000
27	28	0.000	0.000	28	27	-0.000	0.000	0.000	0.000
27	29	0.000	0.000	29	27	-0.000	0.000	0.000	0.000

27	30	0.000	0.000	30	27	-0.000	0.000	0.000	0.000
29	30	0.000	0.000	30	29	-0.000	0.000	0.000	0.000
13	12	0.000	0.000	12	13	-0.000	0.000	0.000	0.000
13	14	0.000	0.000	14	13	-0.000	0.000	0.000	0.000
7	1	0.000	-177.570	1	7	-0.000	186.005	0.000	8.435
11	32	-0.000	84.112	32	11	0.000	-82.598	0.000	1.514
20	33	0.906	18.384	33	20	-0.904	-18.332	0.003	0.051
21	34	-3.378	-67.555	34	21	3.419	68.386	0.042	0.831
23	35	0.000	-336.347	35	23	-0.000	352.928	0.000	16.582
24	36	-4.290	-233.377	36	24	4.562	248.196	0.272	14.819
26	37	-3.021	-116.827	37	26	3.105	120.075	0.084	3.248
3	31	-0.000	0.000	31	3	0.000	0.000	0.000	0.000
30	38	-8.477	-165.294	38	30	8.701	169.674	0.225	4.380
20	21	0.000	0.000	21	20	-0.000	0.000	0.000	0.000
Total Loss							0.913	57.049	

Settling time = 0.85307sec

Total system Inertia H = 33.5sec

Rate of Change of Frequency (ROCOF) = 0.032656Hz/sec

Best Global Power = 539.0675 MW

Part 4: Results of two wind farms with bus 39 generator Tripped.

Network Statistics			
No. of Buses	Lines	Generators	Loads
39.0000	46.0000	10.0000	19.0000

Solution Statistics		
P mismatch	Q mismatch	No of Iterations
-0.0000	-0.0000	10

Newton Raphson Loadflow Analysis

Bus No	V pu	Angle Degree	Injection MW	Injection MVar	Generation MW	Generation Mvar	Load MW	Load MVar
1	1.0475	0.0000	0.000	473.137	9.200	477.737	9.200	4.600
2	1.0160	-31.6659	-4.792	-192.248	-4.792	-192.248	0.000	0.000
3	1.0180	-18.1385	0.000	-186.566	0.000	-186.566	0.000	0.000
4	1.0085	-18.3827	0.000	-34.620	322.000	-32.220	322.000	2.400
5	0.9915	-18.0312	0.000	-24.690	500.000	159.310	500.000	184.000
6	0.9976	-16.9340	-0.000	-16.260	-0.000	-16.260	0.000	0.000
7	1.0028	-15.8360	-0.000	-436.903	-0.000	-436.903	0.000	0.000
8	0.9859	-19.5341	-0.000	-9.550	233.800	74.450	233.800	84.000
9	0.9824	-20.7951	0.000	-30.300	522.000	145.700	522.000	176.000
10	1.0075	-32.2421	-4.792	-198.828	-4.792	-198.828	0.000	0.000

11	1.0136	-13.1801	0.000	-228.891	0.000	-228.891	0.000	0.000
12	1.0086	-14.0792	0.504	3.092	0.504	3.092	0.000	0.000
13	0.9952	-13.9971	-1.001	-27.221	6.499	60.779	7.500	88.000
14	1.0087	-13.8086	0.504	1.422	0.504	1.422	0.000	0.000
15	1.0014	-15.2685	0.000	-33.830	0.000	-33.830	0.000	0.000
16	0.9996	-13.8100	0.000	-26.850	320.000	126.150	320.000	153.000
17	1.0147	-11.5498	-0.000	-46.600	329.000	-14.300	329.000	32.300
18	1.0149	-14.4677	-0.000	-29.390	-0.000	-29.390	0.000	0.000
19	1.0105	-16.4010	0.000	-17.290	158.000	12.710	158.000	30.000
20	1.0381	-2.9318	-39.845	-812.303	-39.845	-812.303	0.000	0.000
21	0.9680	-1.3051	14.925	292.575	642.925	395.575	628.000	103.000
22	1.0176	-8.2402	0.000	-25.570	274.000	89.430	274.000	115.000
23	1.0412	-2.8531	0.000	-524.808	0.000	-524.808	0.000	0.000
24	1.0362	-3.3735	-4.290	-260.657	243.210	-176.057	247.500	84.600
25	1.0210	-11.2283	0.000	-21.450	308.600	-113.450	308.600	-92.000
26	1.0440	-16.3864	-5.672	-252.274	218.328	-205.074	224.000	47.200
27	1.0403	-15.1581	-0.000	-128.090	139.000	-111.090	139.000	17.000
28	1.0229	-16.0369	0.000	-28.060	281.000	47.440	281.000	75.500

29	1.0440	-11.6111	0.000	-51.460	206.000	-23.860	206.000	27.600
30	1.0458	-8.8333	-16.278	-381.328	267.222	-354.428	283.500	26.900
31	1.0000	-15.5271	0.000	134.753	0.000	134.753	0.000	0.000
32	0.9920	-5.2279	0.000	232.835	0.000	232.835	0.000	0.000
33	1.0072	2.2309	21.626	438.689	21.626	438.689	0.000	0.000
34	0.9823	7.6813	5.952	119.040	5.952	119.040	0.000	0.000
35	1.0493	3.5031	0.000	540.721	0.000	540.721	0.000	0.000
36	1.0635	4.5361	4.562	248.196	4.562	248.196	0.000	0.000
37	1.0378	-9.6135	5.976	231.057	5.976	231.057	0.000	0.000
38	1.0265	-1.7534	17.127	333.986	17.127	333.986	0.000	0.000
39	1.0300	-39.6371	9.872	143.367	1113.872	393.367	1104.000	250.000
Total			4.376	-833.167	6101.476	575.933	6097.100	1409.100

Line FLow and Losses

From Bus	To Bus	P MW	Q MVar	From Bus	To Bus	P MW	Q MVar	Line Loss MW	Line Loss MVar
2	3	0.000	0.000	3	2	-0.000	0.000	0.000	0.000
2	39	-4.792	-119.808	39	2	4.936	123.403	0.144	3.594
3	4	0.000	0.000	4	3	-0.000	0.000	0.000	0.000

3	26	0.000	0.000	26	3	-0.000	0.000	0.000	0.000
4	5	0.000	0.000	5	4	-0.000	0.000	0.000	0.000
4	19	0.000	0.000	19	4	-0.000	0.000	0.000	0.000
5	6	0.000	0.000	6	5	-0.000	0.000	0.000	0.000
5	15	0.000	0.000	15	5	-0.000	0.000	0.000	0.000
6	7	0.000	0.000	7	6	-0.000	0.000	0.000	0.000
6	9	0.000	0.000	9	6	-0.000	0.000	0.000	0.000
7	8	0.000	0.000	8	7	-0.000	0.000	0.000	0.000
7	12	0.000	0.000	12	7	-0.000	0.000	0.000	0.000
8	9	0.000	0.000	9	8	-0.000	0.000	0.000	0.000
9	10	0.000	0.000	10	9	-0.000	0.000	0.000	0.000
10	39	-4.792	-119.808	39	10	4.936	123.403	0.144	3.594
11	12	0.000	0.000	12	11	-0.000	0.000	0.000	0.000
11	14	0.000	0.000	14	11	-0.000	0.000	0.000	0.000
14	15	0.000	0.000	15	14	-0.000	0.000	0.000	0.000
15	16	0.000	0.000	16	15	-0.000	0.000	0.000	0.000
16	17	0.000	0.000	17	16	-0.000	0.000	0.000	0.000
17	18	0.000	0.000	18	17	-0.000	0.000	0.000	0.000

17	20	0.000	0.000	20	17	-0.000	0.000	0.000	0.000
17	22	0.000	0.000	22	17	-0.000	0.000	0.000	0.000
17	25	0.000	0.000	25	17	-0.000	0.000	0.000	0.000
18	19	0.000	0.000	19	18	-0.000	0.000	0.000	0.000
18	28	0.000	0.000	28	18	-0.000	0.000	0.000	0.000
22	23	0.000	0.000	23	22	-0.000	0.000	0.000	0.000
23	24	0.000	0.000	24	23	-0.000	0.000	0.000	0.000
24	25	0.000	0.000	25	24	-0.000	0.000	0.000	0.000
26	27	0.000	0.000	27	26	-0.000	0.000	0.000	0.000
27	28	0.000	0.000	28	27	-0.000	0.000	0.000	0.000
27	29	0.000	0.000	29	27	-0.000	0.000	0.000	0.000
27	30	0.000	0.000	30	27	-0.000	0.000	0.000	0.000
29	30	0.000	0.000	30	29	-0.000	0.000	0.000	0.000
13	12	0.000	0.000	12	13	-0.000	0.000	0.000	0.000
13	14	0.000	0.000	14	13	-0.000	0.000	0.000	0.000
7	1	0.000	-177.570	1	7	-0.000	186.005	0.000	8.435
11	32	-0.000	84.112	32	11	0.000	-82.598	0.000	1.514
20	33	0.906	18.384	33	20	-0.904	-18.332	0.003	0.051

---

21 34 -3.378 -67.555 34 21 3.419 68.386 0.042 0.831

---

23 35 0.000 -336.347 35 23 -0.000 352.928 0.000 16.582

---

24 36 -4.290 -233.377 36 24 4.562 248.196 0.272 14.819

---

26 37 -3.021 -116.827 37 26 3.105 120.075 0.084 3.248

---

3 31 -0.000 0.000 31 3 0.000 0.000 0.000 0.000

---

30 38 -8.477 -165.294 38 30 8.701 169.674 0.225 4.380

---

20 21 0.000 0.000 21 20 -0.000 0.000 0.000 0.000

Total Loss 0.913 57.049

Settling time = 0.76394sec

Total system Inertia H = 30sec

Rate of Change of Frequency (ROCOF) = 0.036466Hz/sec

Best Global Power = 740.8843 MW

Part 5: Results of two wind farms with two generators at bus 38 and 39 Tripped.

| Network Statistics |

|No. of Buses | Lines |Generators |Loads |

39.0000 46.0000 10.0000 19.0000

| Solution Statistics |

|P mismatch | Q mismatch|No of Iterations |

-0.0000 -0.0000 10

Newton Raphson Loadflow Analysis

| Bus | V | Angle | Injection | Generation | Load |

| No | pu | Degree | MW | MVar | MW | Mvar | MW | MVar |

1	1.0475	0.0000	0.000	473.137	9.200	477.737	9.200	4.600
2	1.0002	-64.8394	-4.792	-192.248	-4.792	-192.248	0.000	0.000
3	0.9918	-53.7690	0.000	-186.566	0.000	-186.566	0.000	0.000
4	0.9548	-51.6923	0.000	-34.620	322.000	-32.220	322.000	2.400
5	0.8996	-44.6461	0.000	-24.690	500.000	159.310	500.000	184.000
6	0.8887	-38.5520	-0.000	-16.260	-0.000	-16.260	0.000	0.000
7	0.8931	-36.1579	-0.000	-436.903	-0.000	-436.903	0.000	0.000
8	0.8739	-41.6182	-0.000	-9.550	233.800	74.450	233.800	84.000
9	0.8711	-43.6204	0.000	-30.300	522.000	145.700	522.000	176.000
10	0.9360	-61.1604	-4.792	-198.828	-4.792	-198.828	0.000	0.000
11	0.9235	-35.9199	0.000	-228.891	0.000	-228.891	0.000	0.000
12	0.9121	-36.0480	0.504	3.092	0.504	3.092	0.000	0.000
13	0.8993	-36.8921	-1.001	-27.221	6.499	60.779	7.500	88.000
14	0.9188	-37.6007	0.504	1.422	0.504	1.422	0.000	0.000
15	0.9160	-41.7588	0.000	-33.830	0.000	-33.830	0.000	0.000
16	0.9425	-45.8229	0.000	-26.850	320.000	126.150	320.000	153.000
17	0.9706	-45.6827	-0.000	-46.600	329.000	-14.300	329.000	32.300
18	0.9651	-50.2345	-0.000	-29.390	-0.000	-29.390	0.000	0.000

19	0.9596	-51.2807	0.000	-17.290	158.000	12.710	158.000	30.000
20	1.0132	-37.3178	-39.845	-812.303	-39.845	-812.303	0.000	0.000
21	0.9554	-36.2518	14.925	292.575	642.925	395.575	628.000	103.000
22	0.9823	-42.4966	0.000	-25.570	274.000	89.430	274.000	115.000
23	1.0154	-37.1693	0.000	-524.808	0.000	-524.808	0.000	0.000
24	1.0133	-37.5999	-4.290	-260.657	243.210	-176.057	247.500	84.600
25	0.9801	-45.4250	0.000	-21.450	308.600	-113.450	308.600	-92.000
26	1.0042	-54.2788	-5.672	-252.274	218.328	-205.074	224.000	47.200
27	0.9980	-59.9108	-0.000	-128.090	139.000	-111.090	139.000	17.000
28	0.9740	-56.8538	0.000	-28.060	281.000	47.440	281.000	75.500
29	1.0230	-67.3252	0.000	-51.460	206.000	-23.860	206.000	27.600
30	1.0326	-67.8962	-16.278	-381.328	267.222	-354.428	283.500	26.900
31	0.9800	-51.0340	0.000	134.753	0.000	134.753	0.000	0.000
32	0.9420	-26.7192	0.000	232.835	0.000	232.835	0.000	0.000
33	0.9872	-31.9286	21.626	438.689	21.626	438.689	0.000	0.000
34	0.9823	-27.9514	5.952	119.040	5.952	119.040	0.000	0.000
35	1.0293	-31.0798	0.000	540.721	0.000	540.721	0.000	0.000
36	1.0635	-29.5348	4.562	248.196	4.562	248.196	0.000	0.000

37	1.0278	-47.2119	5.976	231.057	5.976	231.057	0.000	0.000
38	1.0265	-67.9519	17.127	333.986	17.127	333.986	0.000	0.000
39	1.0100	-71.3173	9.872	143.367	1113.872	393.367	1104.000	250.000
Total			4.376	-833.167	6101.476	575.933	6097.100	1409.100

Line FLow and Losses

From Bus	To Bus	P MW	Q MVar	From Bus	To Bus	P MW	Q MVar	Line Loss MW	Line Loss MVar
2	3	0.000	0.000	3	2	-0.000	0.000	0.000	0.000
2	39	-4.792	-119.808	39	2	4.936	123.403	0.144	3.594
3	4	0.000	0.000	4	3	-0.000	0.000	0.000	0.000
3	26	0.000	0.000	26	3	-0.000	0.000	0.000	0.000
4	5	0.000	0.000	5	4	-0.000	0.000	0.000	0.000
4	19	0.000	0.000	19	4	-0.000	0.000	0.000	0.000
5	6	0.000	0.000	6	5	-0.000	0.000	0.000	0.000
5	15	0.000	0.000	15	5	-0.000	0.000	0.000	0.000
6	7	0.000	0.000	7	6	-0.000	0.000	0.000	0.000
6	9	0.000	0.000	9	6	-0.000	0.000	0.000	0.000
7	8	0.000	0.000	8	7	-0.000	0.000	0.000	0.000

7	12	0.000	0.000	12	7	-0.000	0.000	0.000	0.000
8	9	0.000	0.000	9	8	-0.000	0.000	0.000	0.000
9	10	0.000	0.000	10	9	-0.000	0.000	0.000	0.000
10	39	-4.792	-119.808	39	10	4.936	123.403	0.144	3.594
11	12	0.000	0.000	12	11	-0.000	0.000	0.000	0.000
11	14	0.000	0.000	14	11	-0.000	0.000	0.000	0.000
14	15	0.000	0.000	15	14	-0.000	0.000	0.000	0.000
15	16	0.000	0.000	16	15	-0.000	0.000	0.000	0.000
16	17	0.000	0.000	17	16	-0.000	0.000	0.000	0.000
17	18	0.000	0.000	18	17	-0.000	0.000	0.000	0.000
17	20	0.000	0.000	20	17	-0.000	0.000	0.000	0.000
17	22	0.000	0.000	22	17	-0.000	0.000	0.000	0.000
17	25	0.000	0.000	25	17	-0.000	0.000	0.000	0.000
18	19	0.000	0.000	19	18	-0.000	0.000	0.000	0.000
18	28	0.000	0.000	28	18	-0.000	0.000	0.000	0.000
22	23	0.000	0.000	23	22	-0.000	0.000	0.000	0.000
23	24	0.000	0.000	24	23	-0.000	0.000	0.000	0.000
24	25	0.000	0.000	25	24	-0.000	0.000	0.000	0.000

26	27	0.000	0.000	27	26	-0.000	0.000	0.000	0.000
27	28	0.000	0.000	28	27	-0.000	0.000	0.000	0.000
27	29	0.000	0.000	29	27	-0.000	0.000	0.000	0.000
27	30	0.000	0.000	30	27	-0.000	0.000	0.000	0.000
29	30	0.000	0.000	30	29	-0.000	0.000	0.000	0.000
13	12	0.000	0.000	12	13	-0.000	0.000	0.000	0.000
13	14	0.000	0.000	14	13	-0.000	0.000	0.000	0.000
7	1	0.000	-177.570	1	7	-0.000	186.005	0.000	8.435
11	32	-0.000	84.112	32	11	0.000	-82.598	0.000	1.514
20	33	0.906	18.384	33	20	-0.904	-18.332	0.003	0.051
21	34	-3.378	-67.555	34	21	3.419	68.386	0.042	0.831
23	35	0.000	-336.347	35	23	-0.000	352.928	0.000	16.582
24	36	-4.290	-233.377	36	24	4.562	248.196	0.272	14.819
26	37	-3.021	-116.827	37	26	3.105	120.075	0.084	3.248
3	31	-0.000	0.000	31	3	0.000	0.000	0.000	0.000
30	38	-8.477	-165.294	38	30	8.701	169.674	0.225	4.380
20	21	0.000	0.000	21	20	-0.000	0.000	0.000	0.000
Total Loss								0.913	57.049

Settling time = 0.68755sec

Total system Inertia H = 27sec

Rate of Change of Frequency (ROCOF) = 0.040518Hz/sec

Best Global Power = 756.4451MW

APPENDIX C.

Coding and Algorithms

NEWTON RAPHSON CODE.

```
% Program for Newton-Raphson Load Flow Analysis
% Bus number 1 is assumed to be slask bus..
clc
Y = ybusppg39();          % Get Y-Bus..
busdata = busdata39();     % Get Bus Data..
linedata = linedata39();   % Get Line Data
BestSol = psoWT39();       % Get PSO in NR

% Calculate reactive power output of a wind farm as a ratio of active power.

Rr = 0.01; % pu value of rotor winding resistance
Xs = 0.10;% pu value of stator winding reactannce
Xr = 0.08; % pu value of rotor winding reactance
Xk= 0.18; % pu value of the sum of stator winding and rotor winding reactance
Xm =  3.00; % pu excitation reactance
W =(BestSol.Position(1,:)); % Get the Rotor speed in rads/Second
Wmax=max(BestSol.Position(1,:)); % without loss of generality because power is a single value then any rotor speed in the selected range gives Best power.
% G=30; % where the Gear Ratio is 1:30 for the DFIG
Ws=2*pi*50; % the Synchronous speed of the DFIG
F=(Ws-(Wmax*pi/30))/Ws;% slip of the DFIG
K =((Rr^2 + Xk*(Xk + Xm)*F^2)*BestSol.Power(1,1))/(Rr*Xm*F*10^6);% Calculate reactive power

% Update Buses with Active and Reactive Power
%busdata(31,5)= (BestSol.Power(1,1)/(1*10^6));% Update Bus 31 with wind farm active power
%busdata(31,6)= K;                        % Update Bus 31 with wind farm reactive power
%busdata(32,5)= (BestSol.Power(1,1)/(1*10^6));% Update Bus 32 with wind farm active power
%busdata(32,6)= K;                        % Update Bus 32 with wind farm reactive power
%busdata(33,5)= (BestSol.Power(1,1)/(1*10^6));% Update Bus 33 with wind turbine active power
%busdata(33,6)= K;                        % Update Bus 33 with wind farm reactive power
busdata(34,5)= (BestSol.Power(1,1)/(1*10^6));% Update Bus 34 with wind turbine active power
busdata(34,6)= K;                        % Update Bus 34 with wind farm reactive power
busdata(35,5)= (BestSol.Power(1,1)/(1*10^6));% Update Bus 35 with wind turbine active power
busdata(35,6)= K;                        % Update Bus 35 with wind farm reactive power

%busdata(36,5)= (BestSol.Power(1,1)/(1*10^6));% Update Bus 36 with wind turbine active power
%busdata(36,6)= K;                        % Update Bus 36 with wind farm reactive power
%busdata(37,5)= (BestSol.Power(1,1)/(1*10^6));% Update Bus 37 with wind turbine active power
%busdata(37,6)= K;                        % Update Bus 37 with wind farm reactive power
%busdata(38,5)= (BestSol.Power(1,1)/(1*10^6));% Update Bus 38 with wind turbine active power
%busdata(38,6)= K;                        % Update Bus 38 with wind farm reactive power
%busdata(39,5)= (BestSol.Power(1,1)/(1*10^6));% Update Bus 39 with wind turbine active power for Hydro plant
%busdata(39,6)= K;                        % Update Bus 39 with wind farm reactive power for Hydro plant


baseMVA = 100;            % Base MVA..
fb = linedata(:,1);        % From bus number...
tb = linedata(:,2);        % To bus number...
nbranch = length(fb);      % Number of branches
bus = busdata(:,1);        % Bus Number..
type = busdata(:,2);       % Type of Bus 1-Slack, 2-PV, 3-PQ..
V = busdata(:,3);          % Specified Voltage..
del = busdata(:,4);        % Voltage Angle..
Vm = pol2rec(V,del);       % Converting polar to rectangular..
Pg = busdata(:,5);         % PGi..
Qg = busdata(:,6);         % QGi..
Pl = busdata(:,7);         % PLi..
Ql = busdata(:,8);         % QLi..
Qmin = busdata(:,9);       % Minimum Reactive Power Limit..
Qmax = busdata(:,10);      % Maximum Reactive Power Limit..
nbus = max(bus);           % To get no. of buses..
```

```
P = Pg - Pl;                % Pi = PGi - PLi..
Q = Qg - Ql;                % Qi = QGi - QLi..
P = P/baseMVA;              % Converting to p.u..
Q = Q/baseMVA;
Qmin = Qmin/baseMVA;
Qmax = Qmax/baseMVA;
Tol = 10;     % Tolerence kept at high value.
Iter = 1;  % iteration starting
Psp = P;
Qsp = Q;
G = real(Y);    % Conductance..
B = imag(Y);    % Susceptance..
pv = find(type == 2 | type == 1); % Index of PV Buses..
pq = find(type == 3); % Index of PQ Buses..
npv = length(pv); % Number of PV buses..
npq = length(pq); % Number of PQ buses..
while (Tol > 1e-5)   % Iteration starting..
   P = zeros(nbus,1);
   Q = zeros(nbus,1);
   % Calculate P and Q
   for i = 1:nbus
      for k = 1:nbus
         P(i) = P(i) + V(i)* V(k)*(G(i,k)*cos(del(i)-del(k)) + B(i,k)*sin(del(i)-del(k)));
         Q(i) = Q(i) + V(i)* V(k)*(G(i,k)*sin(del(i)-del(k)) - B(i,k)*cos(del(i)-del(k)));
      end
   end

   % Checking Q-limit violations..
   if Iter <= 7 && Iter >= 2
      for n = 2:nbus
         if type(n) == 2
            if Q(n) < Qmin(n)
               V(n) = V(n) + 0.01;
            elseif Q(n) > Qmax(n)
               V(n) = V(n) - 0.01;
            end
         end
       end
   end

   % Calculate change from specified value
   dPa = Psp-P;
   dQa = Qsp-Q;
   dQ = zeros(npq,1);
   k = 1;
   for i = 1:nbus
      if type(i) == 3
         dQ(k,1) = dQa(i);
         k = k+1;
      end
   end

   dP = dPa(2:nbus);
   M = [dP; dQ];       % Mismatch Vector

   % Jacobian
   % J1 - Derivative of Real Power Injections with Angles..
   J1 = zeros(nbus-1,nbus-1);
   for i = 1:(nbus-1)
      m = i+1;
      for k = 1:(nbus-1)
         n = k+1;
         if n == m
            for q = 1:nbus
               J1(i,k) = J1(i,k) + V(m)* V(q)*(-G(m,q)*sin(del(m)-del(q)) + B(m,q)*cos(del(m)-del(q)));
            end
            J1(i,k) = J1(i,k) - V(m)^2*B(m,m);
         else
            J1(i,k) = V(m)* V(n)*(G(m,n)*sin(del(m)-del(n)) - B(m,n)*cos(del(m)-del(n)));
         end
```

```
        end
    end

    % J2 - Derivative of Real Power Injections with V..
    J2 = zeros(nbus-1,npq);
    for i = 1:(nbus-1)
        m = i+1;
        for k = 1:npq
            n = pq(k);
            if n == m
                for q = 1:nbus
                    J2(i,k) = J2(i,k) + V(q)*(G(m,q)*cos(del(m)-del(q)) + B(m,q)*sin(del(m)-del(q)));
                end
                J2(i,k) = J2(i,k) + V(m)*G(m,m);
            else
                J2(i,k) = V(m)*(G(m,n)*cos(del(m)-del(n)) + B(m,n)*sin(del(m)-del(n)));
            end
        end
    end

    % J3 - Derivative of Reactive Power Injections with Angles..
    J3 = zeros(npq,nbus-1);
    for i = 1:npq
        m = pq(i);
        for k = 1:(nbus-1)
            n = k+1;
            if n == m
                for q = 1:nbus
                    J3(i,k) = J3(i,k) + V(m)* V(q)*(G(m,q)*cos(del(m)-del(q)) + B(m,q)*sin(del(m)-del(q)));
                end
                J3(i,k) = J3(i,k) - V(m)^2*G(m,m);
            else
                J3(i,k) = V(m)* V(n)*(-G(m,n)*cos(del(m)-del(n)) - B(m,n)*sin(del(m)-del(n)));
            end
        end
    end

    % J4 - Derivative of Reactive Power Injections with V..
    J4 = zeros(npq,npq);
    for i = 1:npq
        m = pq(i);
        for k = 1:npq
            n = pq(k);
            if n == m
                for q = 1:nbus
                    J4(i,k) = J4(i,k) + V(q)*(G(m,q)*sin(del(m)-del(q)) - B(m,q)*cos(del(m)-del(q)));
                end
                J4(i,k) = J4(i,k) - V(m)*B(m,m);
            else
                J4(i,k) = V(m)*(G(m,n)*sin(del(m)-del(n)) - B(m,n)*cos(del(m)-del(n)));
            end
        end
    end

    J = [J1 J2; J3 J4];     % Jacobian

    X = inv(J)*M;           % Correction Vector
    dTh = X(1:nbus-1);
    dV = X(nbus:end);
    del(2:nbus) = dTh + del(2:nbus);
    k = 1;
    for i = 2:nbus
        if type(i) == 3
            V(i) = dV(k) + V(i);
            k = k+1;
        end
    end
    Iter = Iter + 1;
    Tol = max(abs(M));
end
```

```
Iter = Iter - 1; % Number of Iterations took..
V;
Del = 180/pi*del;
E1 = [V Del]; % Bus Voltages and angles..
Px=sum(dP);       % Maximum P mismatch in p.u.
Qx=sum(dQ);       % Maximum Q mismatch in p.u.
nloads=sum(sum(Pl~=0,7)); % Number of loads

Iij = zeros(nbus,nbus);
Sij = zeros(nbus,nbus);
Si = zeros(nbus,1);
% Bus Current Injections..
I = Y*Vm;
Im = abs(I);
Ia = angle(I);
%Line Current Flows..
for m = 1:nbranch
   p = fb(m); q = tb(m);
   Iij(p,q) = -(Vm(p) - Vm(q))*Y(p,q); % Y(m,n) = -y(m,n)..
   Iij(q,p) = -Iij(p,q);

end
%Iij = sparse(Iij);     % Commented out..
Iijm = abs(Iij);
Iija = angle(Iij);
% Line Power Flows..
for m = 1:nbus
   for n = 1:nbus
      if m ~= n
         Sij(m,n) = Vm(m)*conj(Iij(m,n))*baseMVA;
      end
   end
end
%Sij = sparse(Sij);     % Commented out..
Pij = real(Sij);
Qij = imag(Sij);

% Line Losses..
Lij = zeros(nbranch,1);
for m = 1:nbranch
   p = fb(m); q = tb(m);
   Lij(m) = Sij(p,q) + Sij(q,p);
end
Lpij = real(Lij);
Lqij = imag(Lij);

% Bus Power Injections..
for i = 1:nbus
   for k = 1:nbus
      Si(i) = Si(i) + conj(Vm(i))* Vm(k)*Y(i,k)*baseMVA;
   end
end

Pi = real(Si);
Qi = -imag(Si);
Pg = Pi+Pl;
Qg = Qi+Ql;
disp ('-------------------------------------------------------------------------------');
disp ('|  Network Statistics                                    |');
disp ('|No. of Buses | Lines    |Generators   |Loads                |');

   fprintf('    %8.4f', nbus ),fprintf('    %8.4f', nbranch ),fprintf('    %8.4f', npv ),fprintf('    %8.4f', nloads );fprintf('\n');
disp ('-------------------------------------------------------------------------------');
disp ('|  Solution Statistics                        |');
disp ('|P mismatch | Q mismatch|No of Iterations |');

   fprintf('    %8.4f', Px ),fprintf('    %8.4f', Qx ),fprintf('    %4g', Iter );fprintf('\n');
```

```
disp('-----------------------------------------------------------------------------------------');
disp('                          Newton Raphson Loadflow Analysis ');
disp('-----------------------------------------------------------------------------------------');
disp('| Bus |    V   | Angle |     Injection      |     Generation     |         Load      |');
disp('| No  |   pu   | Degree |    MW   |   MVar   |    MW   |  Mvar    |     MW     | MVar | ');
for m = 1:nbus
   disp('-----------------------------------------------------------------------------------------');
   fprintf('%3g', m); fprintf('  %8.4f', V(m)); fprintf('   %8.4f', Del(m));
   fprintf('  %8.3f', Pi(m)); fprintf('   %8.3f', Qi(m));
   fprintf('  %8.3f', Pg(m)); fprintf('   %8.3f', Qg(m));
   fprintf('  %8.3f', Pl(m)); fprintf('   %8.3f', Ql(m)); fprintf('\n');
end
disp('-----------------------------------------------------------------------------------------');
fprintf(' Total                 ');fprintf('  %8.3f', sum(Pi)); fprintf('   %8.3f', sum(Qi));
fprintf('  %8.3f', sum(Pi+Pl)); fprintf('   %8.3f', sum(Qi+Ql));
fprintf('  %8.3f', sum(Pl)); fprintf('   %8.3f', sum(Ql)); fprintf('\n');
disp('-----------------------------------------------------------------------------------------');
disp('                                                                                          ');

disp('-----------------------------------------------------------------------------------------');
disp('                          Line FLow and Losses ');
disp('-----------------------------------------------------------------------------------------');
disp('|From|To |    P    |    Q     | From| To |    P     |    Q     |      Line Loss      |');
disp('|Bus |Bus|   MW    |   MVar   | Bus | Bus|    MW    |  MVar    |     MW    |    MVar  |');
for m = 1:nbranch
   p = fb(m); q = tb(m);
   disp('-----------------------------------------------------------------------------------------');
   fprintf('%4g', p); fprintf('%4g', q); fprintf('  %8.3f', Pij(p,q)); fprintf('   %8.3f', Qij(p,q));
   fprintf('   %4g', q); fprintf('%4g', p); fprintf('   %8.3f', Pij(q,p)); fprintf('   %8.3f', Qij(q,p));
   fprintf('  %8.3f', Lpij(m)); fprintf('   %8.3f', Lqij(m));
   fprintf('\n');
end

disp('-----------------------------------------------------------------------------------------');
fprintf('   Total Loss                                                  ');
fprintf('  %8.3f', sum(Lpij)); fprintf('   %8.3f', sum(Lqij));  fprintf('\n');
disp('-----------------------------------------------------------------------------------------');


%fs=1600;

%t= 0:1/fs:10-1/fs;
%for m=31:nbus
%fi=(1/(2*pi))*Del(m)./t(m);
%y=imag(hilbert(fi,16000))';
%end



word = actxserver('Word.Application');      %start Word
word.Visible =1;                            %make Word Visible
document=word.Documents.Add;                %create new Document
selection=word.Selection;                   %set Cursor
selection.Font.Name='Courier New';          %set Font
selection.Font.Size=9;                      %set Size

selection.Pagesetup.RightMargin=28.34646;   %set right Margin to 1cm
selection.Pagesetup.LeftMargin=28.34646;    %set left Margin to 1cm
selection.Pagesetup.TopMargin=28.34646;     %set top Margin to 1cm
selection.Pagesetup.BottomMargin=28.34646;  %set bottom Margin to 1cm
                                            %1cm is circa 28.34646 points
selection.Paragraphs.LineUnitAfter=0.01;    %sets the amount of spacing
                                            %between paragraphs(in gridlines)



Figure (1)
bar(bus,V);
bar(V,0.5)
title('Voltage Magnitude Profile')
```

```
xlabel('Bus Number')
ylabel('Bus Voltage(pu)')

Figure (2)
bar(bus,Pi);
bar(Pi,0.5);
title('Real Power Injected Profile')
xlabel('Bus Number')
ylabel('Real Power Injected(MW)')

Figure (3)
bar(bus,Qi);
bar(Qi,0.5);
title('Reactive Power Injected Profile')
xlabel('Bus Number')
ylabel('Reactive Power Injected(MVARS)')

Figure (4)
bar(bus,del);
bar(del,0.5);
title('Phase Angle Profile')
xlabel('Bus Number')
ylabel('Angle Degrees')

% close Figure 1 ;
Hi=busdata(:,11);
% Calculating total inertia of the system
Htot=sum(Hi);
% Calculating the rate of change of frequency in Hz/s
rocof=sum(Pi)*50/(2*Htot*100);
% Calculating frequency of the grid.

%fn=2*100*rocof*Htot/sum(Pi);

%%DFIG mimicking the synchronous Generator
%Disturbance = menu('Define the direction of the  disturbance in Power Angle: (1 for +ve and 2 for -ve)', 1,2);

%if Disturbance == 1

   Dpa0 = 1*pi/180; % Displacement of the Power Angle from the initial operating point

%elseif Disturbance == 2

  % Dpa0 = (-1*pi/180);% Negative disturbance in the Power Angle from the initial operating point
%end
%%%%%%%%%Generator Values from IEEE39 Bus System
   Exc_Voltage = 1.0;% Per unit excitation Voltage of Generator to its own base

   Vt= 1.0;% % Per Unit Generator Terminal Voltage to its own base

   X=0.280;% Unsaturated d axis transient reactance in p.u.

   Damp_Coeff=2;% Damping power coefficient

   f0 = 50;% System frequency

   Power_Del=222.8908/100;% Power Delivered to the 'infinite bus'

   Pow_max = Exc_Voltage*Vt/X; % Maximum power of the machine

   d0 = asin (Power_Del/Pow_max);% Initial angle of operation

   Pow_Sync = Pow_max*cos (d0);% Synchronizing power coefficient


    wn = sqrt (pi*50/Htot *Pow_Sync);% Undamped oscillation frequency

    z = Damp_Coeff/2*sqrt (pi*50/(Htot*Pow_Sync));% Damping factor

    wd = wn*sqrt (1-z^2); %Damped oscillation frequency in radians per second
```

```
    fd = wd/(2*pi);% Damped oscillation frequency in hertz

    tau = 1/(z*wn);% Time constant

    t_settling = 4.*tau; % settling time

    th = acos (z);% Phase angle

    t = 0:.01:5; % Time axis parameters

    Dw = Dpa0/sqrt (1-z^2)*exp (-z*wn*t).*(-z*wn*sin (wd*t+th)+wd*cos(wd*t+th)); %transient response of the deviation in frequency

    f = f0+Dw/(2*pi);% Frequency in Hz

    disp(['Settling time  = ' num2str(t_settling) 'sec'])
    disp(['Total system Inertia H = ' num2str(Htot) 'sec'])
    disp(['Rate of Change of Frequency (ROCOF)= ' num2str(rocof) 'Hz/sec'])
    disp(['Best Global Power = ' num2str(BestSol.Power(1,1)/(1*10^6)) 'MW'])

        % Frequency plot
Figure(5)
title('Frequency Profile')
plot(t,f),grid %Plot transient response of frequency
xlabel('Time(s)')
ylabel('Frequency(Hz)')

figtoprint=Figure (5);                    %opens new Figure window
print(figtoprint,'-dmeta');               %print Figure to clipboard
invoke(word.Selection,'Paste');           %paste Figure to Word

hold on;
```

Y BUS CODE.

```
% Program to form Admittance And Impedance Bus Formation....
% with Transformer Tap setting..
function ybus = ybusppg39()  % Returns ybus
linedata = linedata39(); % Calling "linedata3.m" for Line Data...
fb = linedata(:,1);     % From bus number...
tb = linedata(:,2);     % To bus number...
r = linedata(:,3);      % Resistance, R...
x = linedata(:,4);      % Reactance, X...
b = linedata(:,5);    % Ground Admittance, B/2...
a = linedata(:,6);      % Tap setting value..
z = r + 1i*x;           % Z matrix...
y = 1./z;               % To get inverse of each element...
b = 1i*b;               % Make B imaginary...
nbus = max(max(fb),max(tb));    % no. of buses...
nbranch = length(fb);           % no. of branches...
ybus = zeros(nbus,nbus);        % Initialise YBus...
 % Formation of the Off Diagonal Elements...
 for k = 1:nbranch
    ybus(fb(k),tb(k)) = ybus(fb(k),tb(k))-y(k)/a(k);
    ybus(tb(k),fb(k)) = ybus(fb(k),tb(k));
 end

 % Formation of Diagonal Elements....
 for m = 1:nbus
    for n = 1:nbranch
       if fb(n) == m
          ybus(m,m) = ybus(m,m) + y(n)/(a(n)^2) + b(n);
       elseif tb(n) == m
          ybus(m,m) = ybus(m,m) + y(n) + b(n);
       end
    end
 end
```

SHUNT ADMITTANCE CODE.

```
% Line Data for B-Bus (Shunt Admittance)Formation.
function bbus = bbusppg()     % Returns B-bus..
linedata = linedata30();
fb = linedata(:,1);
tb = linedata(:,2);
b = linedata(:,5);
nbus = max(max(fb),max(tb));    % no. of buses...
nbranch = length(fb);           % no. of branches...
bbus = zeros(nbus,nbus);
 for k=1:nbranch
    bbus(fb(k),tb(k)) = b(k);
    bbus(tb(k),fb(k)) = bbus(fb(k),tb(k));
 end
```

BUS DATA.

```
function busdata = busdata39()
%        |Bus | Type | Vsp | theta | PGi | QGi     | PLi | QLi |  Qmin | Qmax|  Hi |
busdata = [ 1     1    1.0475  0       0          0   9.2   4.6       0    0       0;
          2    3    1.00    0       0          0     0     0       0    0       0;
          3    3    1.00    0       0          0     0     0       0    0       0 ;
          4    3    1.0     0       0          0  322.0    2.4     0    0       0 ;
          5    3    1.0     0       0          0  500.0   184.0    0    0       0 ;
          6    3    1.0     0       0          0     0     0       0    0       0 ;
          7    3    1.0     0       0          0    0.0    0.0     0    0       0 ;
          8    3    1.0     0       0          0  233.8   84.0     0    0       0 ;
          9    3    1.0     0       0          0  522.0   176.0    0    0       0  ;
          10   3    1.0     0       0          0    0.0    0.0     0    0       0  ;
          11   3    1.0     0       0          0    0.0    0.0     0    0       0 ;
          12   3    1.0     0       0          0   0.0    0.0      0    0       0 ;
          13   3    1.0     0       0          0   7.5    88.0     0    0       0 ;
          14   3    1.0     0       0          0   0.0    0.0      0    0       0  ;
          15   3    1.0     0       0          0    0.0   0.0      0    0       0 ;
          16   3    1.0     0       0          0   320.0  153.0    0    0       0;
          17   3    1.0     0       0          0   329.0   32.3    0    0       0;
          18   3    1.0     0       0          0    0.0    0.0     0    0       0;
          19   3    1.0     0       0          0   158.0   30.0    0    0       0;
          20   3    1.0     0       0          0    0.0    0.0     0    0       0;
          21   3    1.0     0       0          0   628.0  103.0    0    0       0;
          22   3    1.0     0       0          0   274.0  115.0    0    0       0;
          23   3    1.0     0       0          0    0.0    0.0     0    0       0;
          24   3    1.0     0       0          0   247.5  84.6     0    0       0;
          25   3    1.0     0       0          0   308.6  -92.0    0    0       0;
          26   3    1.0     0       0          0   224.0   47.2    0    0       0;
          27   3    1.0     0       0          0   139.0   17.0    0    0       0;
          28   3    1.0     0       0          0   281.0   75.5    0    0       0;
          29   3    1.0     0       0          0   206.0   27.6    0    0       0;
          30   3    1.0     0       0          0   283.5   26.9    0    0       0;
          31   2    1.0     0       250        0   0.0     0.0     0    0       0;

          32   2    0.9820  0       650        0    0.0    0.0    150  300   6.5;
          33   2    0.9972  0       632        0    0.0    0.0    0    250   6.5;
          34   2    1.0123  0       508        0    0.0    0.0    0    167   3.5;
          35   2    1.0493  0       650        0    0.0    0.0    -100 300   3.5;
          36   2    1.0635  0       560        0    0.0    0.0    0    240   3.5;
          37   2    1.0278  0       540        0    0.0    0.0    0    250   3.5;
          38   2    1.0265  0       0       0    0.0     0.0    -150 300   0;
          39   2    1.0300  0       0       0    1104.0  250.0  -100 300   0;];
```

FITNESS FUNCTION

```
function P = fitnessWT(S,dw,W)

A = 3903.625;          % using R=35.25 M
u = 1.1225;            % the Ro value,?=1.1225 kg/m3
```

```
%S=sym('S',[1,4]);       % Creating variable for speed
%Z=sum(1/2*u*A*C*S.^3);

C = 0.4535;% Normal,Power Coefficient of 0.3617 at 1 degree pitch angle and 7 tip speed ratio,abnormal 0.4535,

for m=1:8
 Z = 1/2*u*A*C*S(m)^3;
end
% syms W;
% f = 1/2*W^2;
%
% T1 = J1*(diff(f));
% T2 = J2*(diff(f));
% T3 = J3*(diff(f));
% T4 = J4*(diff(f));
J = 4.45e5;
%W=sym('W',[1,4]);
%T = sum(J*W*pi/30);

for n=1:8
 T= (J*dw*W*(pi)^2/900);            % the pi/30=2*Pi/60 to convert W to rads/sec
end          % the pi/30=2*Pi/60 to convert W to rads/sec
P1 = 10*(sum(Z-T));
P2= 25*(sum(Z-T));
%P5 = 5*(sum(Z-T));
P=P1+P2;

end


% P = symsum(Zm - Jm*Wdel*(diffWdel/dt),m,1:4);

% KE = 0.5*jm*wdel^2
%syms z
%S_symsum=symsum(z,k,1,4);

LINE DATA

% Line Data of IEEE-39 Bus System..
function linedata = linedata39()
%        | From | To   |  R     |  X     |     B/2  | X'mer |
%        | Bus  | Bus  | pu     | pu     |     pu   | TAP (a) |
linedata = [ 2      3       0.0035    0.0411     0.3494          1
             2      39      0.0010    0.0250     0.3750          1
             3      4       0.0013    0.0151     0.1286          1
             3      26      0.0070    0.0086     0.0730          1
             4      5       0.0013    0.0213     0.1107          1
             4      19      0.0011    0.0133     0.1069          1
             5      6       0.0008    0.0128     0.0671          1
             5      15      0.0008    0.0129     0.0691          1
             6      7       0.0002    0.0026     0.0217          1
             6      9       0.0008    0.0112     0.0738          1
             7      8       0.0006    0.0092     0.0565          1
             7      12      0.0007    0.0082     0.0695          1
             8      9       0.0004    0.0046     0.0390          1
             9      10      0.0023    0.0363     0.1902          1
             10     39      0.0010    0.0250     0.6000          1
             11     12      0.0004    0.0043     0.0365          1
             11     14      0.0004    0.0043     0.0365          1
             14     15      0.0009    0.0101     0.0862          1
             15     16      0.0018    0.0217     0.1830          1
             16     17      0.0009    0.0094     0.0855          1
             17     18      0.0007    0.0089     0.0671          1
             17     20      0.0016    0.0195     0.1520          1
             17     22      0.0008    0.0135     0.1274          1
             17     25      0.0003    0.0059     0.0340          1
             18     19      0.0007    0.0082     0.0660          1
             18     28      0.0013    0.0173     0.1608          1
             22     23      0.0008    0.0140     0.1283          1
             23     24      0.0006    0.0096     0.0923          1
```

```
24    25     0.0022   0.0350   0.1805        1
26    27     0.0032   0.0323   0.2565        1
27    28     0.0014   0.0147   0.1198        1
27    29     0.0043   0.0474   0.3901        1
27    30     0.0057   0.0625   0.5145        1
29    30     0.0014   0.0151   0.1245        1
13    12     0.0016   0.0435   0.0000        1.006
13    14     0.0016   0.0435   0.0000        1.006
7     1      0.0000   0.0250   0.0000        1.070
11    32     0.0000   0.0200   0.0000        1.070
20    33     0.0007   0.0142   0.0000        1.070
21    34     0.0009   0.0180   0.0000        1.009
23    35     0.0000   0.0143   0.0000        1.025
24    36     0.0005   0.0272   0.0000        1.000
26    37     0.0006   0.0232   0.0000        1.025
3     31     0.0000   0.0181   0.0000        1.025
30    38     0.0008   0.0156   0.0000        1.025
20    21     0.0007   0.0138   0.0000        1.060];
```

POLAR TO RECTANGULAR COORDINATES

```
% Polar to Rectangular Conversion
% [RECT] = RECT2POL(RHO, THETA)
% RECT - Complex matrix or number, RECT = A + jB, A = Real, B = Imaginary
% RHO - Magnitude
% THETA - Angle in radians
function rec = pol2rec(rho,theta)
rec = rho.*cos(theta) + 1i*rho.*sin(theta);
```

POWER COEFFICIENT FUNCTION.

```
function Cp=powerCoeff()
clc
clear all
R=35.25; % Radius of the Wind Turbine Blade
S= [4 7 8 9 10 11 12 14]; % Wind velocity input
B=[0 0.5 1 2 3 4 5 6]; % Pitch Angle in Degrees
L=(1:8)'; % Tip Speed Ratio
    W=L.*S./R; % Wind turbine Speed
   Li=((B.^3+1).*(L+0.08.*B))./((B.^3+1)-(0.035.*(L+0.08.*B))); % Lambda i
   Cp=0.5176.*((((116./Li)-(0.6.*B)-5).*exp(-21./Li))+0.0068*L);% Power coefficient



Figure
plot(W,Cp,'b.-','linewidth',1.5)
title('Plot of Increasing Pitch Angle with Wind Turbine Speed,Tip Speed Ratio and Power Coefficient')
xlabel('Wind Turbine Speed')
ylabel('power coefficient')
hold on;
grid on;

plot(L,Cp,'r.-','linewidth',1.5)
xlabel('Tip speed ratio')
ylabel('power coefficient')


disp ('                          |Pitch Angle|');
disp ('|Tip  |');
disp ('|Speed|');
disp ('|Ratio|');
for m=L'


      fprintf('    %8.4f', B );fprintf('\n');fprintf('%3g', m);fprintf('    %8.4f', Cp(m,1:8) );

end;fprintf('\n');
```

```
end
```

PSO CODE.

```
function BestSol = psoWT39()
clc;
clear;
close all;

%% Problem Definition

nVar=8;           % Number of Decision Variables

VarSize=[1 nVar];   % Size of Decision Variables Matrix

VarMin=6;        % Lower Bound of Variables
VarMax=12;         % Upper Bound of Variables


%% PSO Parameters

MaxIt=1000;      % Maximum Number of Iterations

nPop=1000;        % Population Size (Swarm Size)

% PSO Parameters
%w=1;            % Inertia Weight
wmax = 0.9;
wmin = 0.4;
wdamp=0.99;     % Inertia Weight Damping Ratio
c1=1.2;         % Personal Learning Coefficient
c2=1.6;         % Global Learning Coefficient

% If you would like to use Constriction Coefficients for PSO,
% uncomment the following block and comment the above set of parameters.

% % Constriction Coefficients
% phi1=2.05;
% phi2=2.05;
% phi=phi1+phi2;
% chi=2/(phi-2+sqrt(phi^2-4*phi));
% w=chi;          % Inertia Weight
% wdamp=1;        % Inertia Weight Damping Ratio
% c1=chi*phi1;    % Personal Learning Coefficient
% c2=chi*phi2;    % Global Learning Coefficient

% Velocity Limits
VelMax=0.1*(VarMax-VarMin);
VelMin=-VelMax;

%% Initialization

empty_particle.Position=[];
empty_particle.Velocity=[];
empty_particle.Power=[];
empty_particle.Best.Position=[];
empty_particle.Best.Power=[];

particle=repmat(empty_particle,nPop,1);

GlobalBest.Power=inf;
 % Wind Velocity
S= [4 7 8 9 10 11 12 14];


for i=1:nPop

   % Initialize Position
   particle(i).Position=unifrnd(VarMin,VarMax,VarSize);
```

```
    % Initialize Velocity
    particle(i).Velocity=zeros(VarSize);

    % Evaluation
    h=3/7;            % 8 inputs within 3 seconds using finite central difference method
    myW=particle(i).Position;
    if i<6
        dw = myW(i+2)-myW(i)/(2*h);
    end
    particle(i).Power = fitnessWT(S,dw,particle(i).Position);

    % Update Personal Best
    particle(i).Best.Position=particle(i).Position;
    particle(i).Best.Power=particle(i).Power;

    % Update Global Best
    if particle(i).Best.Power<GlobalBest.Power

        GlobalBest=particle(i).Best;

    end

end

BestPower=zeros(MaxIt,1);

%% PSO Main Loop

for it=1:MaxIt

    w = wmax-(wmax-wmin)*it/MaxIt;

    for i=1:nPop

        % Update Velocity
        particle(i).Velocity = w*particle(i).Velocity ...
            +c1*rand(VarSize).*(particle(i).Best.Position-particle(i).Position) ...
            +c2*rand(VarSize).*(GlobalBest.Position-particle(i).Position);

        % Apply Velocity Limits
        particle(i).Velocity = max(particle(i).Velocity,VelMin);
        particle(i).Velocity = min(particle(i).Velocity,VelMax);

        % Update Position
        particle(i).Position = particle(i).Position + particle(i).Velocity;

        % Velocity Mirror Effect
        IsOutside=(particle(i).Position<VarMin | particle(i).Position>VarMax);
        particle(i).Velocity(IsOutside)=-particle(i).Velocity(IsOutside);

        % Apply Position Limits
        particle(i).Position = max(particle(i).Position,VarMin);
        particle(i).Position = min(particle(i).Position,VarMax);

        % Evaluation
        particle(i).Power = fitnessWT(S,dw,particle(i).Position);

        % Update Personal Best
        if particle(i).Power<particle(i).Best.Power

            particle(i).Best.Position=particle(i).Position;
            particle(i).Best.Power=particle(i).Power;

            % Update Global Best
            if particle(i).Best.Power>GlobalBest.Power

                GlobalBest=particle(i).Best;

            end
```

```
        end

    end

%     BestPower(it)=GlobalBest.Power;
%
%     disp(['Iteration ' num2str(it) ': Best Power = ' num2str(BestPower(it))]);

    w=w*wdamp;

    disp(['Iteration' num2str(it), ':  RotorSpeed = ' num2str(particle(i).Position), '   BestPower = ' num2str(GlobalBest.Power)]);

end

BestSol = GlobalBest;



%% Results

% Figure;
% plot(BestPower,'LineWidth',2);
% xlabel('Iteration');
% ylabel('BestPower');
% grid on;
%
%Figure (1);
%semilogy(BestPower,'LineWidth',2);
%plot(it,BestPower)
%xlabel('Iteration');
%ylabel('BestPower');
%hold on;

%x=linspace(0,100);
%Figure
%plot(RotorSpeed,BestPower,'b.-')
%ylabel ('BestPower')
%xlabel ('RotorSpeed')
%ylim([0 1000]);
%xlim([5 15]);
end
```

A Brief Bio

Eng. Terry Lumbasi Chepkania is the Manager, Design at Rural Electrification and Renewable Energy Corporation (REREC). He is passionate about serving others and has a personal commitment to his family and exploiting available opportunities in the society. He values sharing and making contribution to the society and building a career in electrical engineering while also acquiring new skills and knowledge for posterity.

In the past, he served in various roles and capacities with Kenya Power & Lighting Company in Nairobi region and environs for a period of 12 years. Prior to that he worked with Nzoia Sugar Company as Trainee Engineer. He holds a Bachelor of Technology degree in Electrical and Communication Engineering from Moi University received in 2005. In 2014, he graduated with a Master of Business Administration in Finance from University of Nairobi. He is a registered professional Engineer with the Engineers Board of Kenya and a Member of the Institution of Engineers of Kenya. He is also a member of Institute of Electrical & Electronic Engineers. His research interests includes renewable energy generation and power system control, distributed generation and grid integration.

SIMILARITY INDEX

Investigating Power Grid Frequency Stability with Wind Energy using PSO

by Terry Lumbasi

Submission date: 09-Nov-2019 12:04PM (UTC+0300)
Submission ID: 1208973236
File name: Grid_Frequency_Stability_with_Wind_Energy_using_PSO_final_8.docx (1.01M)
Word count: 12650
Character count: 101171

Investigating Power Grid Frequency Stability with Wind Energy using PSO

ORIGINALITY REPORT

13%	6%	2%	13%
SIMILARITY INDEX	INTERNET SOURCES	PUBLICATIONS	STUDENT PAPERS

PRIMARY SOURCES

1	Submitted to University of Nairobi Student Paper	5%
2	eie.uonbi.ac.ke Internet Source	1%
3	scholarworks.uno.edu Internet Source	1%
4	www.scribd.com Internet Source	1%
5	fr.scribd.com Internet Source	1%
6	Submitted to University of Queensland Student Paper	1%
7	Submitted to Ghana Technology University College Student Paper	1%
8	Submitted to Asian Institute of Technology Student Paper	<1%